Biochemical Characterization of Metal-Dependent 3-Deoxy-D-*manno*-Octulosonate 8-Phosphate Synthases from *Chlorobium tepidum* & *Acidithiobacillus ferrooxidans*

Jeffrey Aaron Yeoman

2007

Biochemical Characterization of Metal-Dependent 3-Deoxy-D-*manno*-Octulosonate 8-Phosphate Synthases from *Chlorobium tepidum* & *Acidithiobacillus ferrooxidans*

A thesis presented in partial fulfillment of the requirements for the degree of

Masterate of Science

in

Biochemistry

at Massey University, Turitea, Palmerston North

New Zealand

Jeffrey Aaron Yeoman

2007

ABSTRACT

3-Deoxy-D-*manno*-octulosonate 8-phosphate (KDO8P) synthase is the enzyme responsible for catalyzing the first reaction in the biosynthesis of KDO. KDO is an essential component in the cell wall of Gram-negative bacteria and plants. This compound is not present in mammals; therefore the enzymes responsible for its biosynthesis are potential targets for the development of new antibiotic agents. KDO8P synthase catalyzes the condensation reaction between phosphoenol pyruvate (PEP) and D-arabinose 5-phosphate (A5P) to form KDO8P.

Two types of KDO8P synthase have been identified; a metal-dependent type and a non metal-dependent type. KDO8P synthase from the organism *Chlorobium tepidum* (*Cte*) has been partially purified and partially characterized. In line with predictions based on sequence alone, the activity of this enzyme is dependent on the presence of a divalent metal ion and is sensitive to the presence of the metal chelating agent EDTA. *Cte* KDO8P synthase was found to have the highest activity in the presence of Mn^{2+} or Cd^{2+}.

KDO8P synthase from the organism *Acidithiobacillus ferrooxidans* (*Afe*) has also been cloned, purified and biochemically characterized. *Afe* KDO8P synthase was also found to be a metallo enzyme and the catalytic activity is highest in the presence of Mn^{2+} or Co^{2+}. *Afe* KDO8P synthase was found to exist as a tetramer in solution and is most active within the pH range of 6.8 to 7.5 and within a temperature range of 35 ºC to 40 ºC. Sequence analysis suggests that this enzyme has characteristics conserved throughout the metallo and the non-metallo KDO8P synthases and is closely related to the metal-dependent 3-deoxy-D-*arabino*-heptulosonate 7-phosphate (DAH7P) synthases. The role of several active-site residues of *Afe* KDO8P synthase has been investigated. A C21N mutant of *Afe* KDO8P synthase was found to retain 0.5% of wild-type activity and did not require a divalent metal ion for catalytic activity. This suggests that the metallo and non-metallo KDO8P synthases have similar catalytic mechanisms.

ACKNOWLEDGEMENTS

Thank you to my supervisor Emily Parker for all the help and guidance and for encouraging me to pursue postgraduate studies. She has provided me with a great environment to learn and introduced me to some great people along the way. Also thanks for the coffee and lunch shouts. I will look forward to catching up with you over a wine or two in Lorne sometime in the future.

Thank you to my co-supervisor Geoff Jameson for helping with my work both in this project and throughout my time at Massey University. I wish I had some more exciting crystals for you to help me work with, but thanks for the help at the end and for the pretty pikkies!! Thank you also to Mark Patchett for providing the *C. tepidum* KDO8P synthase for me to work on. We couldn't have chosen a worse protein to try and purify, but thanks anyway!

Thanks to all the team in the EJP research group at Massey University. It has been great to be able to work with a vibrant group of students and researchers. Special thanks to Fiona Cochrane for looking over my shoulder for the first six months of my masters, showing me the way around a research lab, and giving me the odd Post-It note if I had done something wrong! And to Linley Schofield, two words – chocolate cake! I have learnt a lot from everybody in this group.

Thanks to my family for supporting me for five years at Massey University and for all the free meals when I was living off a student allowance! Thanks especially to my wife Monique who encouraged me to go and do what I wanted to do and for doing her best to stay out of my way during the last few weeks of writing up!

TABLE OF CONTENTS

INDEX OF FIGURES

INDEX OF TABLES

ABBREVIATIONS

AEC	Anion exchange chromatography
Afe	*Acidithiobacillus ferrooxidans*
Amp	Ampicillin
ATP	Adenosine triphosphate
A5P	D-Arabinose 5-phosphate
BTP	1,3-*bis*(tris(hydroxymethyl)methylamino)propane
bp	Base pairs
CEC	Cation exchange chromatography
Cte	*Chlorobium tepidum*
Da	Dalton
DAH7P	3-deoxy-D-*arabino*-heptulosonate 7-phosphate
DNA	Deoxyribo nucleic acid
dNTP	Deoxyribo nucleotide triphosphate
DTT	Dithiothreitol
EDTA	Ethylene diamine tetra-acetic acid (di-sodium salt)
E4P	D-Erythrose 4-phosphate
FPLC	Fast protein liquid chromatography
HCl	Hydrochloric acid
HIC	Hydrophobic interaction chromatography
IEC	Ion exchange chromatography
IPTG	Isopropyl-1-thio-β-D-galactopyranoside
k_{cat}	Turnover number
KCl	Potassium chloride
KDO8P	3-deoxy-D-*manno*-octulosonate 8-phosphate
K_m	Michaelis constant
LB broth	Luria-Bertani broth
LPS	Lipopolysaccharide

MW	Molecular weight
MWCO	Molecular weight cut-off
NaCl	Sodium chloride
$(NH_4)_2SO_4$	Ammonium sulfate
NMR	Nuclear magnetic resonance
OD	Optical density
PAGE	Polyacrylamide gel electrophoresis
PCR	Polymerase chain reaction
PEG	Polyethyleneglycol
PEP	Phosphoenolpyruvate
pI	Isoelectric point
P_i	Inorganic phosphate
Psi	Pounds per square inch
SDS	Sodium dodecyl sulfate
SEC	Size exclusion chromatography
Thesit	Polyethyleneglycol dodecyl ether
UV	Ultra violet
V_{max}	Maximum reaction velocity

CHAPTER 1

INTRODUCTION

1.1 KDO8P synthase overview

As pathogenic microorganisms become more resistant to current antibiotics, the need to design novel antibacterial agents becomes greater. Enzymes catalyzing reactions in pathways unique to pathogenic bacteria make attractive targets for such compounds. One such enzyme is 3-deoxy-D-*manno*-octulosonate 8-phosphate (KDO8P) synthase (EC 2.5.1.55), an enzyme found in Gram-negative bacteria and in plants but not in humans.

KDO8P synthase catalyzes the aldol-like condensation reaction between D-arabinose 5-phosphate (A5P) and phosphoenol pyruvate (PEP) to produce the 8 carbon sugar KDO8P and inorganic phosphate.[1] (Figure 1.1)

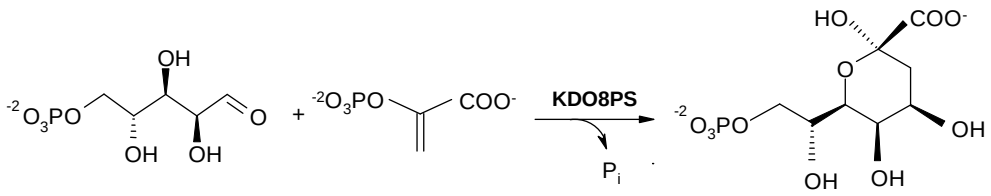

A5P PEP KDO8P

Figure 1.1 **Reaction catalyzed by KDO8P synthase.**

KDO8P is the phosphorylated precursor to KDO, which is an essential part of the lipopolysaccharide (LPS) layer in the cell wall of Gram-negative bacteria[2] and part of the primary cell wall of higher plants.[3] In Gram-negative bacteria KDO forms part of lipid A which links the LPS layer to the outer membrane[4] (Figure 1.2), and is the only sugar residue of the LPS which has been identified in almost all LPS structures that have been investigated.[5] The Lipid A-inner core region is also known as the endotoxin and promotes antigenic response associated with Gram-negative inflammation and sepsis.

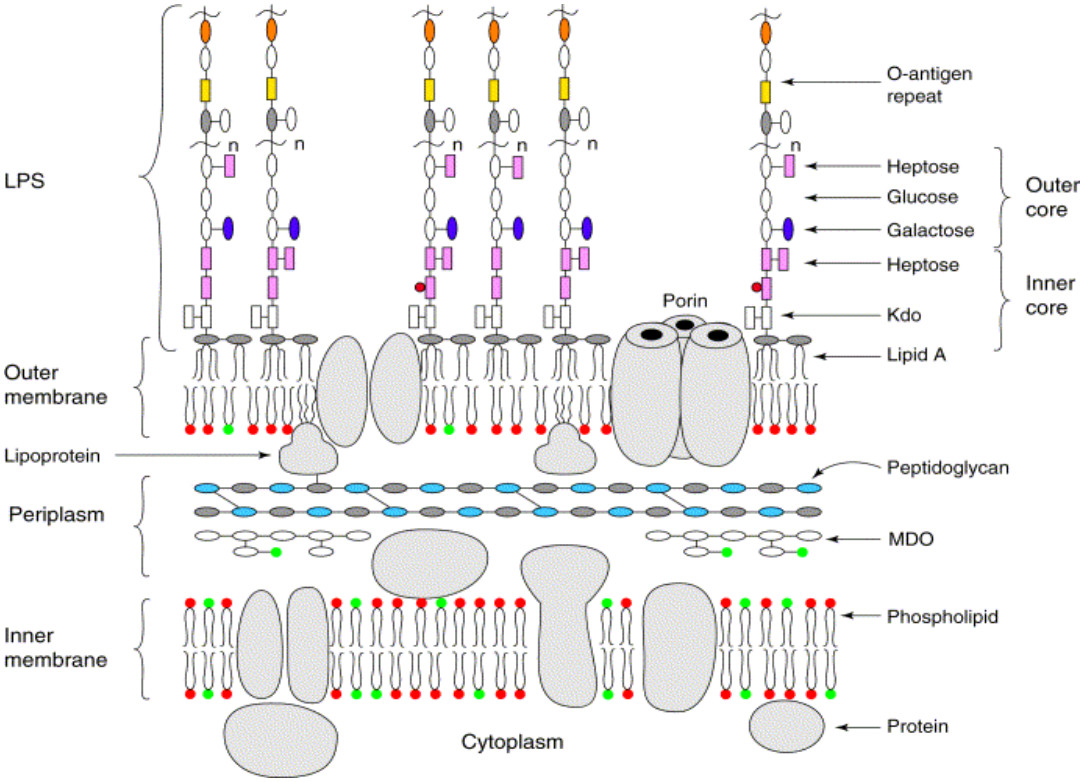

Figure 1.2 **Schematic diagram of the molecular organization of the outer envelope of Gram-negative bacteria.** (Figure taken directly from Wyckoff *et al* (1998).[4]

KDO was shown to be necessary for Gram-negative bacterial growth and homeostasis by elimination of KDO8P synthase activity from a temperature-sensitive mutant of the microorganism *Salmonella typhimurium.*[6] Even microorganisms that do not express an antigenic region such as the K-12 strain of *Escherichia coli* still have the essential components lipid A and KDO.[2] Gram-negative bacteria that have been mutated to produce incomplete LPS layers have also been shown to be less pathogenic and more susceptible to antibiotics.[7] More recently the importance of the structure of the LPS layer has been questioned. Mutants of *E. coli* K-12[8] and *Moraxella catarrhalis,*[9] which contained lipid A but no KDO, were shown to be viable.

KDO8P synthase and other enzymes in the LPS biosynthetic pathway have been identified as targets for new antibacterial agents.[4] Biochemical, functional and structural characterization of KDO8P synthase from many different organisms gives insight into the enzyme's mechanism and will aid the design of novel inhibitors.

1.2 Relationship between KDO8P synthase and DAH7P synthase

The first biochemically characterized KDO8P synthase, from *E. coli*, was shown not to require any metal cofactor for activity.[10] Later characterization of the KDO8P synthase from *Aquifex aeolicus* suggested that there may be another group of KDO8P synthases that require a divalent metal cofactor for catalytic activity.[11] This discovery suggests that there is an evolutionary relationship between KDO8P synthase and the functionally unrelated but mechanistically related enzyme 3-deoxy-D-*arabino*-heptulosonate 7-phosphate (DAH7P) synthase (EC 2.5.1.54). DAH7P synthase is a metal-dependent enzyme that catalyzes the aldol-like condensation reaction between PEP and D-erythrose 4-phosphate (E4P) to produce the 7-carbon sugar DAH7P and inorganic phosphate. This is the first committed step of the shikimate pathway, responsible for the biosynthesis of aromatic compounds.[12] DAH7P synthases can be grouped into two families based on amino-acid sequence and molecular weight. These are referred to as

type I and type II throughout this thesis. Type II DAH7P synthases are much larger than their type I counterparts, with molecular masses of around 54 kDa. Type I DAH7P synthases have molecular masses less than 40 kDa. Sequence identity between the two types is less than 10% but structural analysis of both types reveal a similar core monomer fold and similar arrangement of key residues in the active site, suggesting a common ancestry.[13] All DAH7P synthases that have been characterized to date require a divalent metal ion for activity.[14-16]

The type I DAH7P synthases can be further divided on the basis of primary sequence similarity.[13] These are denoted as subfamilies Iβ and Iα DAH7P synthase. Jensen *et al* (2002) have illustrated the relationship between KDO8P synthase and subfamily Iα and subfamily Iβ DAH7P synthase based on primary sequence similarity[13] (Figure 1.3). Their analysis suggests that the subfamily Iβ DAH7P synthases are more closely related to the KDO8P synthases than to the subfamily Iα DAH7P synthases and that the two enzymes may have emerged from a common ancestor. The properties and structure of *Pyrococcus furiosus* DAH7P synthase suggest that it is the most closely related of all characterized DAH7P synthases to the KDO8P synthases.[17]

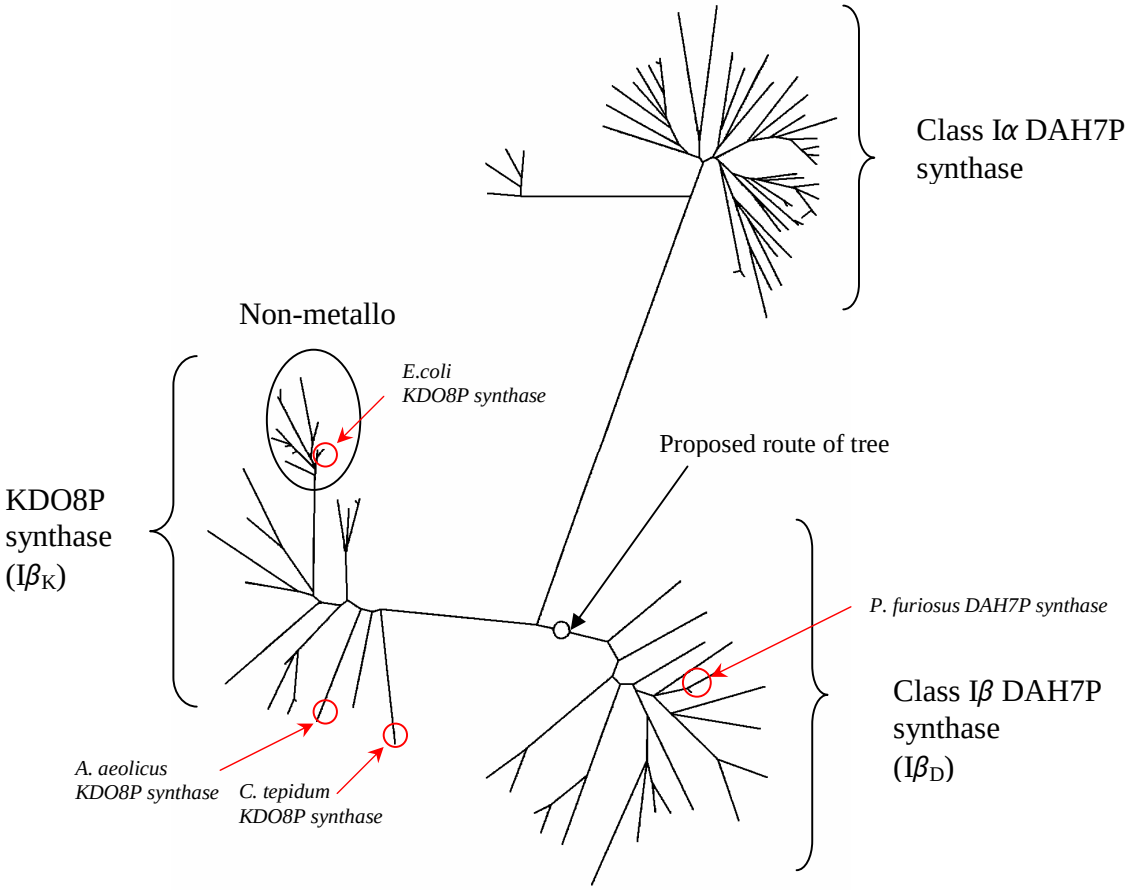

Figure 1.3 **Phylogenetic relationship between KDO8P synthase and type 1 DAH7P synthase.**[13] Phylogenetic tree is based on complete primary amino-acid sequence alignments. The proposed route of the tree is placed closest to the type Iβ DAH7P synthases because of the groups shown, the type Iβ DAH7P synthases are the most widely distributed throughout nature.[18]

1.3 Metal dependency of KDO8P synthase

Although only a small number of metallo and non-metallo KDO8P synthases have been fully or partially characterized, the phylogenetic analysis presented by Jensen *et al* (figure 1.3) separates the two groups on the basis of several highly conserved residues in and around the active site. The sequence analysis shows the non-metallo KDO8P synthases are grouped very close to the metallo KDO8P synthases but the non-metallo group seem slightly more distantly related to the 1β DAH7P synthases.[13] All proposed active site residues of KDO8P synthase are conserved throughout the metallo and non-metallo types except for one, a Cys residue (figure 1.4) common to the known and proposed metallo enzymes (residue 21 in *Acidithiobacillus ferrooxidans* KDO8P synthase, the subject of this thesis) and the corresponding Asn residue (Asn26 in *E. coli*) common to KDO8P synthase of the known and proposed non-metallo enzymes[19] (Figure 1.5). The Cys residue is one of four conserved metal binding residues throughout the primary sequence of all metallo KDO8P synthases (see figure 1.5).[13]

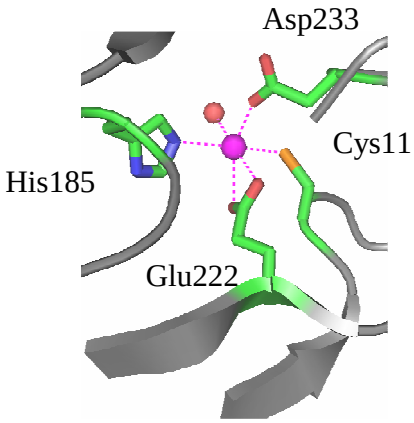

Figure 1.4 **Metal binding site of *A. aeolicus* KDO8P synthase (PDB code 1FWW).[20]** Taken from structure of *A. aeolicus* with A5P, PEP and Cd^{2+} (pink) bound. Red = O; Blue = N; Orange = S; red sphere = water. Dashed lines indicate interactions between Cd^{2+} and conserved metal binding residues and water. The polypeptide backbone with secondary structural elements is shown in grey.

Substitution of the Cys residue in the corresponding position of the *Aquifex pyrophilus*[21] and *A. aeolicus*[22] KDO8P synthases, known metallo enzymes, generated mutant proteins that were shown to be incapable of metal binding. By substituting the Cys with Asn the *A. pyrophilus* and *A. aeolicus* KDO8P synthases became insensitive to EDTA and some metal-independent activity (up to 10% and 70% wild type activity respectively) was shown.[22, 23] Studies by Oliynyk *et al* and Shulami *et al* have shown that substitution of the Asn with a Cys in *E. coli* KDO8P synthase resulted in a mutant enzyme that was capable of metal binding and was activated by Mn^{2+} but still retaining high levels of non-metallo activity.[23, 24] In contrast, studies by Li *et al* have proposed that non-metallo *E. coli* KDO8P synthase can not be converted to a metal-binding enzyme through this single amino acid substitution alone.[22] However, the authors do agree that the role of the metal ion in *A. aeolicus* and *A. pyrophilus* KDO8P synthase is similar to the role of Asn26 in *E. coli* KDO8P synthase. It has been suggested that the metal ion has more of a structural role in maintaining the correct orientation of the substrates and/or reaction intermediates in the active site and is not directly involved in catalysis (see section 1.5 for further details).[23, 25]

The corresponding metal-binding Cys residue is also present in all known DAH7P synthases. The Cys to Asn mutation to DAH7P synthase from *P. furiosus* showed no detectable enzymic activity with or without EDTA or added Mn^{2+} showing the importance of a metal-ion cofactor and the correct metal-binding residues in DAH7P synthases.[25]

Figure 1.5 **ClustalW alignment KDO8P synthase amino-acid sequences**

```
                                                                M
A.aeolicus          ---------------------------MEKFLVIAGPCAIES---EELLLKVGEEIKRLS 30
H.pylori            --------------MKTSKT------KTPKSVLIAGPCVIES---LENLRSIATKLQPLA 37
C.tepidum           --------------MQKFSVGTVSLPGPKGLFLIAGPCLIEN---RRMAMDVAAELDRIR 43
A.ferrooxidans      --------------MRLCGFEAG---LQHPFFLMAGPCAIES---ESLALRTAEDLRDIC 40
N.meningitidis      --------------MDIKIN-DITLGNNSPFVLFGGINVLES---LDSTLQTCAHYVEVT 42
N.gonorrhoeae       --------------MDIKIN-DITLGNNSPFVLFGGINVLED---LDSTLQTCAHYVEVT 42
E.coli              -----------MKQKVVSIG-DINVANDLPFVLFGGMNVLES---RDLAMRICEHYVTVT 45
S.typhimurium       -----------MKQKVVNIG-DIKVANDLPFVLFGGMNVLES---RDLAMRICEHYVTVT 45
                                                  ::.*   :*.

A.aeolicus          EKFKEVEFVFKSSFDKANRSSIHSFRGHGLEYGVKALRKVKEEFGLKITTDIHESWQAEP 90
H.pylori            NNE-RLDFYFKASFDKANRTSLESYRGPGLEKGLEMLQTIKEEFGYKILTDVHESYQASV 96
C.tepidum           KKE-DVRVIFKGSYRKANRSSASSYTGIGDRQALEILREIRDYFGMPVLTDVHETSEVEL 102
A.ferrooxidans      ARL-GIPFIYKSSYDKANRSSGQSFRGPGMDEGLRILEKVRREVGVPVVTDVHEKEDVSA 99
N.meningitidis      RKL-GIPYIFKASFDKANRSSIHSYRGVGLEEGLKIFEKVKAEFGIPVITDVHEPHQCQP 101
N.gonorrhoeae       RKL-GIPYIFKASFDKANRSSIHSYRGVGLEEGLKIFEKVKAEFGIPVITDVHEPHQCQP 101
E.coli              QKL-GIPYVFKASFDKANRSSIHSYRGPGLEEGMKIFQELKQTFGVKIITDVHEPSQAQP 104
S.typhimurium       QKL-GIPYVFKASFDKANRSSIHSYRGPGLEEGMKIFQELKQTFGVKVITDVHEASQAQP 104
                         :   :* *: ****:*     * *   .:  :  ::        **:*.  .

A.aeolicus          VAEVADIIQIPAFLCRQTDLLLAAAKTGRAVNVKKGQFLAPWDTKNVVEKLKFGGA---- 146
H.pylori            AAKVADILQIPAFLCRQTDLIVEVSQTNAIVNIKKGQFMNPKDMQYSVLKALKTRDKSIQ 156
C.tepidum           AASYVDVLQIPAFLCRQTDLIVAAASTGLAVNIKKGQFLAPEDMALAAAKAAATGN---- 158
A.ferrooxidans      VAEVVDVLQTPAFLCRQTDFIQAVAAAGKPVNIKKGQFLAPWDMLHVASKAKATGN---- 155
N.meningitidis      VAEVCDVIQLPAFLARQTDLVVAMAKTGNVVNIKKPQFLSPSQMKNIVEKFHEAGN---- 157
N.gonorrhoeae       VAEVCDVIQLPAFLARQTDLVAAMAETGNVINIKKPQFLSPSQMKNIVEKFREAGN---- 157
E.coli              VADVVDVIQLPAFLARQTDLVEAMAKTGAVINVKKPQFVSPGQMGNIVDKFKEGGN---- 160
S.typhimurium       VADVVDVIQLPAFLARQTDLVEAMAKTGAVINVKKPQFVSPGQMGNIVDKFHEGGN---- 160
                    ...  *::* ****.****::   . :   :::** **: * :      *

                                                                  M
A.aeolicus          ---------KEIYLTERGTTFGYNNLVVDFRSLPIM-KQW---AKVIYDATHSVQLPGGL 193
H.pylori            SPTYETALKNGVWLCERGSSFGYGNLVVDMRSLKIM-REF---APVIFDATHSVQMPGGA 212
C.tepidum           ---------KKIMLTERGTTFGYHNLVVDYRGLPIM-AESG--WPVILDVTHSVQLPGAG 206
A.ferrooxidans      ---------EQIMVCERGASFGYNNLVSDMRSLAVM-RQTG--CPVVFDATHSVQLPGGQ 203
N.meningitidis      ---------GKLILCERGSSFGYDNLVVDMLGFGVM-KQTCGNLPVIFDVTHSLQTRDAG 207
N.gonorrhoeae       ---------GKLILCERGSSFGYDNLVVDMLGFGVM-KQTCGNLPVIFDVTHSLQTRDAG 207
E.coli              ---------EKVILCDRGANFGYDNLVVDMLGFSIM-KKVSGNSPVIFDVTHALQCRDPF 210
S.typhimurium       ---------DKVILCDRGANFGYDNLVVDMLGFSVM-KKVSGNSPVIFDVTHALQCRDPF 210
                              :   :**  :** .*: *  .: ::        :. * **::*  .

                                                  M                 M
A.aeolicus          GDKSGGMREFIFPLIRAAVAVGCDGVFMETHPEPEKALSDASTQLPLSQLEGIIEAILEI 253
H.pylori            NGKSSGDSSFAPILARAAAAVGIDGLFAETHVDPKNALSDGANMLKPDELEQLVTDMLKI 272
C.tepidum           AGVSGGDRRFLMPLARAAVAAGVDGLFFEVHPDPATAMSDASTQAPLAGFGEMVRELMQL 266
A.ferrooxidans      GDRSGGQREFIPVLARAAVAAGVSGLFMETHPNPADALSDGPNAWPLGRMEDLLRILQHI 263
N.meningitidis      SAASGGRRAQALDLALAGMATRLAGLFLESHPDPKLAKCDGPSALPLHLLEDFLIRIKAL 267
N.gonorrhoeae       SAASGGRRAQALDLALAGMATRLAGLFLESHPDPKLAKCDGPSALPLHLLENFLIRIKAL 267
E.coli              GAASGGRRAQVAELARAGMAVGLAGLFIEAHPDPEHAKCDGPSALPLAKLEPFLRQMKAI 270
S.typhimurium       GAASGGRRGQVTELARAGMAVGLAGLFLESHPDPANAKCDGPSALPLAKLEQFLTQIKAI 270
                      *.*       *  :. .    :: * * :*  * .*..       :  ::

A.aeolicus          REVASK--YYETIPVK-- 267
H.pylori            QNLF-------------- 276
C.tepidum           QRCMQS--IREEFHSR-- 280
A.ferrooxidans      DHVVKNQDFPENYPEELV 281
N.meningitidis      DDLIKSQPILTIE----- 280
N.gonorrhoeae       DDLIKSQPILTIE----- 280
E.coli              DDLVKGFEELDTSK---- 284
S.typhimurium       DDLVKSFDELDTEN---- 284
```

* Conserved residues
: Conservative substitution
. Semi-conservative substitutions
M Metal binding residues
--- Proposed A5P binding residues in *A. aeolicus* KDO8P synthase
--- Proposed PEP binding residues in *A. aeolicus* KDO8P synthase

1.4 Functional and structural studies of KDO8P synthase

Since the characterization of *A. aeolicus* KDO8P synthase[11], the KDO8P synthases from *A. pyrophilus*[21] and *Helicobacter pylori* J99[26] have also been shown to require a metal ion for activity. The KDO8P synthases from *E. coli*, *S. typhimurium*, *Neisseria gonorrhoeae* and *Neisseria meningitidis* are among those which have been shown to be non-metallo.[6, 10, 27, 28] The only plant KDO8P synthase to be functionally and biochemically characterized is from *Arabidopsis thaliana* and this enzyme does not require a metal ion for catalytic activity.[29]

The monomeric molecular masses of all KDO8P synthases studied to date are around 30 kDa. All microbial KDO8P synthases have been predicted to occur as trimers or tetramers according to size-exclusion chromatography experiments.[19, 30, 31] The *E. coli* and *A. aeolicus* KDO8P synthase structures have been determined by X-ray crystallography and both crystallized as similar tetramers.[20, 32]

The monomer fold of the *E. coli* and *A. aeolicus* KDO8P synthase resembles that of the type I DAH7P synthases and is based around a $(\beta/\alpha)_8$ barrel (figure 1.6). The *P. furiosus* DAH7P synthase structure shows a two-stranded β-hairpin covering the N-terminal of the barrel similar to that observed for *E. coli* KDO8P synthase[17] (figure 1.6). Other DAH7P synthases that have been structurally characterized such as *Thermotoga maritima* DAH7P synthase, show more elaborate N-terminal extensions and these are thought to be associated with allosteric regulation with shikimate-pathway end products.[17, 33, 34] No KDO8P synthases characterized so far show allosteric regulation, nor does *P. furiosus* DAH7P synthase.[17]

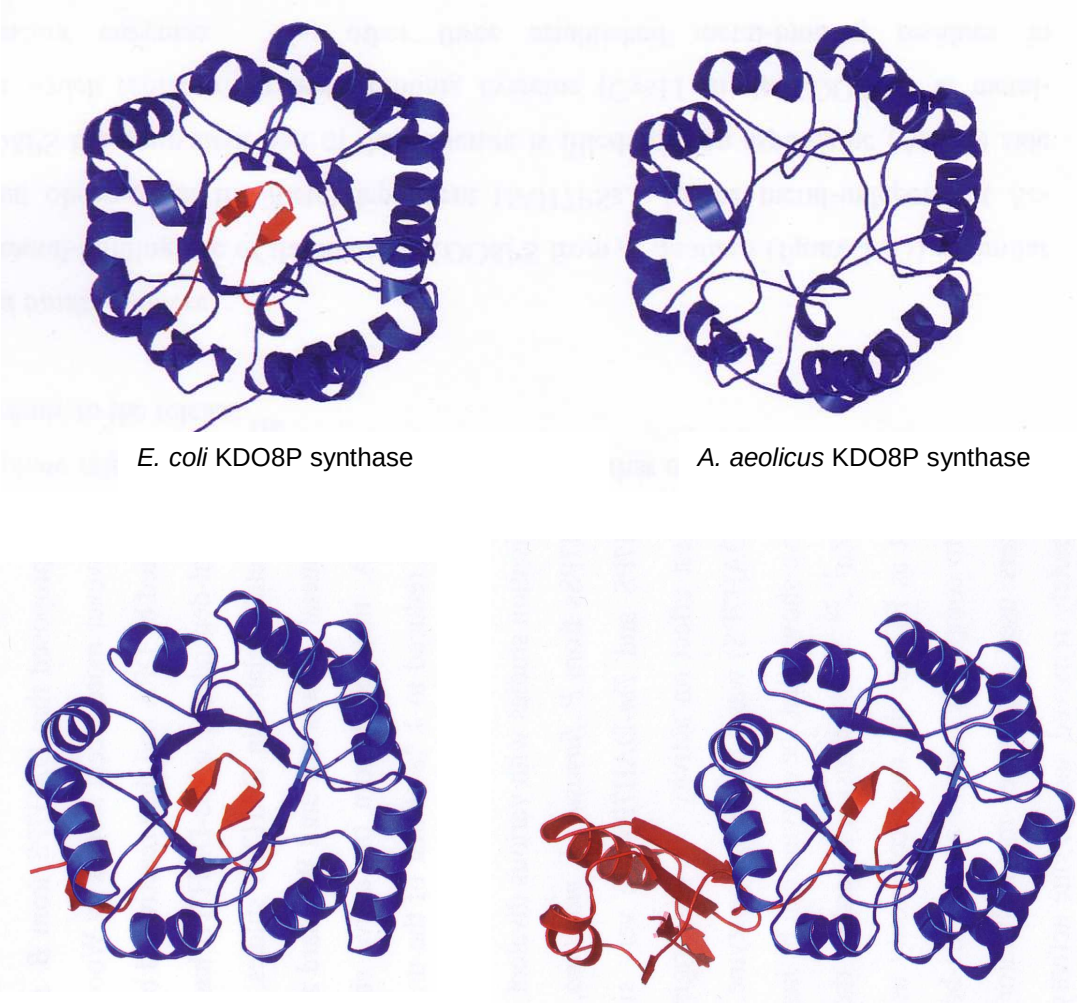

Figure 1.6 **Comparison of monomer fold of *E. coli* KDO8P synthase (PDB code 1X8F) and *A. aeolicus* KDO8P synthase (PDB code 1FWS) to monomer fold of *P. furiosus* DAH7P (PDB code 1ZCO) synthase and *T. maritima* DAH7P synthase.** The N-terminal extension of the β-barrel is shown in red.

The crystal structure of *A. aeolicus* KDO8P synthase has also been determined in complex with PEP, A5P and a Cd^{2+} ion[20] (figure 1.7) as well as with PEP and ribose 5-phosphate (R5P); PEP and E4P; and with API, a bi-substrate inhibitor (**A**5P **P**EP **I**nhibitor), bound.[35] This was achieved by performing all the crystallography at 4 ^{o}C

which is cold enough to render *A. aeolicus* KDO8P synthase inactive even in the presence of both substrates. These studies have given an insight into the positions of residues in the active site (including the Cys, Asp, Glu and His that are conserved throughout the primary sequences of metallo KDO8P synthases) in relation to the substrates. Figure 1.7 highlights the four conserved metal-binding residues as well as other residues that are conserved throughout metallo and non-metallo KDO8P synthases. PEP is shown being held in the active site by a number of polar or positively charged residues surrounding the carboxyl and phosphate groups (Gln99, Lys41, Lys46, Lys124, Arg154). A5P is shown to be held in a position to be attacked by C3 of PEP (discussed in the following section). The residues involved include Asn48, Arg49 and Ser50, part of the LysAla**AsnArgSer** motif which is conserved throughout all KDO8P synthases, but is not present in DAH7P synthase. The Cd^{2+} is also shown to be holding A5P in position by coordinating to the C2 hydroxyl group *via* a water molecule. The metal-binding residue Asp233 also appears to be in a position to interact with the C4 hydroxyl of A5P.

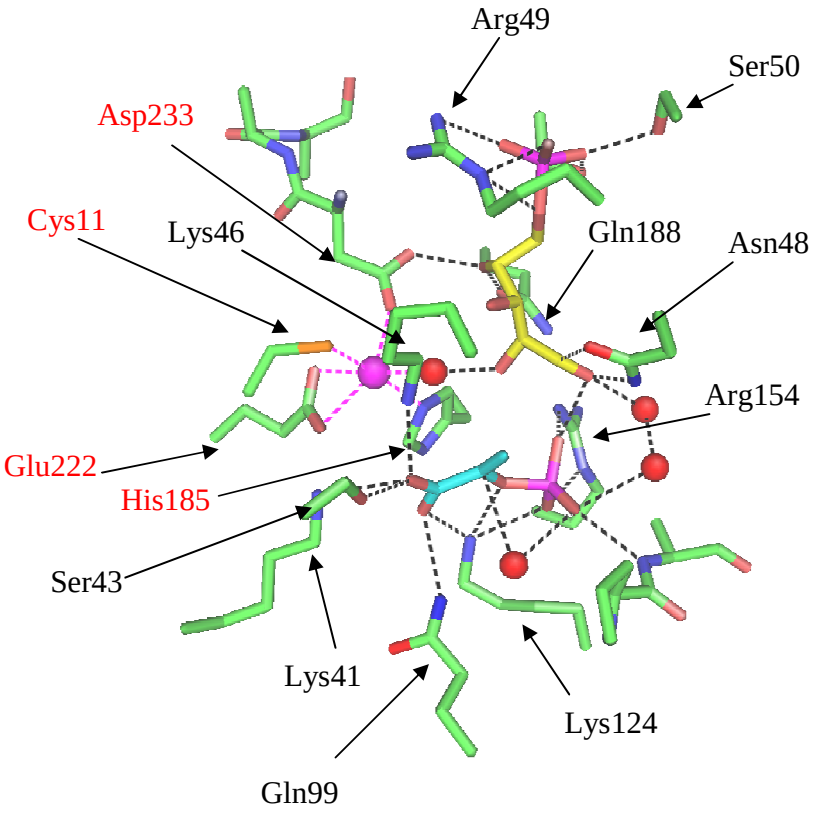

Figure 1.7 **The active site of *A. aeolicus* KDO8P synthase with A5P, PEP and Cd^{2+} bound (PDB code 1FWW).[20]** Oxygen = red; Nitrogen = blue; Phosphorus = pink; Water molecules are represented by red spheres. Pink dashed lines represent interactions between Cd^{2+} (pink sphere) and the surrounding residues and water molecules. Black dashed lines represent hydrogen bonding interactions between amino-acid residues or water molecules and the substrates. The *si* face of PEP is shown facing towards the top of the page, with the *re* face of the A5P carbonyl facing towards it. The four conserved metal-binding residues are labeled in red.

1.5 Mechanism of KDO8P synthase

Not all the mechanistic details of the reaction catalyzed by KDO8P synthase are fully understood. The structural similarities between KDO8P synthase and DAH7P synthase suggest that the mechanisms may be similar but the difference in metal dependency indicates that there must be differences.[11, 32, 36] The ability to convert a metallo KDO8P synthase into a non-metallo KDO8P synthase by mutating the metal-binding Cys to an Asn (found conserved in the non-metallo KDO8P synthases) suggests that both types of KDO8P synthase catalyze the condensation reaction using similar chemistry.[22, 37] The inability of DAH7P synthase to be converted to a non-metallo enzyme by this single mutation suggests a different role for the metal ion in catalysis.[25]

It has been determined that for both KDO8P synthase and DAH7P synthase the condensation reaction proceeds *via* cleavage of the C-O bond of PEP rather than the P-O bond, which is more typical of PEP-utilizing enzymes.[38-40] It has also been determined that the reaction proceeds *via* attack of the *si* face of PEP onto the *re* face of the A5P carbonyl.[41, 42]

A key step in the mechanism of DAH7P synthase and KDO8P synthase is the attack of C3 of PEP on the carbonyl group of E4P and A5P respectively. The importance of this step has been highlighted by substrate-specificity studies showing that the C2 hydroxyl group of E4P and A5P plays different roles in the respective enzymes. In KDO8P synthase it has been proposed that the C2 hydroxyl of A5P plays a critical role as the dihedral angle about the C1-C2 bond is controlled *via* coordination of the C2 hydroxyl to an Asn residue or to a metal (most likely *via* a water molecule). Therefore altering the stereochemistry about C2 of A5P is catastrophic to catalytic activity.[25] This suggests that the position of A5P in the active site is critical. The structure of *A. aeolicus* in complex with ribose-5-phosphate (R5P), which has the opposite stereochemistry about C2 to A5P, shows that the carbonyl functionality has adopted a different orientation and is not in an appropriate position for the addition of C3 of PEP.[35] However, 2-deoxy R5P

has been shown to be an extremely poor substrate, suggesting that without the interaction at C2, 2-deoxy R5P has a much reduced likelihood of accessing the correct conformation in the active site.[25, 43]

Earlier studies proposed two possible mechanistic pathways for the reaction catalyzed by KDO8P synthase (figure 1.8). The first hypothesis (mechanism I) suggests that a water molecule attacks at C2 of PEP and C3 of PEP adds to the aldehyde of A5P or E4P. This process would involve a linear intermediate.[39] The second hypothesis (mechanism II) suggests the formation of a cyclic intermediate and suggests that condensation of C3 of PEP with the carbonyl carbon of A5P is concurrent with an attack by C3-OH of A5P on C2 of PEP.[38, 44]

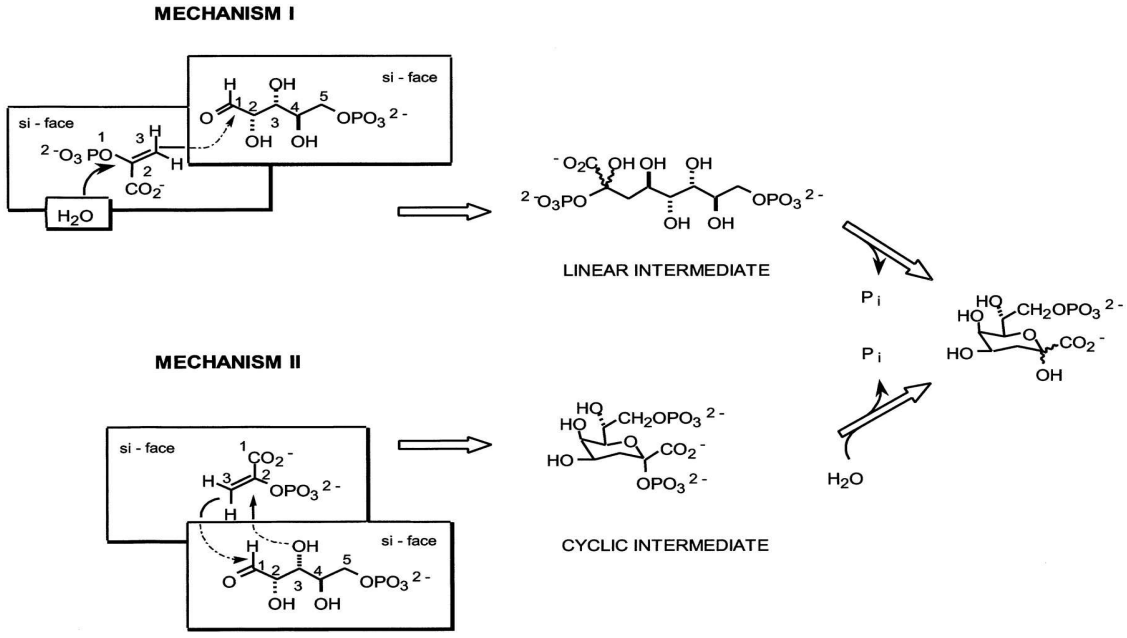

Figure 1.8 **Proposed mechanisms of KDO8P synthase.**[32]

Evidence for the linear intermediate was provided by Baasov *et al* who synthesized analogues of the proposed cyclic and acyclic intermediates and investigated their inhibition of *E. coli* KDO8P synthase.[45] They found that the cyclic compounds were

very poor inhibitors of KDO8P synthase indicating such compounds were not substrates for the enzyme but analogues of the postulated linear intermediate were good inhibitors. This suggests that the linear intermediate is a compatible fit into the active site of KDO8P synthase but a cyclic intermediate is not. More recently, this group has used time-resolved electrospray mass spectrometry (ESI-MS) to monitor the KDO8P synthase-catalyzed reaction with its natural substrates on a millisecond timescale.[46] This study has provided for the first time direct evidence of the linear intermediate by detecting the formation and decay of the enzyme-bound intermediate on a time scale consistent with substrate decay and product formation.

The crystal structures of *A. aeolicus* KDO8P synthase in complex with PEP and A5P[20] and with API (a bi-substrate inhibitor mimicking the postulated linear intermediate[35]), also provide evidence to support the first hypothesis. The structures of the enzyme in complex with PEP and A5P show the distance between C2 of PEP and C3-OH of A5P to be greater than 5 Å, which is too far for a bond to form between them and create a cyclic intermediate without large conformational changes to the active site. The structures of the enzyme in complex with API show the inhibitor sitting in the active site with its phosphate and phosphonate moieties occupying the positions of the phosphate moieties of the two substrates. This compound was also found to be a potent inhibitor of *E. coli* and *A. aeolicus* KDO8P synthases with K_i values of 3.3 μM and 7.0 μM respectively.[35]

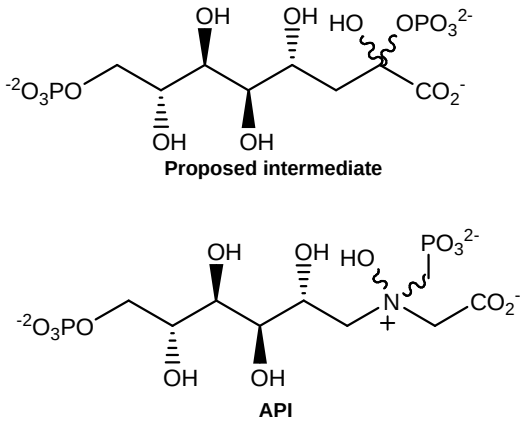

Figure 1.9 **The bi-substrate inhibitor API and the proposed intermediate of the KDO8P synthase catalyzed reaction.**

The current debate is centered on whether C3 of PEP attacks the carbonyl carbon (C1) of A5P first and the water molecule attacks the transient linear intermediate (figure 1.10, scheme 1) or whether the attack by the water molecule on C2 of PEP occurs first (figure 1.10, scheme 2).[43, 47] Two water molecules which could be involved have been identified in several KDO8P synthase structures but it is unclear whether the water molecule located on the *re* or *si* face is responsible for the attack on PEP[20] (see figure 1.11). Structures of *E. coli* KDO8P synthase and *A. aeolicus* KDO8P synthase with PEP bound suggested that the metal-coordinated water in metallo KDO8P synthases may be activated by the metal ion and a carbanion intermediate may be formed (figure 1.10, scheme 2) but in non-metallo KDO8P synthase it may be the other water involved and a carbocation intermediate may be formed (figure 1.10, scheme 1). This was originally proposed to be the difference between the metallo and the non-metallo KDO8P synthases.[20, 23, 47] A direct catalytic role of the metal ion in activation of a water molecule has been largely discounted due to the findings that a single metal binding Cys to Asn mutation can affect the metal dependency of the enzyme, as discussed earlier.[22, 23]

Further evidence for a common mechanism between metallo and non-metallo KDO8P synthases comes from studies using (*E*)- and (*Z*)-phosphoenol-3-fluoropyruvate (fluoro

PEP) as alternative substrates and analyzing the products by ^{19}F NMR.[48] The non-metallo *E. coli* KDO8P synthase and the metallo *A. pyrophilus* KDO8P synthase both showed high selectivity for (*E*)-fluoro PEP versus (*Z*)-fluoro PEP suggesting that PEP must take up the same orientation in the active site of both enzymes for optimal catalytic activity. DAH7P synthase from *E. coli* showed no preference for either isomer, again suggesting mechanistic differences between DAH7P synthase and KDO8P synthase and mechanistic similarities between the metallo and non-metallo KDO8P synthases.

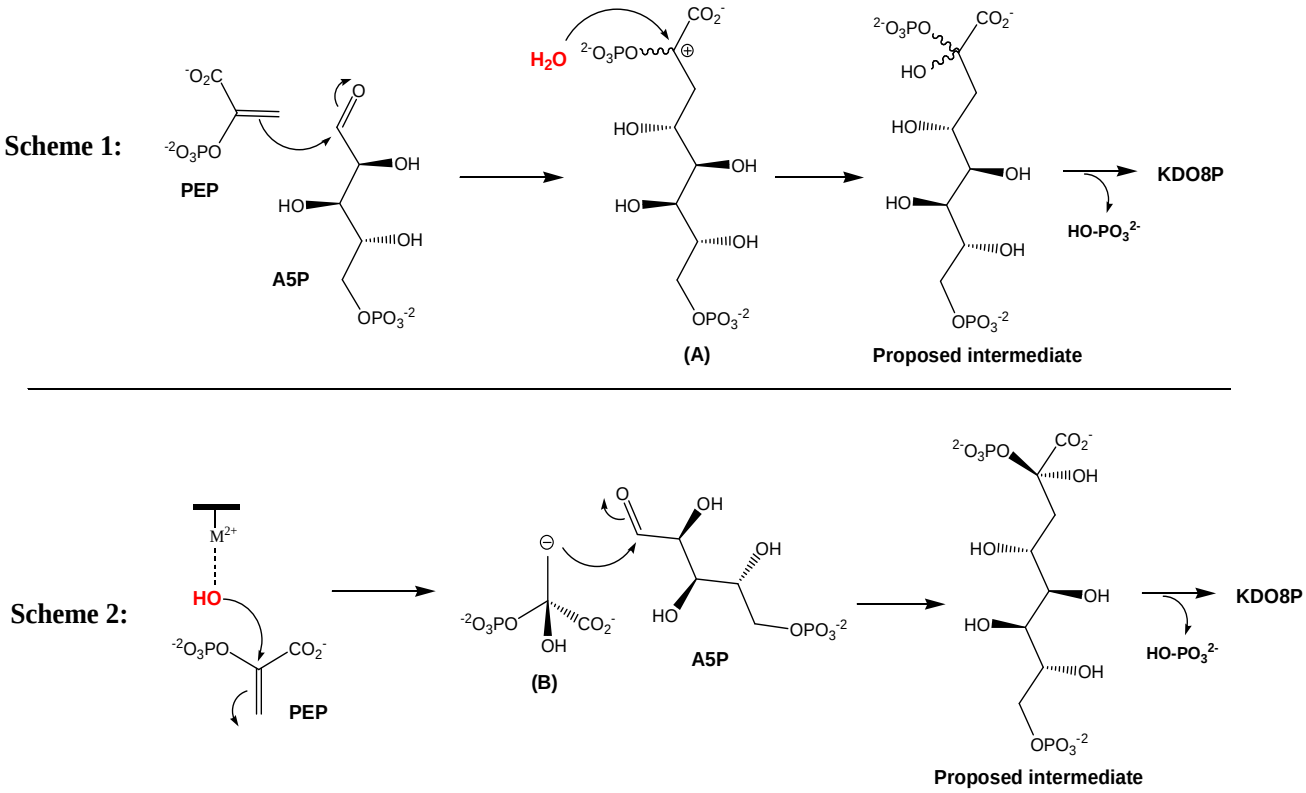

Figure 1.10 **Proposed mechanisms of KDO8P synthesis via a linear intermediate.**
(A) = transient oxocarbenium intermediate; (B) = PEP carbanion.

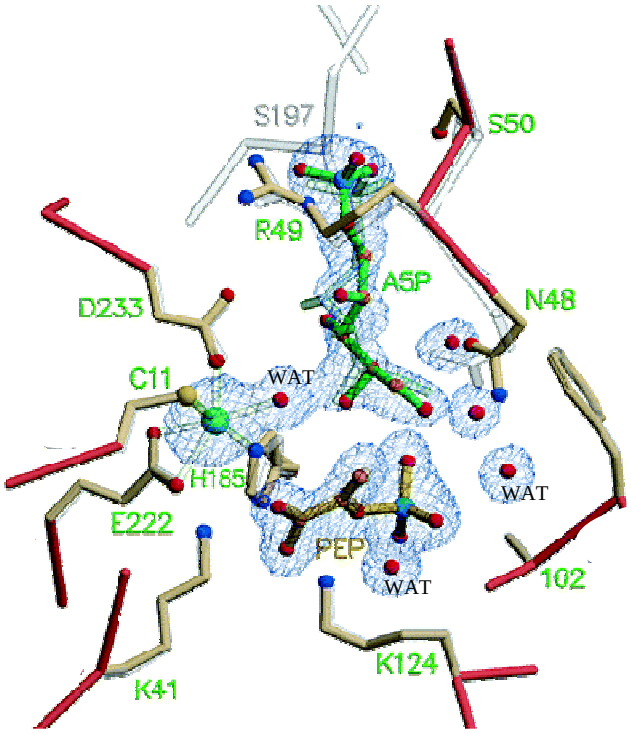

Figure 1.11 ***A. aeolicus* KDO8P synthase structure with Cd^{2+}, A5P and PEP bound (PDB code 1T8X).**[49] Cd^{2+} coordination is shown with transparent bonds. WAT = water. Nitrogen, blue; oxygen, red; carbon, orange; sulfur, yellow; phosphorus, pale blue; cadmium, green. The *si* face of PEP is pointing up and the *re* face is pointing down. Either the water molecule shown coordinated to the cadmium ion or the water molecule just off the *re* face of PEP could be involved in the catalytic mechanism. The water molecule coordinated to the metal is also in a position to be able to hydrogen bond with the C2 hydroxyl of A5P (see section 1.6). Figure taken directly from Xu *et al* (2005).[49]

1.6 The role of the metal ion in KDO8P synthase

The function of the metal ion in KDO8P synthase is still being debated. It has been suggested through structural analysis and substrate specificity studies that it is involved in stabilizing the substrate in the active site (probably *via* an associated water molecule) as it has been shown to be too far away from the aldehyde moiety of A5P to be involved in direct electrophilic activation.[22, 25, 37]

In the DAH7P synthase catalyzed reaction, structural and modeling studies show that the metal ion directly activates the aldehyde moiety of E4P (Lewis acid catalysis) and is not involved in the structural role as proposed for KDO8P synthase.[16, 25, 33, 47] The activation of the aldehyde moiety of A5P is proposed to be through protonation (Brønsted acid catalysis) by the phosphate group of PEP.[25] Structural and functional characterisation of more metallo and non-metallo KDO8P synthases and further analysis of relevant mutants will help define the mechanistic and evolutionary relationship between the two groups.

Structural studies have shown that C2-OH of A5P is coordinated to the metal ion either directly or through a water molecule in order to orient the monosaccharide into the correct position to be attacked by PEP (figure 1.12).[20]

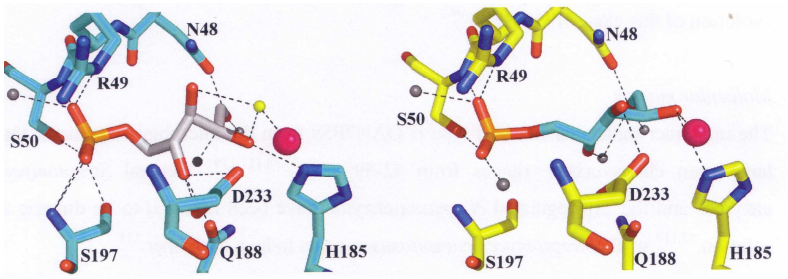

(A) **(B)**

Figure 1.12 **Two different conformations of A5P in the active site of KDO8P synthase.** (A) Shows coordination of A5P to Cd^{2+} (pink) through a water molecule (yellow) (PDB code 1FWW). The structure was solved with A5P, PEP and Cd^{2+} bound. PEP binds first in the enzymatic cycle which forces A5P to another location allowing the water molecule to coordinate to Cd^{2+}. (B) Shows coordination of C2-OH of A5P directly to the Cd^{2+} ion (PDB code 1FY6). The structure was solved with A5P and Cd^{2+} bound.[20]

Since the X-ray crystal structures of *E. coli* and *A. aeolicus* KDO8P synthase have been solved, comparisons can be made between the active sites of a metallo and a non-metallo KDO8P synthase. An overlay of *E. coli* and *A. aeolicus* KDO8P synthase shows that there are four *A. aeolicus* residues bound to the metal ion (Cd^{2+}), Cys11, His185, Glu222 and Asp233 (Figure 1.13).[23] The His, Glu and Asp are conserved residues throughout the KDO8P synthase (and DAH7P synthase) primary sequences for both metallo and non-metallo KDO8P synthases, whereas the fourth metal-binding ligand, the Cys residue, is conserved only throughout the metallo KDO8P synthases and in its place in the non-metallo enzymes is an absolutely conserved Asn.

When the structures of the non-metallo *E. coli* KDO8P synthase and the metallo *A. aeolicus* enzyme are compared in the region of the metal binding site, it is clear that only two of the three conserved residues, the His (202 in *E. coli*, 185 in *A. aeolicus*) and the Glu (239 in *E. coli*, 232 in *A. aeolicus*) are found occupying the same positions in their respective active sites (figure 1.13).[23] The conserved Asn of *E. coli* KDO8P synthase and its equivalent conserved Cys in the metal binding *A. aeolicus* enzyme occupy similar positions. The Cys11 of *A. aeolicus* has been replaced by Asn26 of *E. coli*. The fourth residue, an Asp in the primary sequence of both types of enzymes, appears to occupy a significantly different position in the non-metallo enzyme from that found for the metal binding *A. aeolicus* enzyme. It should be noted that in other structures of the *E. coli* KDO8P synthase and the closely related *N. meningitidis* enzyme, this Asp residue is in a disordered part of the structure, suggesting, at least in the absence of substrates, that there is considerable mobility for this residue in the non-metallo enzymes.[27, 32] Sequence and structural analysis suggests surrounding residues such as the conserved Pro252 (*E. coli*), may be responsible for the altered position of this residue in non-metallo KDO8P synthases (Figure 1.5) but no studies of such residues have been reported to date. The effects of mutations to the Pro245 and Asp243 residues in the metallo *A. ferrooxidans* KDO8P synthase are presented and discussed in chapter four of this thesis.

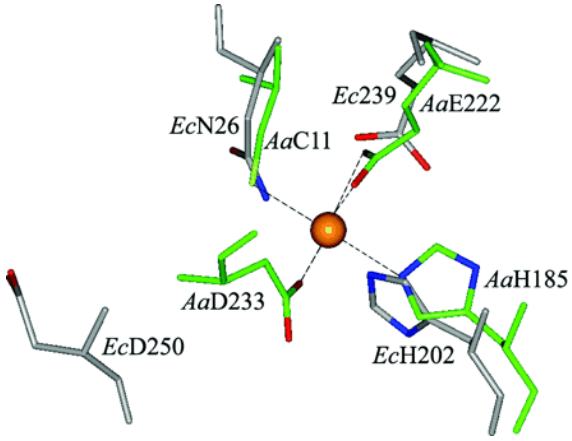

Figure 1.13 **Overlay of *E. coli* (*Ec*) (PDB code 1G7U[47]) and *A. aeolicus* (*Aa*) (PDB code 1FWS[20]) metal-binding sites in KDO8P synthase.** Figure taken directly from Shulami *et al* (2004).[23]

The His (His202 in *E. coli*, His185 in *A. aeolicus*) has been shown to be involved with PEP binding in both the metallo and non-metallo KDO8P synthases as well as being conserved throughout all DAH7P synthases and is important to the activity of both enzymes (figure 1.12).[32, 37] The His185 residue of *A. aeolicus* has been mutated to Gly with the enzyme only retaining 8% activity when compared to the wild type but still able to bind Cd^{2+} ions.[37] Mutation to the His202 residue of *E. coli* rendered the enzyme virtually inactive with only 1% to 4% of wild type activity retained.[50] Shulami *et al* suggest that the *E. coli* Asn26 plays an important role in stabilizing His202 to enable it to interact correctly with PEP.[23] In the metallo KDO8P synthases, the divalent metal ion appears to take on this role suggesting that the catalytic mechanism remains the same for the metallo and non-metallo KDO8P synthases.

1.7 Aims of this project

The aim of this project was to clone, express, purify and biochemically characterize a metallo KDO8P synthase. The KDO8P synthases from the green sulfur bacterium *Chlorobium tepidum* (*Cte*) and from the chemolithoautotrophic bacterium *Acidithiobacillus ferrooxidans* (*Afe*) were chosen. *Cte* KDO8P synthase was chosen as its primary amino acid sequence is closer to that of the Iβ DAH7P synthase subfamily according to analysis of Jensen *et al*.[13] *Afe* KDO8P synthase has the Cys residue typical of all metallo KDO8P synthases, but also has the AspGlyPro (at position 243 in *A. ferrooxidans* KDO8P synthase) motif which is conserved throughout all non-metallo KDO8P synthases but is only present in some of the metallo enzymes (See figure 1.5).

Additional aims of this project include the cloning, expression, purification and biochemical characterization of site-specific mutants of *Afe* KDO8P synthase in order to further explore the role of important residues in and around the metal binding site.

Finally, exploring crystallization conditions of *Afe* KDO8P synthase may help lead to elucidation of the structure and ultimately assist in the design of specific inhibitors for the KDO8P synthases of Gram-negative bacteria.

CHAPTER 2

EXPRESSION AND PURIFICATION OF *CHLOROBIUM TEPIDUM* KDO8P SYNTHASE

2.1 Introduction

Chlorobium tepidum (*Cte*) is a thermophilic Gram-negative green sulfur bacterium which was originally isolated in New Zealand.[51] It generally grows in dense mats in the base of hot pools and grows best at temperatures between 45 ºC and 55 ºC and at a pH of 4.5 – 6. The genome has been completely sequenced and was found to have one circular DNA molecule with 2,154,946 base pairs[52], among which is the gene encoding KDO8P synthase (*kds*A).

Cte KDO8P synthase was chosen as a target to characterize for this project because of its reported close phylogenetic relationship with the type 1β DAH7P synthases.[13] *Cte* KDO8P synthase contains 280 amino-acids, has a calculated molecular mass of 30318 Da and has a theoretical isoelectric point (pI) of 6.97. There are no reports of the isolation or characterization of this protein in the current literature.

This chapter describes the expression, attempted two-step purification and partial characterisation of *Cte* KDO8P synthase.

2.2 Expression and solubility of *Cte* KDO8P synthase

2.2.1 Initial expression trials

Glycerol stocks of BL21(DE3)/pT7-7-*Cte* KDO8P were provided for this project by Dr Mark Patchett (Massey University, Palmerston North, New Zealand). The cloning methods did not incorporate any additional N or C terminal residues into *Cte* KDO8P synthase.

Cultures of BL21(DE3)/pT7-7-*Cte* KDO8P synthase (5 mL) were grown and expression was induced with IPTG as described in the general methods. SDS-PAGE analysis of the whole cell lysate showed an over-expressed protein of the predicted subunit molecular weight for *Cte* KDO8P synthase (MW ~31 kDa). Following cell lysis, a large proportion of this protein was seen in the insoluble fraction (figure 2.1, lanes 6, 9 and 12). To try to recover a higher proportion of soluble protein the growth conditions (temperature and time) and lysis conditions were varied and the results are discussed in the following sections of this chapter.

The soluble protein fraction underwent a standard activity assay monitoring the loss of PEP at 232 nm at 37 ºC as described in chapter 5. It was found that there was activity in the presence of both substrates (100 μM A5P and 200 μM PEP) and a divalent metal cofactor (100 μM Mn^{2+}) but no activity when either a substrate or the metal ion was missing. When more protein solution was added to the reaction mixture, the rate increased proportionally. The absence of activity before the addition of A5P suggests that the observed activity is due to KDO8P synthase. Mn^{2+} was used as the divalent metal cofactor in initial activity assays because this had been found to be the most activating metal in the characterization of metallo KDO8P synthases from *A. aeolicus* and *H. pylori*.[11, 26] No quantitative measurements of activity were made at this stage.

Parameters which may affect the solubility or expression levels of the protein include the concentration of IPTG used, the expression vector used (alternatives to pT7-7

include pET or pUC expression vectors), the media used for growth of the cells or the buffers used in cell lysis (Tris-HCl or acetate buffers instead of BTP). The protein could also have been co-expressed with the chaperone proteins GroEL and GroES which could assist with achieving the correct tertiary structure (protein fold) and may have helped produce a higher proportion of the correctly folded soluble protein.

2.2.2 Effect of DTT, PEP and KCl on solubility

Cultures of BL21(DE3)/pT7-7-*Cte* KDO8P synthase (5 mL) were grown, induced, harvested and lysed, as described in chapter five, using a range of different lysis buffers. The different lysis conditions trialed to try to maximize the proportion of soluble protein recovered were:

A: 10 mM BTP pH 8.5, 1 mM EDTA, 1 mM DTT

B: 10 mM BTP pH 8.5, 1 mM EDTA, 1 mM DTT, 200 μM PEP

C: 10 mM BTP pH 8.5, 1 mM EDTA, 1 mM DTT, 200 μM PEP, 200 mM KCl

Portions of the whole cell lysate, the soluble fraction and the insoluble fractions were run side-by-side on an SDS-PAGE gel. Comparisons between the intensity of the insoluble and soluble bands were made to determine which lysis buffer would be best suited (figure 2.1).

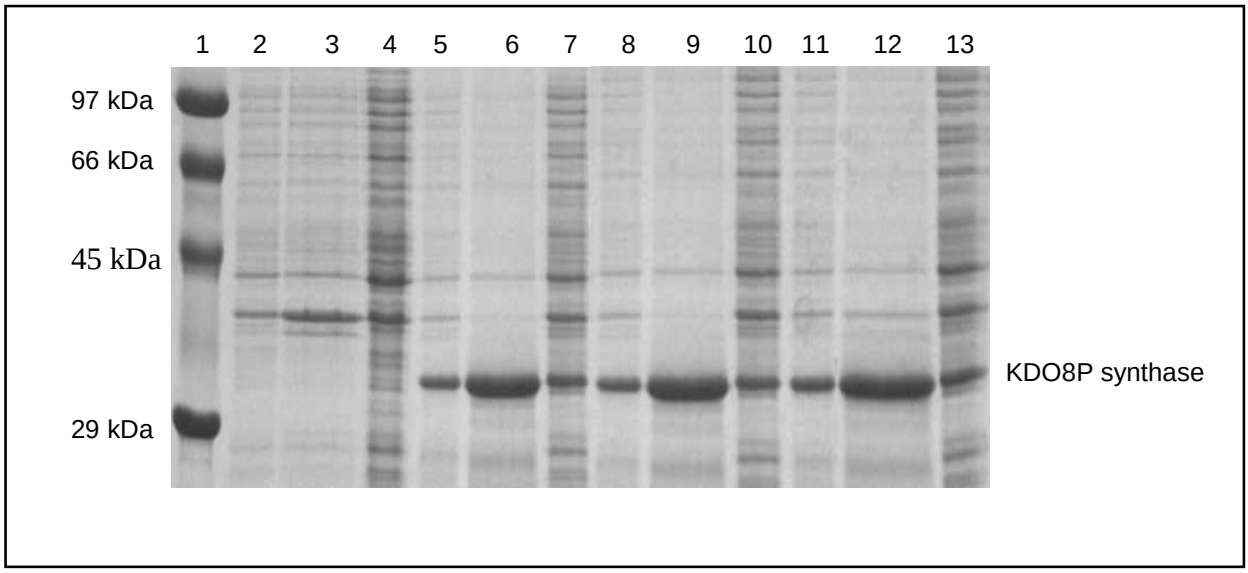

Figure 2.1 **Expression and solubility of *Cte* KDO8P synthase in varying lysis conditions.** Lanes 2 – 4: 2 μL Whole cell lysate (lane 2), 10 μL insoluble fraction resuspended in 400 μL 1:1 6 M urea / 20 % SDS (lane 3), 10 μL soluble fraction (lane 4) of growth *without* induction with IPTG (control); Lanes 5 – 7: Whole, insoluble and soluble fractions in lysis buffer A; Lanes 8 – 10: Whole, insoluble and soluble fractions in lysis buffer B; Lanes 11 – 13: Whole, insoluble and soluble fractions in lysis buffer C.

The lysis buffer that was chosen to use for subsequent *Cte* KDO8P synthase experiments was buffer B. Although the soluble portion of the protein appeared to be very similar under all three conditions, lysis in the presence of buffer C appeared to produce more of the insoluble KDO8P synthase than the other two. The reducing agent DTT was included in the lysis buffer because of its reported ability to protect protein, such as *Helicobacter pylori* DAH7P synthase, from losing activity during a multi-step purification.[53] The decision to use BTP buffer and keep EDTA and DTT present was based on other successful purifications of DAH7P synthases[53, 54] in the Parker laboratory at Massey University, where this project was carried out, although other reported KDO8P synthase purifications use different lysis buffers and do not include any of these additives.[21, 26, 55] It should be noted that partial solubility is not the only

cause of low activity in this protein (as discussed in section 2.4), but increasing the solubility may help produce a higher yield of active protein after purification.

2.2.3 Effect of Thesit™ and Complete™ protease inhibitor on solubility of *Cte* KDO8P synthase

To try to further improve the proportion of soluble protein expressed, the additives Thesit™ (polyethyleneglycol dodecyl ether) and EDTA-free Complete™ protease inhibitor (Roche) were added to the lysis buffer. SDS-PAGE analysis showed that neither additive improved the amount of soluble *Cte* KDO8P synthase expressed (figure 2.2). Although the lanes in figure 2.2 that contain soluble protein (lanes 2, 4, 6, 8) are over loaded, the relative intensity of the bands in the lanes that contain insoluble protein (lanes 3, 5, 7, 9) can be visually compared.

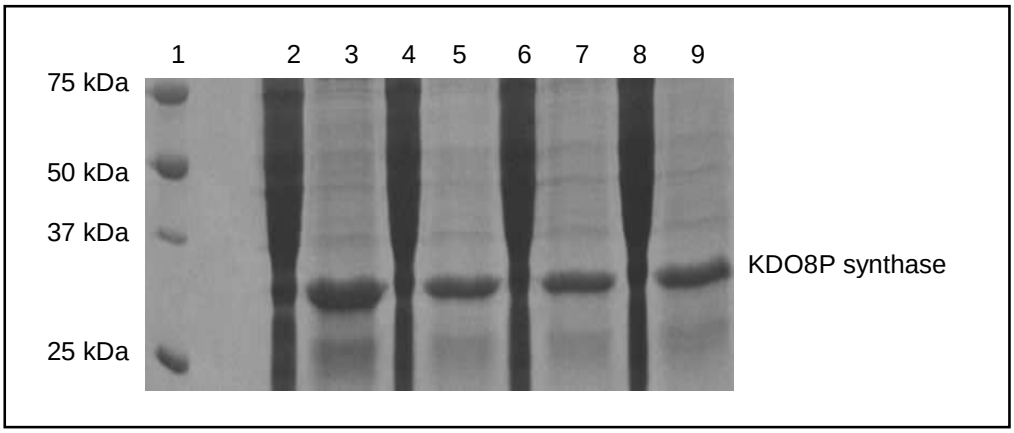

Figure 2.2 **Effect of Thesit™ and Complete™ protease inhibitor on solubility of *Cte* KDO8P synthase.** Lanes 2 – 3: Soluble (lane 2) and insoluble (lane 3) fractions. Cells lysed in buffer A (10 mM BTP pH 8.5, 1 mM EDTA, 1 mM DTT, 200 μM PEP) with 0.005 % (v/v) Thesit; Lanes 4 – 5: Soluble and insoluble fractions, Cells lysed in buffer A + 2 % (v/v) Complete protease inhibitor; Lanes 6 – 7: Soluble and insoluble fractions, Cells lysed in buffer A with no additive; Lanes 8 – 9: Soluble and insoluble fractions, Cells lysed in buffer A with 0.005 % (v/v) Thesit and Complete protease inhibitor.

There was no difference in activity when equivalent volumes of each soluble fraction underwent a standard assay. The lysis buffer used for all subsequent experiments with *Cte* KDO8P synthase was 10 mM BTP pH 8.5, 1 mM EDTA, 1 mM DTT, 200 μM PEP. The buffer used was at pH 8.5 because this pH is the same as the pH used in the buffers for purification by anion exchange chromatography (AEC) (see section 2.3).

2.2.4 Effect of temperature on expression and solubility

Three 5 mL cultures of BL21(DE3)/pT7-7-*Cte* KDO8P synthase were grown at 37 ºC as described above. After induction with IPTG, the respective cultures were incubated at 25 ºC, 30 ºC and 37 ºC for 4 hours. The cells were harvested, resuspended and lysed as described in the section 2.2.1. SDS-PAGE analysis of the whole cell lysate, soluble fraction, and insoluble fraction, revealed that growth at 37 ºC produced the highest proportion of soluble *Cte* KDO8P synthase compared to insoluble (figure 2.3).

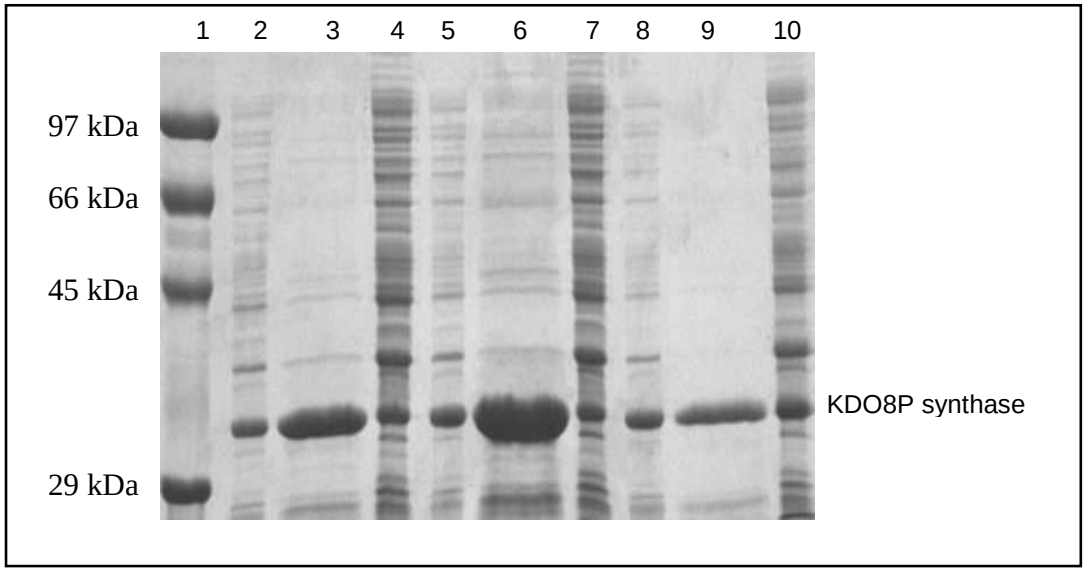

Figure 2.3 **Effect of growth temperature on expression and solubility of *Cte* KDO8P synthase.** Lanes 2 – 4: Whole cell lysate, insoluble fraction, soluble fraction, cells grown at 25 ºC after induction; Lanes 5 – 7: Whole cell lysate, insoluble fraction, soluble fraction, cells grown at 30 ºC after induction; Lanes 8 – 10: Whole cell lysate, insoluble fraction, soluble fraction, cells grown at 37 ºC after induction.

All subsequent cultures of BL21(DE3)/pT7-7-*Cte* KDO8P synthase were grown at 37 ºC before and after induction.

2.2.5 Effect of growth time on expression and solubility

Five 5 mL cultures of BL21(DE3)/pT7-7-*Cte* KDO8P synthase were grown at 37 ºC as described above. After induction with IPTG, the respective cultures were incubated at 37 ºC for 0, 3, 6, 12, and 20 hours. The cells were harvested, resuspended and lysed as described in the section 2.2.1. SDS-PAGE analysis of the whole cell lysate, soluble fractions, and insoluble fractions, revealed that growth for 3, 6, and 9 hours produced the best expression levels of soluble protein and growth for 0 and 20 hours produced the worst. The experiment was repeated, but with growth times of 4 and 8 hours after induction. SDS-PAGE analysis suggested that there was not a significant difference in the proportion of soluble to insoluble protein between the two conditions (figure 2.4).

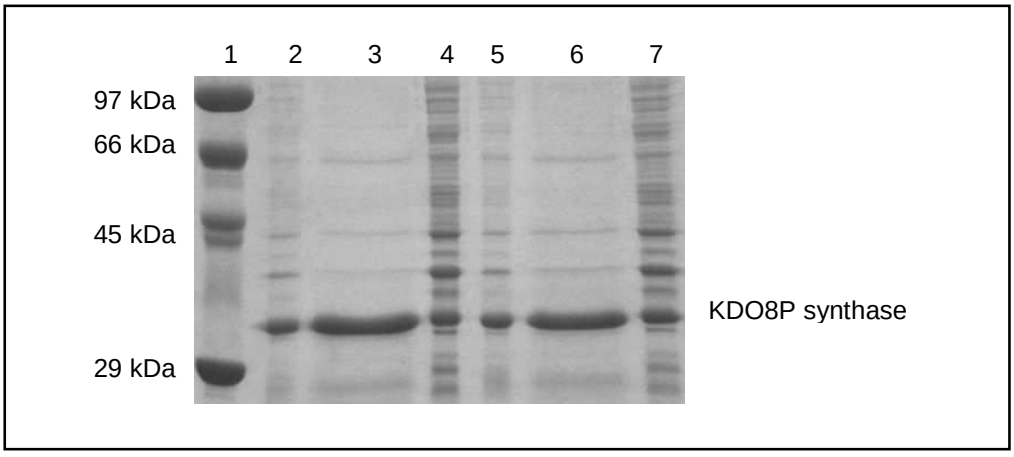

Figure 2.4 **Effect of growth time on expression and solubility of *Cte* KDO8P synthase.** Lanes 2 – 4: Whole cell lysate, insoluble fraction, soluble fraction, cell growth at 37 ºC for 4 hours after induction with IPTG; Lanes 5 – 7: Whole cell lysate, insoluble fraction, soluble fraction, cell growth at 37 ºC for 8 hours after induction.

All subsequent cultures of BL21(DE3)/pT7-7-*Cte* KDO8P synthase were grown for 4 – 5 hours after induction. This growth time is a compromise between finding the best conditions for expression and solubility, and fitting the experiments into an 8-hour working day.

2.3 Attempted two-step purification of *Cte* KDO8P synthase

2.3.1 Purification by anion exchange chromatography (AEC)

Cultures of BL21(DE3)/pT7-7-*Cte* KDO8P synthase were grown, induced, harvested and lysed as described in chapter 5. The soluble fraction of the protein was diluted with buffer A (10 mM BTP pH 8.5, 1 mM EDTA, 1 mM DTT) and loaded onto a SOURCE™ 15Q column (Amersham). Bound protein was eluted with a 90 mL linear gradient between buffer A and buffer A + 0.2 M NaCl, as described in chapter 5.

The fractions of eluent (3 mL) were collected and those that corresponded to a peak in the UV (218 and 280 nm) trace were analyzed by SDS-PAGE to see if they contained KDO8P synthase (figure 2.5). The fractions that were identified as containing a protein of the size corresponding to that of *Cte* KDO8P synthase (~31 kDa) were assayed for activity using the standard assay described in chapter 5.

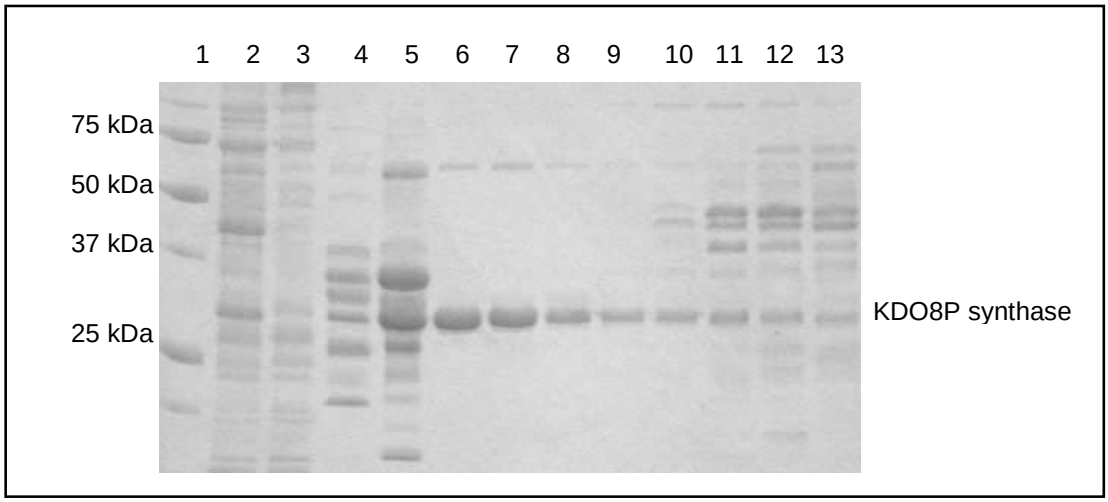

Figure 2.5 **SDS-PAGE analysis of soluble *Cte* KDO8P synthase after anion exchange chromatography.** Lane 2: 2 μL crude cell lysate (soluble fraction, before loading to column); Lane 3: 10 μL Flow through from SOURCE™ 15Q column while loading protein; Lanes 4 – 13: 10 μL of fractions as they were eluted from the column.

2.3.2 Purification by cation exchange chromatography (CEC)

The fractions that contained *Cte* KDO8P synthase of reasonable purity (figure 2.5, lanes 6 - 9) were pooled and buffer and the buffer was changed to pH 6.0 in preparation for cation exchange chromatography. It should be noted that the pooled fractions were chosen for purity rather than total protein recovery. A pH of 6.0 was chosen for cation exchange chromatography to ensure that the surface amino-acids of the *Cte* KDO8P synthase (pI = 6.97) would have an overall positive charge and so adsorb to the column. The protein solution was filtered and immediately loaded onto a SOURCE™ 15S column (Amersham). The bound protein was eluted with a 90 mL linear gradient between buffer B and buffer B + 0.2 M NaCl, as described in chapter 5. Fractions of eluent were collected and fractions that corresponded to a peak on the UV trace were analyzed by SDS-PAGE to see if they contained KDO8P synthase (figure 2.6). Fractions that were identified as containing a protein of the size corresponding to that of *Cte* KDO8P synthase were assayed for activity using the standard assay described in chapter 5.

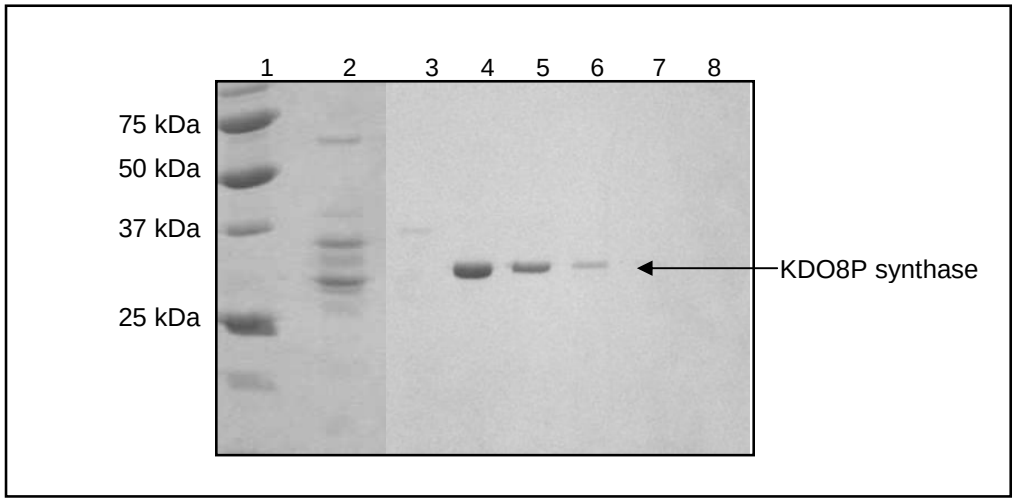

Figure 2.6 **SDS-PAGE analysis of *Cte* KDO8P synthase after cation exchange chromatography.** Lane 2: 5 μL pooled anion exchange fractions (before loading to column); Lane 3: 10 μL Flow through from SOURCE™ 15S column while loading protein; Lanes 4 – 8: 10 μL of fractions as they were eluted from the column.

Activity assays showed that there was more KDO8P synthase activity in the pooled AEC fractions (0.41 U mg^{-1}) than in the crude soluble fraction before AEC (0.27 U mg^{-1}), but very little activity was detected in fractions after CEC (0.22 U mg^{-1}) (see table 2.1). The small amount of KDO8P synthase detected by SDS-PAGE after CEC compared to the amount recovered after AEC suggests that the protein may be precipitating out of solution either during the buffer exchange or while the being loaded onto the SOURCE™ 15S column.

2.3.3 Purification by hydrophobic interaction chromatography (HIC)

HIC was performed after anion exchange as an alternative to cation exchange. Performing this step eliminated the buffer exchange step performed between AEC and CEC as there is no need to eliminate salt or change the pH of the buffer before loading onto the column. AEC was carried out exactly as described above, fractions containing KDO8P synthase were pooled and $(NH_4)_2SO_4$ was added to a final concentration of 1

M. HIC was carried out using a SOURCE™ 15Phe column (Amersham). Bound protein was eluted with a 100 mL linear gradient between 100 % buffer C (10 mM BTP pH 8.5, 1 mM EDTA, 1 mM DTT, 1 M $(NH_4)_2SO_4$) and 100 % buffer A as described in chapter 5. The fractions were analyzed for KDO8P synthase by SDS-PAGE (figure 2.7) and standard activity assays.

KDO8P synthase activity was detected in the protein solution before being loaded onto the SOURCE™ 15Phe column (0.4 U mg^{-1}) but very little activity was detected in the fractions as they came off the column (0.07 U mg^{-1}) (table 2.1). This suggests that the problem with stability may not only be during buffer exchange before CEC. The protein may not be robust enough to be subjected to 2 columns in a row or may not be stable in the presence of a high salt concentration. SDS-PAGE analysis (figure 2.7) suggests that there is less *Cte* KDO8P synthase present in solution after HIC than there was after AEC, again suggesting that protein may be precipitating out of solution after AEC or while being loaded onto the next column. Tests of the stability of *Cte* KDO8P synthase at each stage of the attempted purification are discussed in the following section.

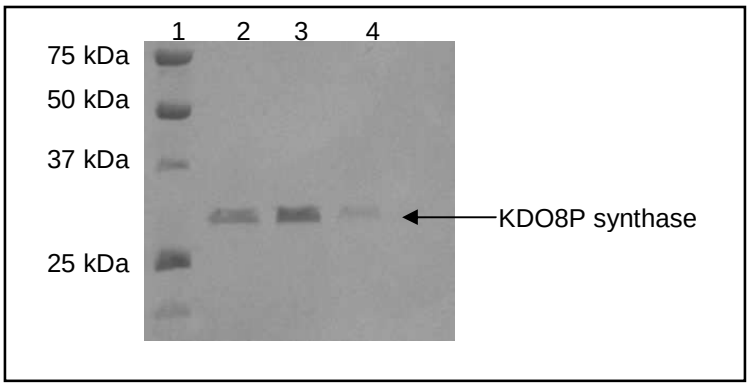

Figure 2.7 **SDS-PAGE analysis of *Cte* KDO8P synthase after hydrophobic interaction chromatography.** Lane 1: 5 μL Precision Plus protein standards (Bio-Rad); Lanes 2 – 4: 10 μL of fractions as they were eluted from the column.

Purification Step	Total protein (mg)	Total enzyme activity (Units)[b]	Specific activity (Units mg^{-1})	% Yield	Relative purity
1. Crude lysate	**100**	**27**	**0.27**	**100**	**1.0**
2. Anion exchange	**8.1**	**3.3**	**0.41**	**12**	**1.5**
3a. Cation exchange	**3.0**	**0.65**	**0.22**	**2.4**	**0.81**
3b. Hydrophobic interaction	**4.0**	**0.28**	**0.07**	**1.0**	**0.26**

Table 2.1 **Summary of attempted purification of *Cte* KDO8P synthase**[a]

[a] Purification of 250 mL culture of BL21(DE3)/pT7-7-*Cte* KDO8P synthase

[b] Determined by following the loss of PEP at 232 nm at 37 ºC.

2.4 Stability of *Cte* KDO8P synthase

The purification by the methods described above (section 2.3) was found to be unsuccessful as there was a loss in specific activity between AEC and the following step(s). In order to determine when and why the enzyme was losing activity, tests of stability were performed on the crude lysate (10 mg mL^{-1}, 0.27 U mg^{-1} activity) and on the pooled fractions after AEC but before buffer exchange (2.7 mg mL^{-1}, 0.42 U mg^{-1} activity).

When left at 4 ºC for 12 hours in the presence of 200 μM PEP, there was no change in activity in either the crude lysate or the fractions directly after AEC. The CEC or HIC steps took place within 2 hours of AEC in the examples reported in section 2.3 so no enzymic activity should have been lost during this time.

To test the effect the buffer exchange step has on the protein after AEC, 1 mL aliquots of each sample (crude lysate and pooled AEC fractions) were added to 3 mL of buffer

(10 mM BTP, 1 mM EDTA, 1 mM DTT) at pH 6.0, 7.5 and 8.5 and resultant solutions were concentrated down to ~300 μL using an Amicon Ultra 4 mL concentrator (Millipore) by centrifugation at 4500 rpm for 15 minutes. The recovery of the protein was the same at each pH and there was similar activity in all of the samples at this point. After 4 hours at 4 ºC there was no detectable activity in any of the samples. Because there is no loss of protein or enzymic activity immediately after concentration and buffer exchange, this suggests that the concentration process may be destabilizing the protein and it loses its native fold or falls out of solution in the following hours. The CEC and HIC steps both take around 3 hours to complete and this appears to be too long for the unstable protein to retain activity in dilute solution, regardless of the buffer conditions.

It should be noted that initially Vivaspin concentrators (polyethersulfone membranes, VivaScience) were used and there was a large amount of protein lost during the process so very little protein was able to be loaded onto the SOURCE™ 15S column. The purification reported in this chapter used Amicon Ultra (Ultracel regenerated cellulose membranes, Millipore) concentrators in the buffer exchange and concentration steps. These concentrators provided much better protein recovery based on SDS-PAGE analysis.

The small amount of detectable activity present after cation exchange chromatography was also lost after 4 hours at 4 ºC. This made it too difficult and too inaccurate to perform any characterization using fractions coming off the SOURCE™ 15S column. Only the crude lysate and SOURCE™ 15Q fractions were stable enough to perform any characterization on, but it appeared that the protein was very vulnerable at this point and could not sustain being subjected to any further treatment (concentration or passing through another column).

2.5 Metal-dependency of *Cte* KDO8P synthase

The effect of different metals on enzyme activity was tested immediately after anion exchange chromatography using the fraction that contained the highest amount of KDO8P synthase (lane 6, figure 2.5) as this was the stage when the highest specific activity was measured. The protein was not concentrated or washed in a salt-free buffer due to lack of stability when undergoing these processes.

Cte KDO8P synthase was found to be dependent on a divalent metal ion for activity as there was no activity at all without the addition of metal in the standard activity assay. Furthermore, when EDTA was included to a final concentration of 10 mM in the standard assay reaction mixture (including both substrates and 100 μM $MnSO_4$), no activity was detected (figure 2.8, table 2.2). The assay buffer consisted of 50 mM BTP pH 7.5 with 10 μM EDTA and was pre-treated with Chelex100 resin to minimize the presence of metal ions from other sources.

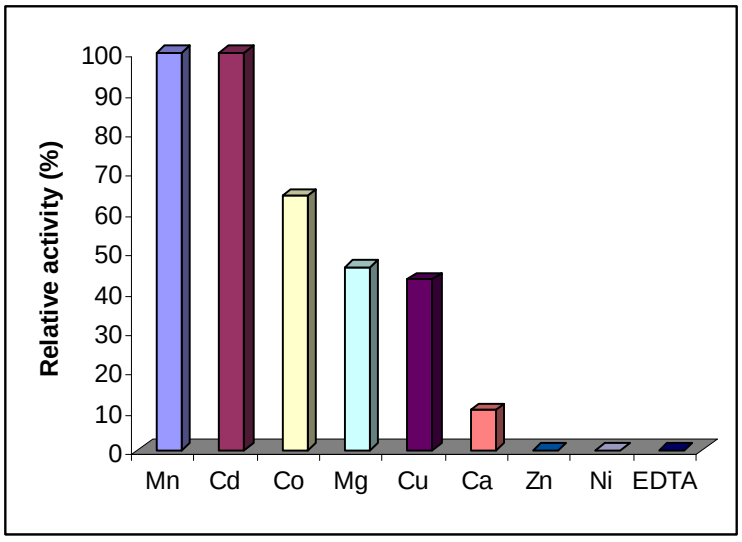

Figure 2.8 **Effect of divalent metal ions on *Cte* KDO8P synthase activity.**

Divalent Metal ion	Relative activity (%)
Mn^{2+}	100
Cd^{2+}	100
Co^{2+}	64
Mg^{2+}	46
Cu^{2+}	43
Ca^{2+}	10
Zn^{2+}	<1
Ni^{2+}	<1
EDTA	0

Table 2.2 **Relative activity of *Cte* KDO8P synthase in the presence of divalent metal ions or EDTA.** Activity was determined by following the absorbance change at 232 nm due to the consumption of PEP. Reaction mixtures consisted of 100 μM A5P, 200 μM PEP, 110 μM metal ion and 10 μL of anion exchange purified *Cte* KDO8P synthase (8 mg mL^{-1}) in BTP buffer (pH 7.4) with 10 μM EDTA in a total volume of 1 mL. Reactions were initiated by the addition of A5P.

The metal ions that were found to activate *Cte* KDO8P synthase the most were Mn^{2+}, Cd^{2+} and Co^{2+} but activity was also detected in the presence of Cu^{2+}, Mg^{2+} and Ca^{2+} ions. Assays were carried out using 10 μL of the protein solution in order to produce measurable and comparable rates.

2.6 Cloning and expression of C24N *Cte* KDO8P synthase and D246A *Cte* KDO8P synthase

The C24N mutation to *Cte* KDO8P synthase was chosen because this Cys residue has been found to be conserved throughout all known metallo KDO8P synthases and some non-metallo activity has been reported when it has been replaced by Asn in *A. aeolicus* KDO8P synthase.[22] The Asp233 (corresponding to Asp246 in *Cte* KDO8P synthase) residue has also been shown to be a metal-binding residue in *A. aeolicus* KDO8P

synthase.[20] The D246A mutation to *Cte* KDO8P synthase was chosen to determine if this residue is absolutely required for metal-binding and for catalytic activity.

The C24N and D246A mutations were performed using a QuikChange® II Site-Directed Mutagenesis Kit (Stratagene) using pT7-7-*Cte* KDO8P synthase as the double-stranded DNA template. The mutations were introduced using synthetic oligonucleotide primers (as described in chapter 5) and the resulting plasmids were transformed into competent BL21(DE3) cells. Cells were grown, induced and harvested using conditions identical to those used for the wild type protein.

Expression levels of soluble KDO8P synthase in these conditions were similar for both mutations and at similar levels to the wild type *Cte* KDO8P synthase (figure 2.9).

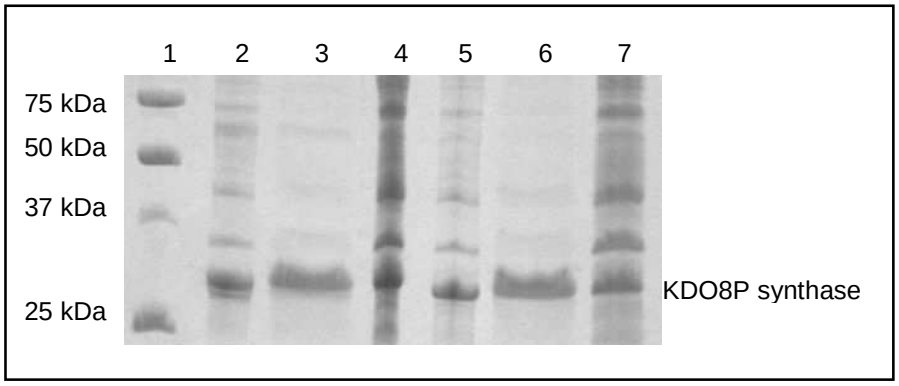

Figure 2.9 **Expression and solubility of C24N and D246A *Cte* KDO8P synthase**. Lanes 2–4: C24N *Cte* KDO8P synthase whole cell lysate, insoluble fraction, soluble fraction; Lanes 5–7: D246A *Cte* KDO8P synthase whole cell lysate, insoluble fraction, soluble fraction.

The soluble fractions were tested for activity using a standard assay and no activity was detected in the presence or absence of metal (Mn^{2+}, Cd^{2+}) for either sample. No purification or further testing was performed on these proteins.

2.7 Discussion

Purification of *Cte* KDO8P synthase by anion exchange chromatography was successful and increased purity of the enzyme by 1.5 fold (based on specific activity). The protein was then stable on ice or at 4 ºC for at least 12 hours and this sample was used for partial characterization. It lost activity when subjected to either concentration or another chromatography column. The well characterized metallo KDO8P synthases from hyperthermophiles *A. aeolicus* and *A. pyrophilus* were both purified by heat treatment followed by one chromatography step (anion exchange) so were not subjected to an intermediate concentration step or a second column.[21, 30] *Cte* KDO8P synthase would have to be as thermostable as the KDO8P synthase from the two *Aquifex* organisms to be able to be purified by this method. The thermostability of *Cte* KDO8P synthase was not examined during this project. KDO8P synthase from *H. pylori* was purified by anion exchange followed by hydrophobic exchange chromatography.[26, 55] This method proved to be unsuccessful for purification of *Cte* KDO8P synthase.

The primary amino-acid sequence of *Cte* KDO8P synthase shows that this enzyme has the four residues that have been shown to be responsible for metal-binding and are conserved throughout the metallo KDO8P synthases. The purification and characterization presented in this chapter is incomplete but it has shown that *Cte* KDO8P synthase is sensitive to the presence of EDTA and is activated by the addition of Mn^{2+} or Cd^{2+} suggesting that it is in fact a metallo enzyme as predicted by the primary sequence. This result is consistent with other more well characterized metallo KDO8P synthases with respect to the metal ions by which they are most activated. KDO8P synthase from the organism *A. aeolicus* has also shown greatest activation in the presence of Mn^{2+} or Cd^{2+} ions.[11] *A. pyrophilus* KDO8P synthase shows highest activity in the presence of Cd^{2+} or Mn^{2+} ions[21] and *H. pylori*J99 is most activated by Cd^{2+} ions.[26] *A. ferrooxidans* KDO8P synthase shows greatest activity in the presence of Mn^{2+}, Co^{2+} and Cd^{2+} (discussed in detail in chapter three of this thesis). This comparison shows that all characterized metallo KDO8P synthases to date are activated

by Mn^{2+} or Cd^{2+}. KDO8P synthase from *C. psittaci* has also been partially characterized and also shows activation by Mn^{2+} ions.[19]

Further characterization of *Cte* KDO8P synthase was not carried out in this study due to the instability of the enzyme after purification. It is unclear whether the protein was denaturing due to the buffers, chromatography or concentration processes used, or was remaining in solution but losing activity over the time period taken for purification using the described methods. What is clear is that the expression of soluble *Cte* KDO8P synthase was very poor as SDS-PAGE analysis of the crude lysate of BL21(DE3)/pT7-7-*Cte* KDO8P synthase showed a higher portion of the protein in the insoluble fraction than in the soluble fraction. This suggests that *Cte* KDO8P synthase is not very stable when expressed using this system in *E. coli*. Co-expression of *Cte* KDO8P synthase with the *E. coli* chaperone proteins GroEL and GroES may reduce misfolding and assist in achieving expression of more soluble protein, but it is not certain whether this would give rise to a more stable *Cte* KDO8P synthase. Alternate expression vectors such as pET or pGEM, or to use expression cells such as Origami B systems may need to be tried to produce a more stable *Cte* KDO8P synthase. Careful analysis of the conditions including temperature, buffer additives and buffer concentrations needs to be carried out to determine which factors are important for *Cte* KDO8P synthase stability. This was not carried out as part of this project due to the successful cloning, expression and solubilization of KDO8P synthase from *A. ferrooxidans* (*Afe*) which was carried out in parallel to the *Cte* KDO8P synthase work. Further characterization of *Afe* KDO8P synthase is presented in the following two chapters of this thesis.

CHAPTER 3

CLONING, EXPRESSION, PURIFICATION AND CHARACTERIZATION OF *ACIDITHIOBACILLUS FERROOXIDANS* KDO8P SYNTHASE

3.1 Introduction

Acidithiobacillus ferrooxidans (Afe), formerly *Thiobacillus ferrooxidans,* is a chemolithoautotrophic Gram-negative bacterium.[56] It uses energy and electrons from ferrous iron, sulfur and various reduced sulfur compounds by using oxygen as the electron acceptor.[57] The organism is found in places where iron and sulfur are abundant such as mines and coal deposits. It grows best at temperatures between 30 ºC and 35 ºC and at a pH between pH 1.3 and pH 4.5.[58]

The KDO8P synthase gene from *Afe* (ATCC 23270) is 846 nucleotides long and the encoded protein product is 281 amino-acids in length with a calculated molecular weight of 30603.96 Da and a theoretical pI of 5.54. The protein was chosen for this project because: a) *Afe* KDO8P synthase is grouped among the metallo KDO8P synthases based on amino-acid sequence but it had not been isolated or characterized previously; b) *Afe* KDO8P synthase has the AspGlyPro243 motif which is conserved among the non-metallo KDO8P synthases but is only sometimes present among the metallo.[13]

This chapter presents the cloning of the KDO8P synthase gene from the genomic DNA of *Afe* (ATCC 23270), the expression and solubility, the two-step purification used to isolate *Afe* KDO8P synthase and the subsequent biochemical characterization. The results are discussed alongside, and compared to, other well characterized metallo KDO8P synthases.

3.2 Cloning of the *Afe* KDO8P synthase open reading frame

Synthetic oligonucleotide primers were used to amplify the *Afe* KDO8P synthase open reading frame (ORF) from the genomic DNA of *Afe* (ATCC 23270) as described in detail in chapter 5. The resulting PCR product of the correct size was identified on an agarose gel (figure 3.1) and gel purified.

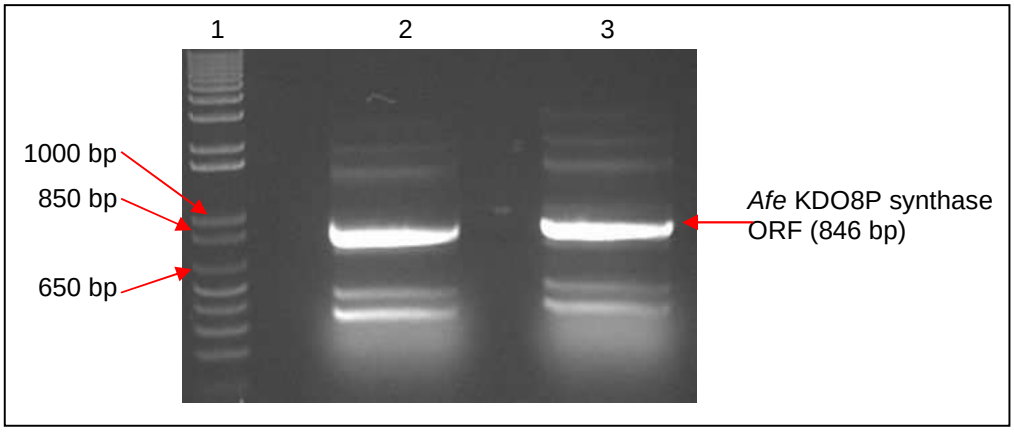

Figure 3.1 **Agarose gel electrophoresis of amplified *Afe* KDO8P synthase gene**

Lane 1: 5 μL DNA ladder (Invitrogen); Lanes 2 and 3: Duplicate 50 μL PCR reactions containing ~1 μg genomic DNA, 15 pmol of each primer, 250 μM of each of the dNTPs, 1x polymerase buffer + $MgSO_4$ and 2 units of *Pwo* DNA polymerase. The brightest band (indicated with a red arrow) was cut from the gel and purified.

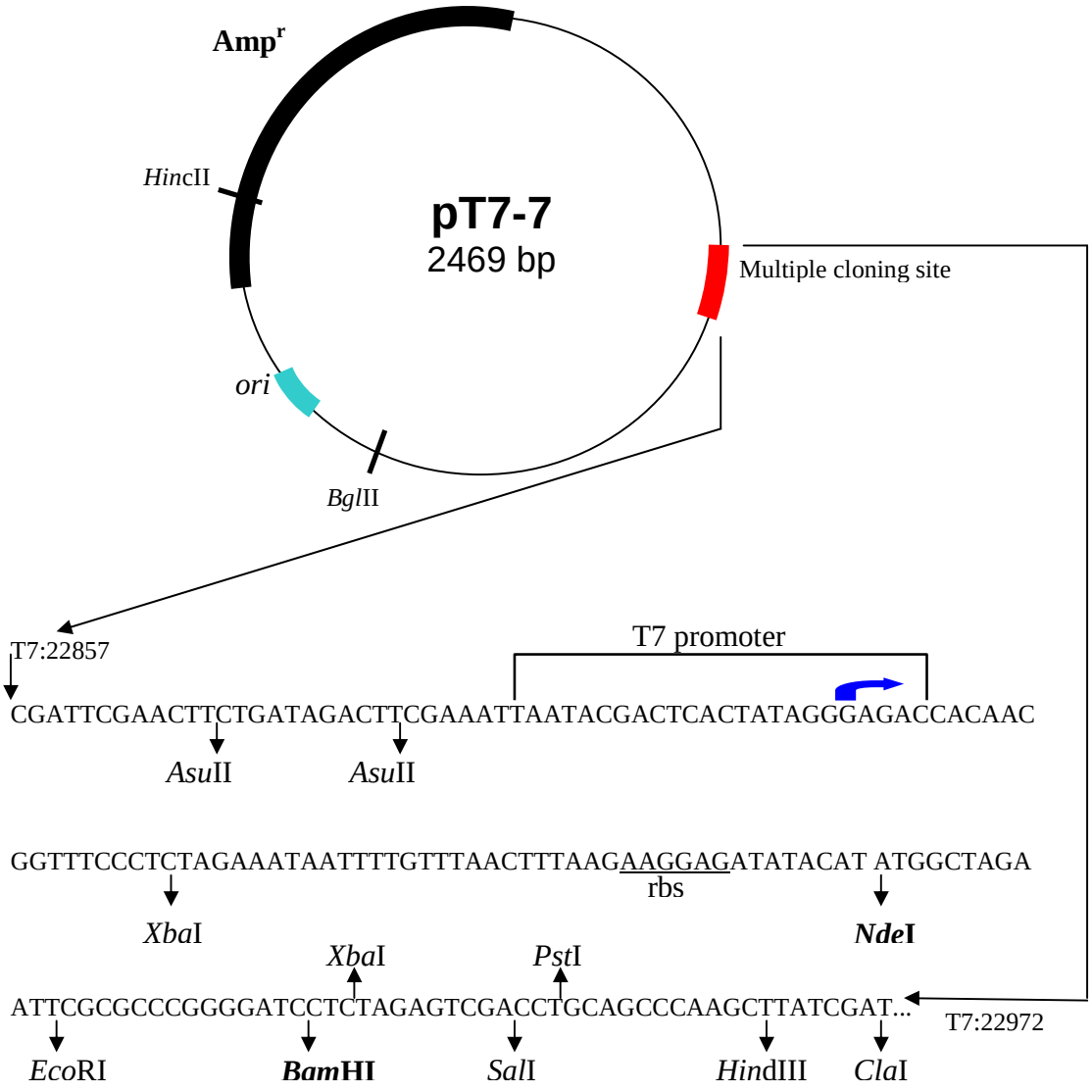

Figure 3.2 **Map of pT7-7 vector.** A schematic diagram of pT7-7 showing the various restriction endonuclease cleavage sites (short arrows) including *Nde*I and *Bam*HI, the ribosome binding site (rbs), T7 promoter region, ampicillin resistance gene (Amp^r) and origin of replication site (*ori*).

The resulting PCR product (*Afe* KDO8P synthase gene) was digested with *Nde*I and *Bam*HI and ligated into *Nde*I / *Bam*HI digested pT7-7 (see figure 3.2) to form the construct pT7-7-*Afe* KDO8P synthase. The pT7-7-*Afe* KDO8P synthase was used to transform *E. coli* XL1-Blue cells. The cloning process was found to be successful by obtaining the DNA sequence of plasmid prepared from these cells, and the plasmid was used to transform *E. coli* BL21(DE3) cells (for further details refer to chapter 5).

3.3 Expression and solubility of *Afe* KDO8P synthase

BL21(DE3)/pT7-7-*Afe* KDO8P synthase cultures were grown and expression was induced with IPTG as described in the general methods. SDS-PAGE analysis of the whole cell lysate showed an over-expressed protein of the predicted subunit molecular weight for *Afe* KDO8P synthase (MW ~31 kDa) (figure 3.3, lanes 2, 5, 8 and 11). Following centrifugation a large proportion of the protein was present in the soluble fraction (figure 3.3, lanes 4, 7, 10 and 13). Several different lysis buffers were used to identify any changes in solubility due to a given additive.

The lysis conditions used were:

A 10 mM BTP pH 7.0, 1 mM EDTA

B 10 mM BTP pH 7.0, 1 mM EDTA, 1 mM DTT

C 10 mM BTP pH 7.0, 1 mM EDTA, 1 mM DTT, 200 μM PEP

D 10 mM BTP pH 7.0, 1 mM EDTA, 1 mM DTT, 200 μM PEP, 0.2 M KCl

The soluble fractions were all tested for activity using a standard assay at 37 ºC with Mn^{2+} as the metal cofactor (refer to chapter 4, section 4.2 for discussion of activating metal ions for *Afe* KDO8P synthase). All fractions had KDO8P synthase activity and the fractions in lysis buffers C and D were shown to be the most active. Lysis was performed at pH 7.0 as this is more than 1 pH unit above the theoretical isoelectric point

(pI) of *Afe* KDO8P synthase (5.56). At this pH the protein would be expected to have an overall negative charge and therefore be in a form suitable for purification by anion exchange chromatography (AEC). Lysis buffer D was used for all subsequent experiments with *Afe* KDO8P synthase.

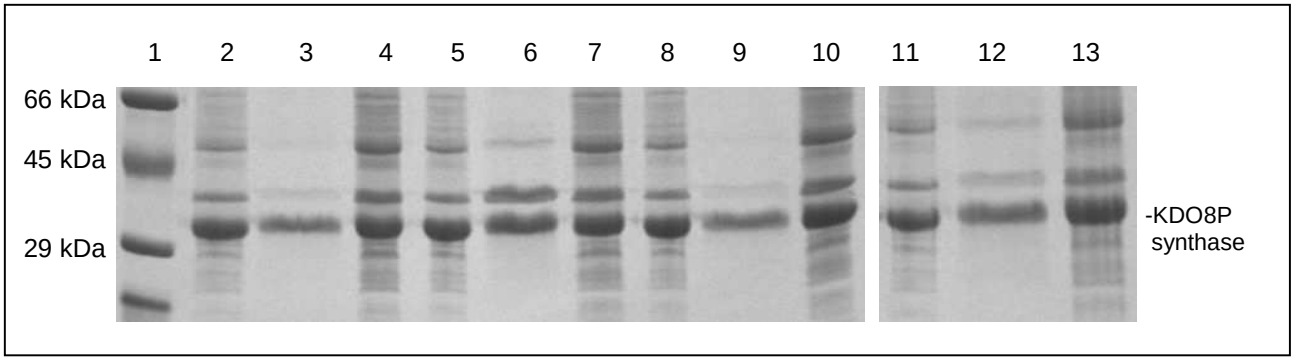

Figure 3.3 **Expression and solubility of *Afe* KDO8P synthase in varying lysis conditions.** Lanes 2 – 4: 2 μL Whole cell lysate (lane 2), 10 μL insoluble fraction resuspended in 400 μL 1:1 6 M urea / 20 % SDS (lane 3), 10 μL soluble fraction (lane 4) in lysis buffer A; Lanes 5 – 7: Whole, insoluble and soluble fractions in lysis buffer B; Lanes 8 – 10: Whole, insoluble and soluble fractions in lysis buffer C; Lanes 11 – 13: Whole, insoluble and soluble fractions in lysis buffer D.

3.4 Two-step purification of *Afe* KDO8P synthase

3.4.1 Purification by anion exchange chromatography (AEC)

A culture of BL21(DE3)/pT7-7-*Afe* KDO8P synthase was grown. Cells were harvested by centrifugation 5 hours after induction with IPTG and stored at -80 ºC overnight. The frozen cell pellet was thawed and resuspended in lysis buffer (as described above) and lysed by French Press followed by sonication. After cell debris were removed by centrifugation, the soluble protein was diluted with buffer A (10 mM BTP pH 7.0, 1 mM EDTA, 1 mM DTT) and loaded onto a SOURCE™ 15Q column (see chapter 5 for

details). Bound protein was eluted from the column with a 90 mL linear gradient between buffer A and buffer A + 0.2 M NaCl.

Fractions of eluent were collected and fractions that corresponded to a peak in the UV trace were analyzed by SDS-PAGE to see if they contained KDO8P synthase (figure 3.3). The fractions that were identified as containing a protein of the size corresponding to that of *Afe* KDO8P synthase (~31 kDa) were assayed for activity using a standard assay as described in chapter 5.

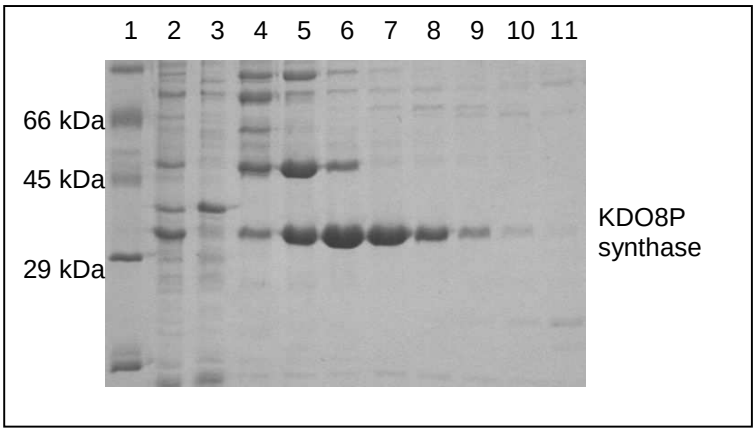

Figure 3.4 **SDS-PAGE analysis of *Afe* KDO8P synthase after anion exchange chromatography.** Lane 2: 2 μL crude cell lysate (soluble fraction before loading to column); Lane 3: 10 μL Flow through from SOURCE™ 15Q column while loading protein; Lanes 4 – 11: 10 μL of fractions collected as they were eluted from the column.

AEC proved to be an effective method for partially purifying *Afe* KDO8P synthase. A major protein contaminant of ~37 kDa is present in the flow through (figure 3.3, lane 3) indicating that it has not adsorbed to the column. Other major contaminants (~50 kDa and ~90 kDa) still remain in some fractions (figure 3.4, lanes 4 – 6) but the *Afe* KDO8P synthase is more pure (purification factor = 2.05 fold) and the recovery of the protein

off the column (45% yield, see table 3.1) is higher than when the same technique was used for purification of *Cte* KDO8P synthase (12% yield).

3.4.2 Purification by hydrophobic interaction chromatography

The fractions corresponding to lanes 5 – 10 of figure 3.3 were pooled and $(NH_4)_2SO_4$ was added to a final concentration of 1 M. HIC was carried out using a SOURCE™ 15Phe column as described in chapter 5. Bound protein was eluted from the column with a 100 mL linear gradient between 100 % buffer C and 100% buffer A. It should be noted that the fractions pooled after AEC were chosen for purity rather than for total KDO8P synthase recovery, thus some protein was lost in this step.

The chromatogram was dominated by a strong peak eluting from the column when the buffer contained ~0.2 M $(NH_4)_2SO_4$ suggesting the presence of a relatively pure protein in the corresponding fractions of eluent. SDS-PAGE analysis of the fractions as they came off the column shows that *Afe* KDO8P synthase is present in a much higher amount than any other protein present (figures 3.4 and 3.5). The fractions were pooled and concentrated to 10 mg mL^{-1} and tested for activity using a standard assay at 37 ºC with Mn^{2+} as the metal cofactor (refer to section 3.8 for discussion of activating metal ions for *Afe* KDO8P synthase).

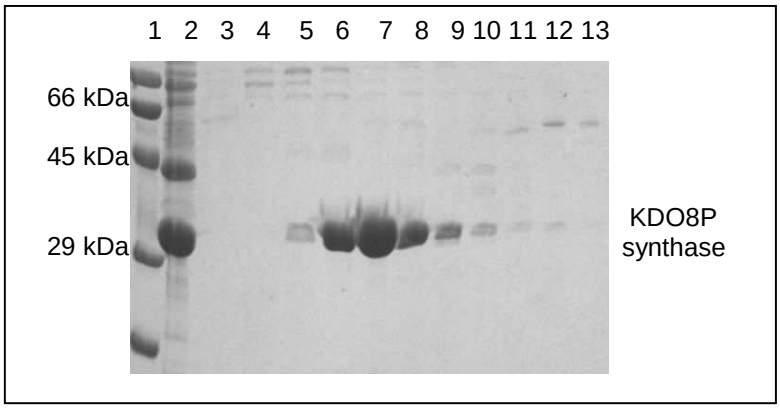

Figure 3.5 **SDS-PAGE analysis of *Afe* KDO8P synthase after hydrophobic interaction chromatography.** Lane 2: 10 μL pooled AEC fractions (before addition of

$(NH_4)_2SO_4$ and loading to SOURCE™ 15Phe column); Lane 3: 10 μL Flow through from SOURCE™ 15Phe column while protein was being loaded; Lanes 4 -13: 10 μL of fractions collected as they were eluted from the column. Fractions corresponding to lanes 6 – 10 were pooled and concentrated for characterization.

3.5 Purification Summary

After purification by AEC and HIC the specific activity of *Afe* KDO8P synthase had increased almost 10 fold over the specific activity of the crude lysate (Table 3.1), which indicates a successful purification even though there are traces of contaminating protein still present (figure 3.6, lane 5).

The purification of *Afe* KDO8P synthase by these methods is consistent with the purification of other metallo KDO8P synthases. KDO8P synthase from *A. aeolicus* and *A. pyrophilus* were both purified using a two-step procedure involving heat treatment followed by anion exchange chromatography which gave 4.3 fold and 8 fold overall purification respectively.[21, 30] The percentage yield of *Afe* KDO8P synthase (17%) is lower than that achieved for the *A. aeolicus* (47%) and *A. pyrophilus* (35%) proteins. This could be due to the loss of *Afe* KDO8P synthase between AEC and HIC as the AEC fractions were chosen according to purity and some fractions containing significant levels of KDO8P synthase, but with major contamination from other proteins, were discarded. This is justified by the end result of achieving a 10-fold more pure protein which is soluble and stable.

The protein was further purified by size-exclusion chromatography (SEC), but only for crystallization trials as discussed in the following chapter and not for characterization and kinetic studies. The specific activity after the two-step purification was deemed sufficiently high, such that subjecting the protein to another column just to eliminate very minor contaminants was not considered beneficial at this stage.

The *Afe* KDO8P synthase was flash frozen in liquid nitrogen and stored at -80 ºC in 100 μL aliquots. These samples were used in the characterization and kinetic studies described later in this chapter.

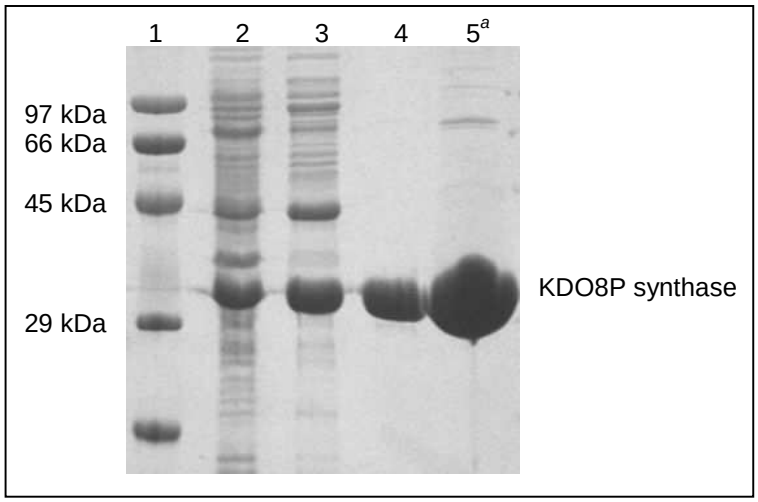

Figure 3.6 **SDS-PAGE summary of two-step purification of *Afe* KDO8P synthase.**
(2) 2 μL crude lysate; (3) 10 μL pooled AEC fractions; (4) 5 μL pooled HIC fractions; (5) 1 μL pooled HIC fractions concentrated to ~10 mg mL^{-1}. Lane 5 highlights the fact that there are minor contaminants of high molecular mass still present after purification by HIC.
[a]Lane 5 of the gel has been overloaded to emphasize the trace contaminants in the protein sample.

Purification Step	Total protein (mg)	Total enzyme activity (Units)[b]	Specific activity (Units mg^{-1})	% Yield	Relative purity
1. Crude lysate	**230**	**79**	**0.34**	**100**	**1.0**
2. Anion exchange	**50**	**35**	**0.7**	**45**	**2.1**
3. Hydrophobic interaction	**4.0**	**14**	**3.4**	**17**	**9.9**

Table 3.1 **Summary of two-step purification of *Afe* KDO8P synthase**[a]

[a] Purification of 250 mL culture of BL21(DE3)/pT7-7 *Afe* KDO8P synthase

[b] Determined by following the loss of PEP at 232 nm at 37 ºC.

3.6 Characterization of wild-type *Afe* KDO8P synthase

Pure samples of *Afe* KDO8P synthase as prepared by the methods discussed above (concentrated to 10 mg mL^{-1} and stored at -80 ºC) were used for the biochemical characterization presented in the following sections of this chapter. Discussed in the following sections is determination of the quaternary structure, metal-dependency, pH and temperature effects, kinetic characterization and preliminary crystallization trials of *Afe* KDO8P synthase. These results are discussed alongside (and compared to) results for other more well characterized KDO8P synthases.

3.7 Quaternary structure of *Afe* KDO8P synthase in solution

To determine the quaternary structure of *Afe* KDO8P synthase in solution SEC was used with protein standards of a known molecular mass. The mass of *Afe* KDO8P synthase was estimated off a standard curve of log of the molecular mass of protein standards against elution time from the Superdex200 column (Amersham). The

calculated monomeric molecular mass of *Afe* KDO8P synthase is 30604 kDa. The molecular mass of *Afe* KDO8P synthase determined by this method was found to be approximately 123 kDa which is consistent with it being tetrameric in solution (figure 3.7). This is the expected result as all other microbial KDO8P synthases that have been characterized have also been found to be tetrameric in solution.[19, 30, 31]

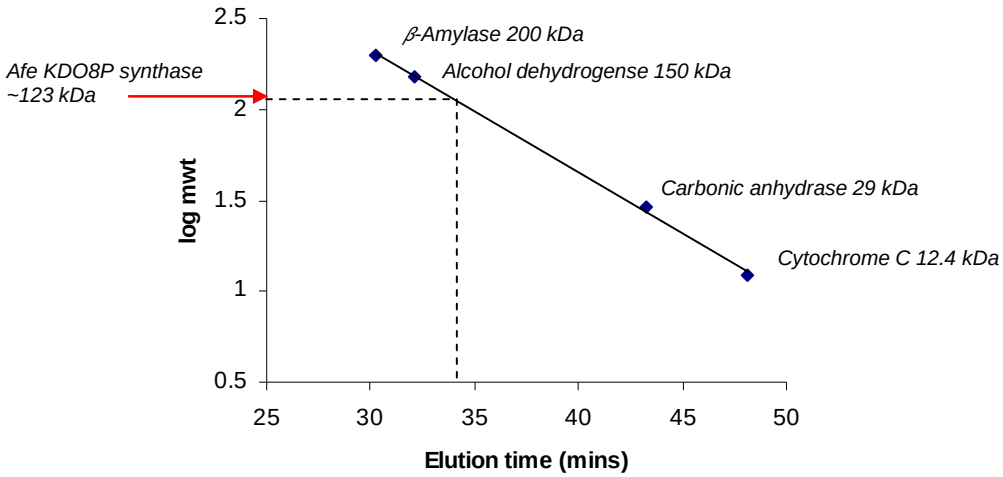

Figure 3.7 **Standard curve of log (molecular mass) vs. elution time for *Afe* KDO8P synthase.** SEC was carried out using buffer consisting of 10 mM BTP pH 7.0, 10 μM EDTA, 200 μM PEP and 50 mM KCl at a flow rate of 0.4 ml min^{-1}. The molecular mass of *Afe* KDO8P synthase was determined to be 123 kDa by this method which is approximately 4 times the size of the monomeric unit (30604 Da). Experimental details of SEC are explained in chapter 5.

3.8 Metal-dependency of *Afe* KDO8P synthase

Afe KDO8P synthase was found to have metal-dependent activity and was sensitive to the presence of the metal-chelator EDTA. There was no detectable activity without a divalent metal ion present or when including 10 mM EDTA in the standard activity assay. Activity could be restored with the inclusion of a variety of divalent metal ions

(figure 3.8). Activity was best in the presence of Mn^{2+}, Co^{2+} and Cd^{2+} but Ni^{2+}, Fe^{2+}, Zn^{2+} and Cu^{2+} were also found to be activating (figure 3.8, table 3.2). All buffers and substrate solutions had been pre-treated with Chelex100 resin to minimize the presence of metal ions from other sources. These results were as expected since *Afe* KDO8P synthase has the same primary amino-acid sequence characteristics that have defined the metal-dependent KDO8P synthases in other studies[13]. The most well characterized of the metallo KDO8P synthases are from *A. aeolicus* and *A. pyrophilus*.[21, 30] These enzymes have shown highest levels of activity in the presence of Mn^{2+} and Cd^{2+} respectively (although Mn^{2+} was the most activating metal ion for *A. pyrophilus* KDO8P synthase after incubation with 10 mM EDTA). Mn^{2+} was also shown to be the most activating metal ion for KDO8P synthase from *C. psittaci*[19] and *C. tepidum* (as discussed in chapter two of this thesis) whereas Cd^{2+} is the preferred metal ion cofactor for *H. pylori*.[26]

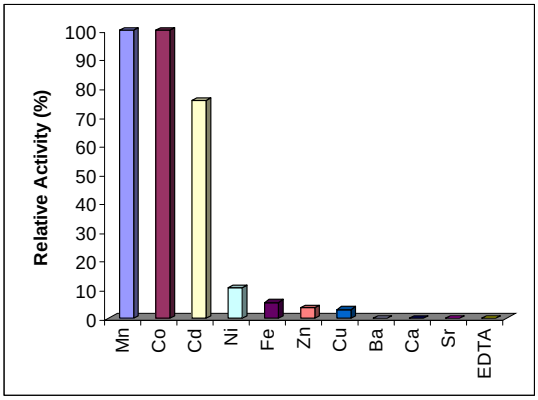

Figure 3.8 **Effect of divalent metal ions on *Afe* KDO8P synthase activity.** Assays were carried out at 37 ºC using 100 μM A5P, 200 μM PEP and 110 μM of the respective metal ions and 1 μL *Afe* KDO8P synthase (10 mg mL^{-1}) in a final volume of 1 mL in BTP buffer (pH 7.2) with 10 μM EDTA. Reaction mixtures containing BTP buffer, PEP, $MnSO_4$ and enzyme were incubated for six minutes and the reaction was initiated by the addition of A5P.

Divalent (2^+) Metal Ion	Relative Activity (%)
Mn^{2+}	100
Co^{2+}	98
Cd^{2+}	76
Ni^{2+}	10
Fe^{2+}	5.4
Zn^{2+}	3.6
Cu^{2+}	2.9
Ca^{2+}	0
Ba^{2+}	0
EDTA	0

Table 3.2 **Relative activity of *Afe* KDO8P synthase in the presence of divalent metal ions.** Activity was measured by following the change in absorbance at 232 nm due to the consumption of PEP.

To determine the affinity of the metal ions for *Afe* KDO8P synthase, standard activity assays were performed with constant and saturating levels of A5P and PEP and varying concentrations of the metal (10 μM to 400 μM). Mn^{2+}, Co^{2+} and Cd^{2+} show the most activation of *Afe* KDO8P synthase activity when present at levels of 50 μM to 100 μM (figure 3.9). Although Mn^{2+} and Co^{2+} activate activity to similar levels, Co^{2+} appears to have an inhibitory effect if present in concentrations over 100 μM, as does the lesser activating metal ion Cd^{2+}. Inhibition of activity has also been shown by Cd^{2+} and Mn^{2+} for KDO8P synthase from both *A. aeolicus* and *A. pyrophilus* but only at metal ion concentrations of 1 mM or above.[11, 21] *H. pylori* KDO8P synthase shows inhibition of activity by Cu^{2+} and, to a lesser extent Zn^{2+}, at concentrations above 100 μM[26] which resembles the results shown here for *Afe* KDO8P synthase in the presence of Co^{2+} or Cd^{2+}. The overall effect of Cu^{2+} on *H. pylori* KDO8P synthase is unusual, for it also enhanced enzymatic activity with higher potency than Cd^{2+} did at lower concentrations (1 μM – 10 μM), but Cd^{2+} is considered the most activating metal ion due to greater activation through to saturating levels.[26] All subsequent assays for further biochemical characterization of wild-type *Afe* KDO8P synthase were performed using Mn^{2+} as the

metal-ion cofactor at levels of 100 μM to 200 μM to ensure there was saturation but not inhibition of activity.

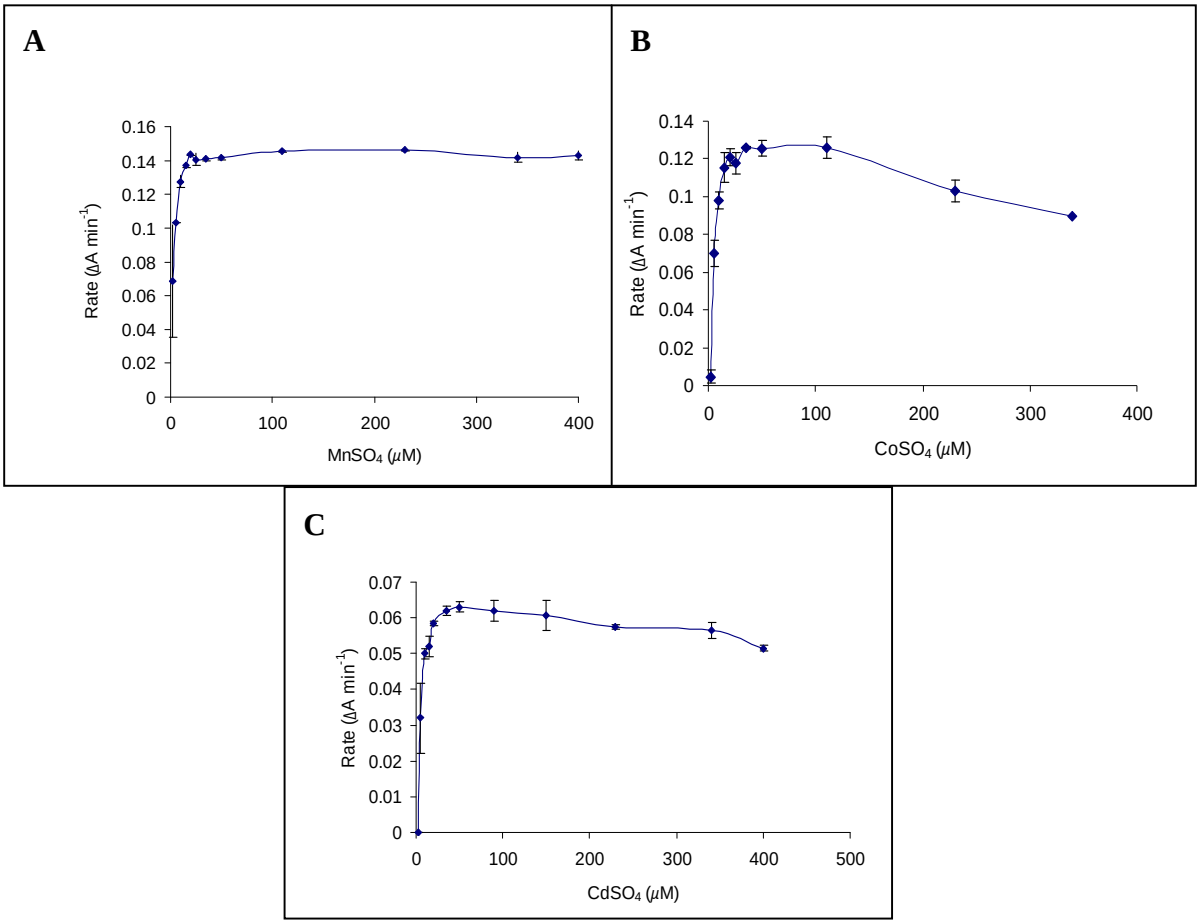

Figure 3.9 **Binding affinity for Mn^{2+} (A), Co^{2+} (B) and Cd^{2+} (C).** Duplicate assays were performed with 100 μM A5P, 200 μM PEP, 1 μL purified *Afe* KDO8P synthase (10 mg mL^{-1}) in BTP buffer (50 mM, pH 7.2) at 37 ºC. The same sample of purified protein was used for A, B and C. All reactions were initiated by the addition of A5P and activities were determined in duplicate. Error bars indicate standard deviation values. Apparent K_m values for Mn^{2+}, Co^{2+} and Cd^{2+} were 2 ± 0.2 μM, 6 ± 2.0 μM and 5.6 ± 1.6 μM respectively indicating that Mn^{2+} binds more efficiently than the other activating metal ions.

3.9 pH profile of *Afe* KDO8P synthase

Afe KDO8P synthase is active over a broad pH range with at least 75% of maximum activity being between pH 6.8 and pH 8.3 (figure 3.10). The range of pH over which there was significant activity was similar to the pH range observed for *H. pylori* KDO8P synthase for which the highest activity was observed between pH 6.5 and pH 7.5. KDO8P synthase from *A. aeolicus* and *A. pyrophilus* are both most active between pH 5.5 and pH 6.0.[21, 30] All subsequent assays for characterisation of *Afe* KDO8P synthase were performed at pH 7.2 as this was the highest point on the pH profile plot and also would not dramatically alter the conditions under which the enzyme was purified and stored (pH 7.0).

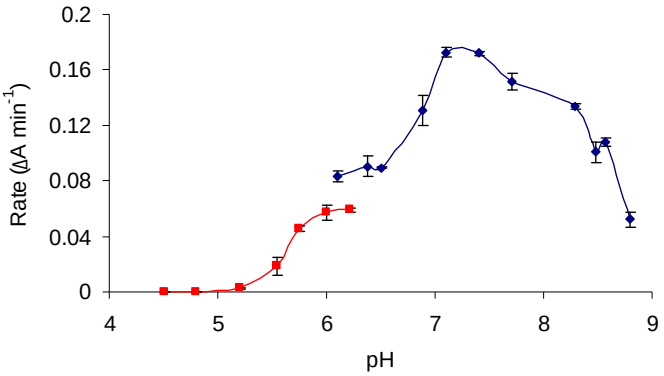

Figure 3.10 **pH profile of *Afe* KDO8P synthase.** ΔA min^{-1} = change in absorbance per minute at 232 nm as PEP is consumed. BTP (50 mM) was used to buffer solutions in the range pH 6.1 to pH 8.8 (blue), whereas acetate (50 mM) was used to buffer solutions between pH 4.5 and pH 6.2 (red). All assays included 100 μM A5P, 200 μM PEP, 100 μM $MnSO_4$ and 1 μL of purified *Afe* KDO8P synthase (10 mg mL^{-1}) in a total volume of 1 mL of buffer at 37 ºC. Reactions were initiated by the addition of A5P. Activity was measured in duplicate with error bars indicating standard deviation values.

3.10 Temperature profile of *Afe* KDO8P synthase

Afe KDO8P synthase was shown to have high levels of enzymic activity over a broad temperature range (30 ºC to 50 ºC). The temperature at which *Afe* KDO8P synthase was found to be most active under the standard assay conditions used was 37 ºC (figure 3.11). The reaction mixtures were all equilibrated to the given temperature for exactly six minutes to ensure the conditions would be consistent for every assay. All subsequent assays for characterization of *Afe* KDO8P synthase were performed at 37 ºC. This assay temperature has been used for characterization of KDO8P synthase from other mesophilic and thermophilic organisms. As the enzymes from the hyperthermophilic organisms *A. aeolicus* and *A. pyrophilus* show greatest activity at 95 ºC and 80 ºC respectively, assays for these enzymes were carried out at these temperatures.[21, 30]

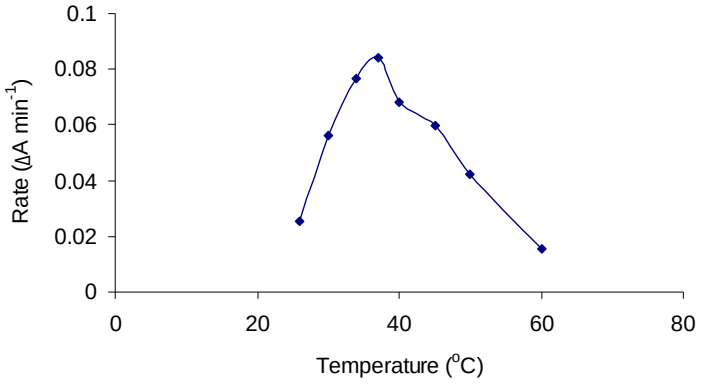

Figure 3.11 **Temperature profile of *Afe* KDO8P synthase.** ΔA min^{-1} = change in absorbance per minute at 232 nm as PEP is consumed. All assays included 100 μM A5P, 200 μM PEP, 100 μM $MnSO_4$ and 1 μL of purified *Afe* KDO8P synthase (10 mg mL^{-1}) in a total volume of 1 mL of buffer at 37 ºC. Reactions were initiated by the addition of A5P. The assay buffers used were 50 mM BTP adjusted to pH 7.2 after equilibration to each temperature tested.

3.11 Kinetic parameters for *Afe* KDO8P synthase

The steady-state kinetic parameters for purified *Afe* KDO8P synthase were measured by following the consumption of PEP at pH 7.2 and 37 ºC. Initial rate values were determined as a function of various concentrations of one substrate at fixed concentration of the other. The Michaelis-Menten constant (K_m) and turnover number (k_{cat}) were determined by fitting the data to the Michaelis-Menten equation using Enzfitter (Biosoft). The apparent K_m values for A5P and PEP were 5.3 ± 0.6 μM and 34 ± 3.0 μM respectively and the k_{cat} (A5P and PEP) was 3.4 ± 0.1 s^{-1} (figure 3.12).

The kinetic parameters from this study are within the range reported from characterization of other KDO8P synthases; however, the range of parameters reported is broad. Table 3.3 summarizes the properties of *Afe* KDO8P synthase alongside the properties of some other well characterized KDO8P synthases.

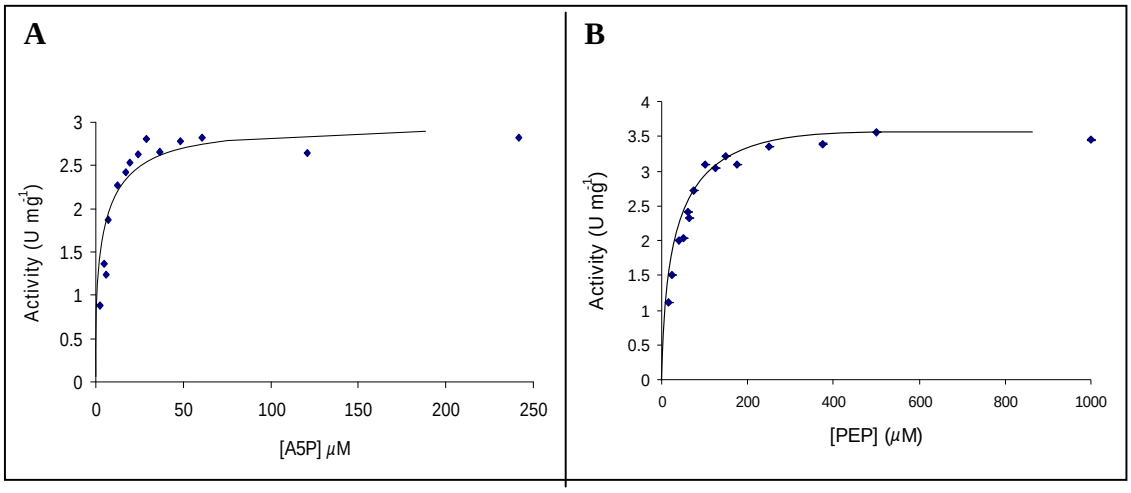

Figure 3.12 **Michaelis-Menten plots for determination of K_m for A5P (A) and PEP (B).** The reaction consisted of A5P (2.4 μM to 240 μM), PEP (15 μM to 1 mM), $MnSO_4$ (100 μM) and 1 μL of purified *Afe* KDO8P synthase (10 mg mL^{-1}) in BTP buffer (50 mM, pH 7.2) at 37 ºC. All reactions were equilibrated without A5P for 6 minutes and initiated by the addition of A5P.

Source of KDO8P synthase	Assay temperature (°C)	K_m A5P (μM)	K_m PEP (μM)	k_{cat} (s^{-1})	Activation by divalent metal (decreasing order of effect)	Reference
A. ferrooxidans	37	5.3 ± 0.6	34 ± 3	3.4 ± 0.1	Mn^{2+}, Co^{2+}, Cd^{2+}, Ni^{2+}, Fe^{2+}, Zn^{2+}, Cu^{2+}	This study
A. aeolicus	90	74 ± 8	28 ± 4	2.0 ± 0.11	Mn^{2+}, Cd^{2+}, Co^{2+}, Ni^{2+}, Cu^{2+}, Ca^{2+}, Zn^{2+}, Mg^{2+}	11
H. pylori J99	37	4.8 ± 0.3	1.8 ± 0.5	1.2 ±0.03	Cd^{2+}, Cu^{2+}, Zn^{2+}, Mg^{2+}	26
N. gonorrhoeae	37	8.5 ± 0.1	3.1 ± 0.2	1.0 ± 0.1	non metallo	59
N. meningitidis	37	5.7 ± 0.5	2.5 ± 0.2	8.0 ± 0.1	non metallo	27
E. coli	37	20	5.9	2.5	non metallo	10

Table 3.3 **Comparison of properties of microbial KDO8P synthase.**

3.12 Crystallography trials

3.12.1 Purification by size-exclusion chromatography (SEC)

Stored aliquots of purified *Afe* KDO8P synthase were pooled (500 μL final volume) and further purified by SEC for crystallization trials (refer to chapter 5 for details). The fractions that corresponded to a peak in the UV trace were analyzed by SDS-PAGE (figure 3.13). The results show *Afe* KDO8P synthase being eluted from the column without the minor contaminants it had after HIC (see section 3.5 for details). The chromatogram showed a major peak corresponding to KDO8P synthase and a very small peak with a lower retention time which suggests the presence of another protein of higher molecular weight, as indicated by the HIC results. The two peaks do not overlap and no trace of the contaminant has been detected by SDS-PAGE (figure 3.13).

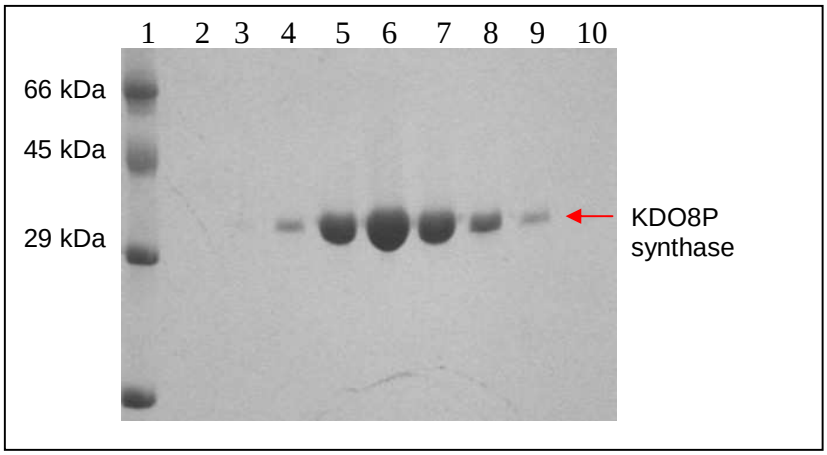

Figure 3.13 **SDS-PAGE analysis of *Afe* KDO8P synthase after size-exclusion chromatography.** Lanes 2 – 10: 8 μL of 0.5 mL fractions as they came off the column. Buffer used contained 10 mM BTP pH 7.0, 10 μM EDTA, 200 μM PEP and 50 mM KCl at a flow rate of 0.4 ml min^{-1} through a Superdex200 SEC column. Fractions corresponding to lanes 4 – 9 were pooled and concentrated for crystallization trials.

3.12.2 Initial crystal screening

The initial screenings for crystallization conditions were performed using hanging-drop vapor diffusion (1 μL protein + 1 μL reservoir solution) on 24-well plates at room temperature with a concentrated solution of *Afe* KDO8P synthase (50 mg mL^{-1}). The Hampton Crystal screens I and II (Hampton Research) were used and the following conditions produced crystals within 24 hours:

A: 0.1 M Hepes-Na pH 7.5, 1.5 M lithium sulfate monohydrate

B: 0.1 M Tris-HCl pH 8.5, 0.2 M lithium sulfate monohydrate, 30% (w/v) polyethyleneglycol (PEG) 4000

C: 0.1 M Tris-HCl pH 8.5, 0.2 M tri-sodium citrate dihydrate, 30% (v/v) PEG 400

D: 0.2 M Magnesium formate

50% of the initial conditions resulted in precipitation and 20% did not form crystals or precipitate. Crystals formed in conditions C and D (as listed above) did not diffract X-rays at all so may not have contained protein crystals or the crystals may have been of poor quality (disordered). Crystals from conditions A and B both diffracted poorly, but showed some signs characteristic of protein crystals. The crystals were approximately 0.2 mm in length and 0.1 mm wide with rounded edges and uneven faces, and there were many small droplet-like crystals forming simultaneously in the background which indicates the protein concentration may have been too high causing the crystals to form too quickly (figure 3.14, A). The diffraction patterns indicated multiple protein crystals may be stacked together which could be why the faces and edges appear so uneven.

The conditions A and B were repeated using 20 mg mL^{-1} and 10 mg mL^{-1} *Afe* KDO8P synthase and preparing and storing the crystal trays at 4 ºC as well as at room temperature to try slowing crystal formation. At 20 mg mL^{-1} crystals grown in condition A formed within the same time frame as for the 50 mg mL^{-1} solution but they were much smaller and ordered in shape, although they still had rough faces (figure 3.14, B). There were still many crystals forming simultaneously in the background but they were needle-like and 1-dimensional. At 10 mg mL^{-1} no crystals formed at either room temperature or at 4 ºC in any of the standard crystal screening conditions trialed.

The Hampton Additive Screen I (Hampton Research) was performed using sitting-drop vapor diffusion on 96-well plates with condition A (0.1 M Hepes-Na pH 7.5, 1.5 M lithium sulfate monohydrate) as the reservoir solution and the *Afe* KDO8P synthase concentration at 20 mg mL^{-1}. The various additives to the original reservoir solution changed the morphology of the crystals (producing needle-, rod- and plate-like crystals) and in some cases produced fewer, larger, and smoother-looking crystals, which was the intended short-term goal. However, most crystals did not diffract X-rays, and those that did (figure 3.14, C) produced very similar diffraction patterns to the patterns produced by the large crystals from the original 24-well plates. This indicated that there may have

still been multiple layers of 2-dimensional crystals stuck together, even in the apparently thin, needle-like crystals.

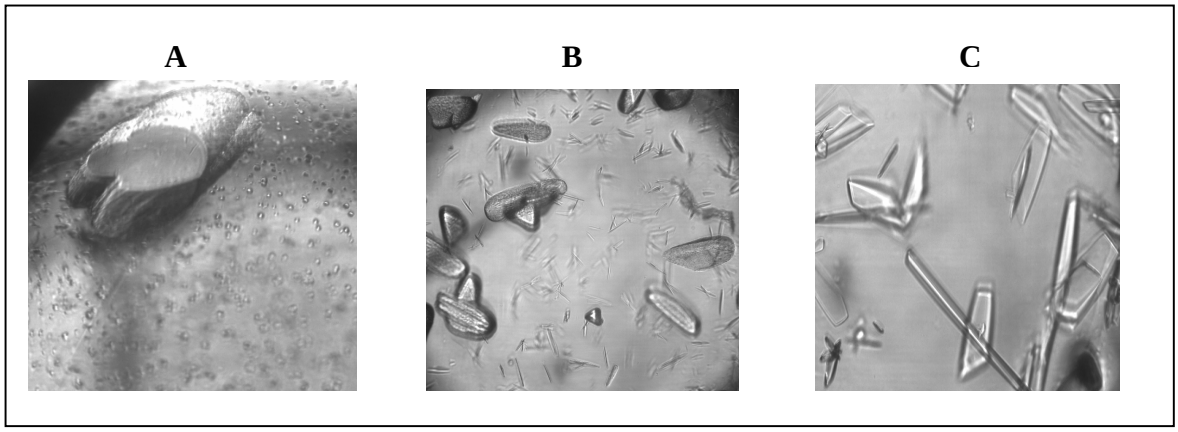

Figure 3.14 **Initial crystallization of *Afe* KDO8P synthase.** Crystals were grown at 22 ºC using hanging-drop (*A* and *B*) or sitting-drop (*C*) vapor diffusion and a reservoir solution of 0.1 M Hepes-Na pH 7.5, 1.5 M lithium sulfate monohydrate. (*A*) 50 mg mL^{-1} protein concentration. Crystal dimensions approximately 0.2 mm x 0.1 mm. (*B*) 20 mg mL^{-1} protein concentration. Dimensions of largest crystals: 0.1 mm x 0.05 mm. (*C*) 20 mg mL^{-1} protein concentration with 30% (v/v) isopropanol. Dimensions of largest crystals: 0.1 mm x 0.05 mm. Crystals shown in *C* showed diffraction patterns of multiple crystals stacked together.

3.13 Summary of characterization

The results presented in this chapter indicate that *Afe* KDO8P synthase is sensitive to the metal chelating agent EDTA and is dependent on a divalent metal ion for activity, as predicted from the primary amino-acid sequence.[13] The most activating metal ions are Mn^{2+}, Co^{2+} and Cd^{2+} with apparent K_m values of 2.0 μM, 6.0 μM and 5.5 μM for the respective metal ions, which is similar to what is observed for the metallo KDO8P synthases from *A. aeolicus*, *A. pyrophilus*, *H. pylori* and *C. tepidum*.[11, 21, 26] The preferred activating metal ion *in vitro* is Mn^{2+} as inhibition of *Afe* KDO8P synthase activity is shown in the presence of Co^{2+} and Cd^{2+} at levels of 200 μM or more.

Afe KDO8P synthase was found to exist as a tetramer in solution and is most active within the pH range of 6.8 to 7.5 and within a temperature range of 35 ºC to 40 ºC.

In the presence of 100 μM Mn^{2+} at 37 ºC and pH 7.2, *Afe* KDO8P synthase has an apparent K_m of 5.3 μM for A5P, 34 μM for PEP and a turnover number (k_{cat}) of 3.4 s^{-1}. These kinetic constants are consistent with what is observed for all characterized metallo and non-metallo KDO8P synthases.

Preliminary crystallization trials show that *Afe* KDO8P synthase can form crystals in solution in a range of conditions, with the best crystals produced using 0.1 M Hepes-Na pH 7.5, 1.5 M lithium sulfate monohydrate with 30 % v/v isopropanol as the reservoir solution. A condition which produced crystals able to diffract X-rays sufficient for data collection was not found during the course of this work. Further methodical manual or automated screening, or further refinement of the conditions mentioned above, may help to produce such crystals and lead to the determination of the structure of *Afe* KDO8P synthase.

CHAPTER 4

INVESTIGATING THE ROLE OF IMPORTANT AMINO-ACIDS IN AND AROUND THE ACTIVE SITE OF *ACIDITHIOBACILLUS FERROOXIDANS* KDO8P SYNTHASE

4.1 Introduction

The KDO8P synthase residues that play an important role in the positioning of A5P, PEP and the divalent metal ion have been identified through structural characterization of the KDO8P synthases from *E. coli* and *A. aeolicus.*[20, 32] Introducing mutations to some of these key residues may inhibit catalytic activity or change the characteristics of the protein, giving an insight into what may be happening in the active site and the role of specific residues.

The following site specific mutations were introduced to *Afe* KDO8P synthase to investigate the effect each residue has on metal-binding and catalytic activity (refer also to figure 4.1).

C21N

This Cys residue has been shown to be essential for metal-binding in other characterized metallo KDO8P synthases. The Asn in this position is conserved throughout all known non-metallo KDO8P synthases and Cys to Asn mutations in the metallo KDO8P synthases from *A. aeolicus* and *A. pyrophilus* have reportedly resulted in metal independent activity.[13,22, 23]

N57A

This Asn residue is part of the conserved LysAla**Asn**Arg motif that is conserved throughout the metallo and the non-metallo KDO8P synthases and is involved in the binding of A5P in the active site (see figure 1.7).[20] Structures of *A. aeolicus* KDO8P synthase with A5P bound suggest that this residue interacts with A5P to hold it in the correct orientation in the active site and close enough to PEP for a hydrogen bond between the phosphate group of PEP and the aldehyde functionality of A5P to occur.[20, 25] This proposed interaction could activate the aldehyde functionality of A5P (Brønsted acid catalysis) to make it susceptible to attack by the C3 of PEP.[25]

D243A, D243E

This Asp residue is conserved throughout metallo and non-metallo KDO8P synthases and is involved in metal-binding and A5P binding at the active site of the metallo type.[13] When overlaid, the structures of the KDO8P synthase metal-binding sites from the organisms *A. aeolicus* and *E. coli* suggest that this residue may adopt a different position in metallo KDO8P synthase and in non-metallo enzymes.[20, 23, 47] However, in other KDO8P synthase structures this part of the enzyme appears disordered which suggests high mobility, possibly due to a Pro residue two amino-acids downstream (discussed below).[20, 27, 32] Mutation of Asp243 to Ala eliminates the functional group altogether to help determine the importance of this residue as an essential metal-binding ligand. Mutation to a Glu residue changes the length of the side chain but retains the same functional group to help determine the importance of both charge and position at this point in the active site.

P245A

The Pro residue at this position (mentioned above) is conserved throughout all known non-metallo KDO8P synthases but is only present in some metallo KDO8P synthases. This region in metallo and non-metallo KDO8P synthases that have been structurally characterized is very disordered which suggests high mobility.[20, 27, 32] Pro is conformationally restrictive and the Pro residue at this position may limit the conformations that other residues can access. Substitution for an Ala residue may therefore have an effect on the relative position of surrounding residues, including the metal-binding Asp two residues upstream. This Pro has not been implicated directly in catalytic activity of KDO8P synthase in the current literature.

This chapter describes the site-directed mutagenesis, purification and biochemical characterization of the *Afe KDO8P* synthase mutants mentioned above.

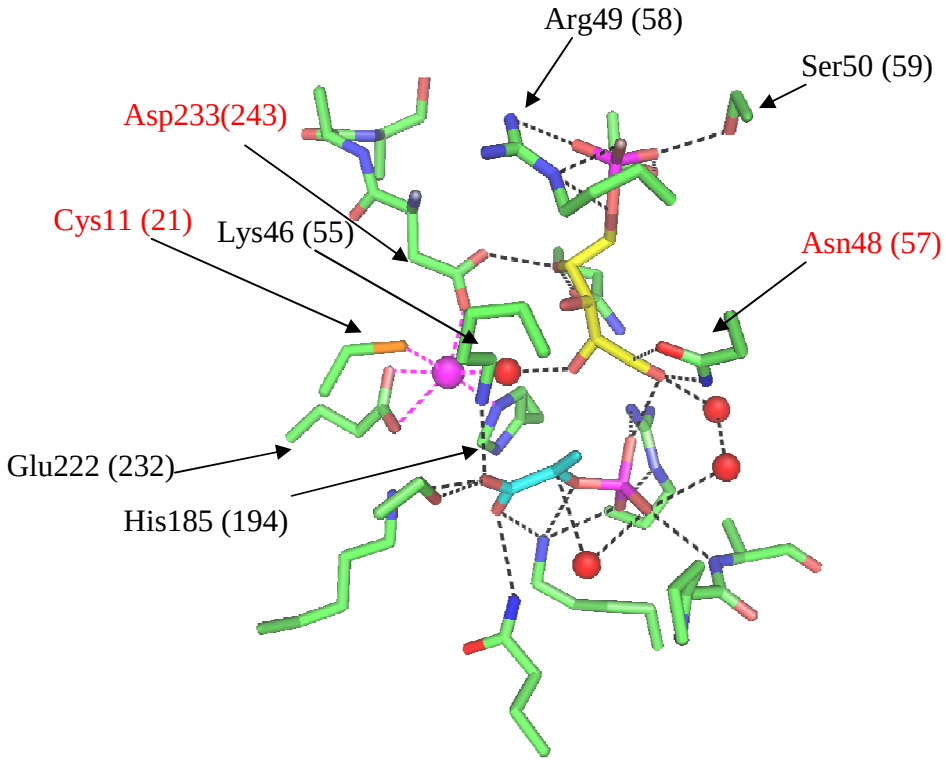

Figure 4.1 **Active site of *A. aeolicus* KDO8P synthase with A5P (yellow), PEP (blue) and Cd^{2+} (pink) bound (PDB code 1FWW).** Oxygen = red. Nitrogen = blue. Phosphorus = purple. Water molecules are represented by red spheres. Pink dashed lines represent interactions between Cd^{2+} and the surrounding residues and water molecules. Black dashed lines represent interactions between amino-acid residues or water molecules and the substrates. The numbers in brackets refer to the corresponding residues from *Afe* KDO8P synthase. Those residues that are being mutated in this project are labeled in red. The *Afe* KDO8P synthase Pro245 residue is not indicated, as the corresponding residue in the *A. aeolicus* structure is a Ser.

4.2 Cloning of *Afe* KDO8P synthase mutants

The amino-acid substitutions were performed using a QuikChange® II Site-Directed Mutagenesis Kit (Stratagene) and pT7-7-*Afe* KDO8P synthase as the double-stranded plasmid template. The substitutions were introduced by designing synthetic oligonucleotide primers complementary to opposite strands of pT7-7-*Afe* KDO8P synthase containing the desired mutation (details of the primer sequences and the PCR program used are given in chapter 5). The resulting plasmids were digested with *Bam*HI and checked for size on a 1 % agarose gel (figure 4.2).

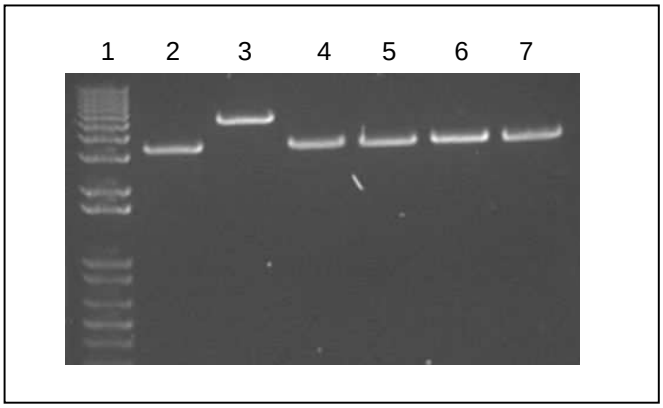

Figure 4.2 **Agarose gel analysis of pT7-7-*Afe* KDO8P synthase plasmid DNA after site-directed mutagenesis.** Lanes 2 – 7 show *Bam*HI digested pT7-7-Afe KDO8P synthase incorporating C21N, N57A, D243A, D243E, P245A mutations and wild-type (control) respectively.

Sequencing results showed that the site-directed mutagenesis successfully produced the C21N, D243A, D243E and P245A mutant proteins but not the N57A mutant. Agarose gel electrophoresis (AGE) analysis of the digested plasmids showed that the N57A mutation produced plasmid DNA that is not of the size expected which suggests that either the primers were faulty or the conditions of the PCR program are not suitable for these particular primers. The original thermo-cycling program consisted of an annealing

temperature of 55 ºC for 1 minute. A gradient PCR reaction was performed using reaction mixture volumes of just 6 μL and screening annealing temperatures from 40.3 ºC to 54.8 ºC. At lower annealing temperatures (40.3 ºC – 43 ºC) a DNA product of the correct size can be seen (figure 4.3).

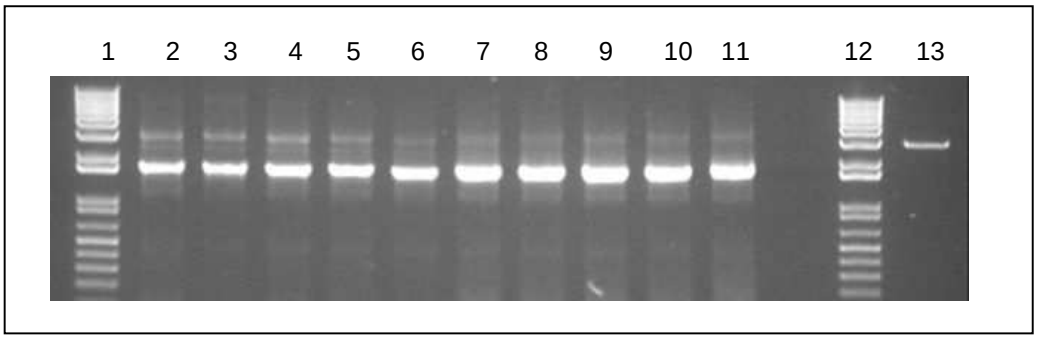

Figure 4.3 **Gradient PCR of N57A primers with pT7-7-*Afe*KDO8P synthase template.** Lanes 2 – 11: PCR performed with annealing temperatures (ºC) of 40.3, 40.6, 41.6, 43.0, 44.8, 46.8, 48.8, 50.8, 52.5, 53.9, 54.8 respectively. Lane 13 (control): PCR performed with P245A primers on pT7-7-AfeKDO8P synthase template with annealing temperature of 55 ºC. Lanes 2 to 5 show that at lower annealing temperatures a greater proportion of correctly sized plasmid is produced.

The PCR reaction for N57A was repeated on a larger scale (25 μL total volume) using an annealing temperature of 40 ºC. If the different sized bands on the agarose gel shown in figure 4.2 represent different products then only the transformants which take up the correct plasmid (carrying an ampicillin resistance gene) will grow on the LB (Amp) plates. All the resulting plasmids were sequenced to confirm that the correct substitutions hade been carried out. The plasmid DNA was then transformed into competent BL21(DE3) cells and cultures of the cells (5 mL) were grown, induced and harvested using conditions identical to those used for wild-type *Afe* KDO8P synthase as described in chapter 3.

4.3 Expression and solubility of *Afe* KDO8P synthase mutant proteins

SDS-PAGE analysis shows that each mutant *Afe* KDO8P synthase protein expressed at levels similar to the wild-type protein when grown and lysed using the same conditions (figure 4.4). There appears to be more KDO8P synthase in the soluble fractions than in the resuspended pellet after lysis and centrifugation.

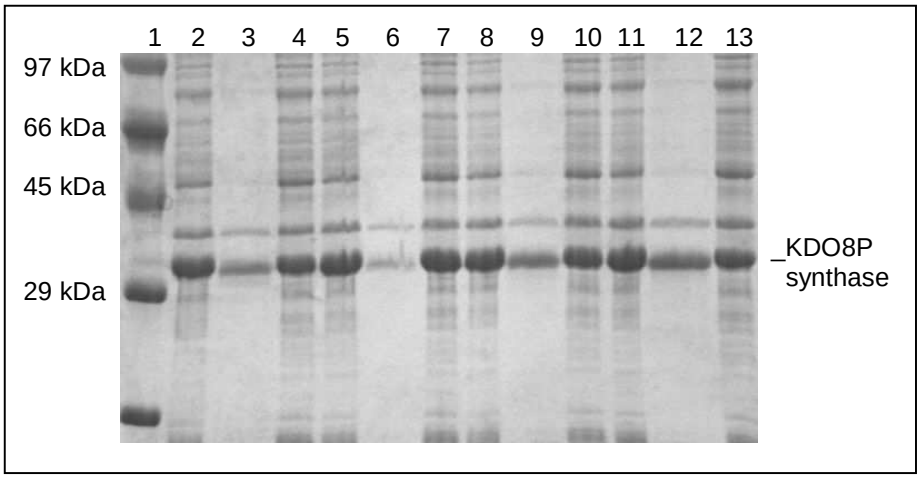

Figure 4.4 **Expression and solubility of *Afe* KDO8P synthase mutant proteins.** Lanes 2 – 4: 2 μL Whole cell lysate (lane 2), 10 μL insoluble fraction resuspended in 400 μL 1:1 6 M urea / 20 % SDS (lane 3), 10 μL soluble fraction (lane 4) of C21N *Afe* KDO8P synthase; Lanes 5 – 7: Whole, insoluble and soluble fractions of D243A *Afe* KDO8P synthase; Lanes 8 – 10: Whole, insoluble and soluble fractions of D243E *Afe* KDO8P synthase; Lanes 11 – 13: Whole, insoluble and soluble fractions of P245A *Afe* KDO8P synthase. Expression of N57A *Afe* KDO8P synthase is not shown.

4.4 Purification of *Afe* KDO8P synthase mutant proteins

The soluble fractions of the *Afe* KDO8P synthase mutant proteins were purified by AEC and HIC using the same conditions that had produced pure wild-type *Afe* KDO8P synthase. Each mutant protein was eluted from the SOURCE™ 15Q and SOURCE™ 15Phe columns at exactly the sodium chloride concentration as the wild-type *Afe*

KDO8P synthase did. The fractions containing KDO8P synthase were pooled, concentrated and stored in 100 μL aliquots at -80 ºC. These fractions were used for all characterization of the mutant proteins that is discussed in this chapter.

4.5 Catalytic activity of *Afe* KDO8P synthase mutant proteins

The activity of each mutant protein was tested after purification using the standard assay conditions described in chapter 5 with Mn^{2+} as the divalent metal cofactor. The C21N and D243A *Afe* KDO8P synthases were both found to have less than 1 % relative specific activity when compared to the wild-type (table 4.1). This result shows that these residues are important for KDO8P synthase activity. No further kinetic studies were carried out on either of these proteins. The P245A mutation did not alter the specific activity of *Afe* KDO8P synthase. The N57A and D243E mutations both lowered the specific activity of *Afe* KDO8P synthase under these conditions.

Mutation	Activity (U mg^{-1})	% Activity (c/a WT)
Wild-type (WT)	3.4	100
P245A	3.4	100
D243E	1.2	35
N57A	0.8	25
D243A	0.01	0.2
C21N	0.02	0.5

Table 4.1 **Comparison of mutant *Afe* KDO8P synthase specific activity after purification.** Specific activity was measured by monitoring absorbance change due to the consumption of PEP at 232 nm. Assay mixtures contained 200 μM A5P, 200 μM PEP, 100 μM Mn^{2+} and 1 μL of purified protein (10 – 20 mg mL^{-1}).

4.6 Metal activation of *Afe* KDO8P synthase mutants

The P245A, D243E and N57A *Afe* KDO8P synthases were assayed using a range of different divalent metal ions using the standard assay conditions. The metal activation profiles were compared with that of the wild-type *Afe* KDO8P synthase (figure 4.5, table 4.2). The resulting profiles are different for each mutant protein. Whereas the wild-type, P245A and N57A are all most active in the presence of Mn^{2+}, there are large differences in activity in the presence of other divalent metal ions. The D243E mutant protein was most active in the presence of Cd^{2+}, with the specific activity measuring 80% of the specific activity of Mn^{2+} activated wild-type *Afe* KDO8P synthase. When activated by Cd^{2+}, wild-type *Afe* KDO8P synthase specific activity was only 95% compared to Cd^{2+} activated D243E *Afe* KDO8P synthase.

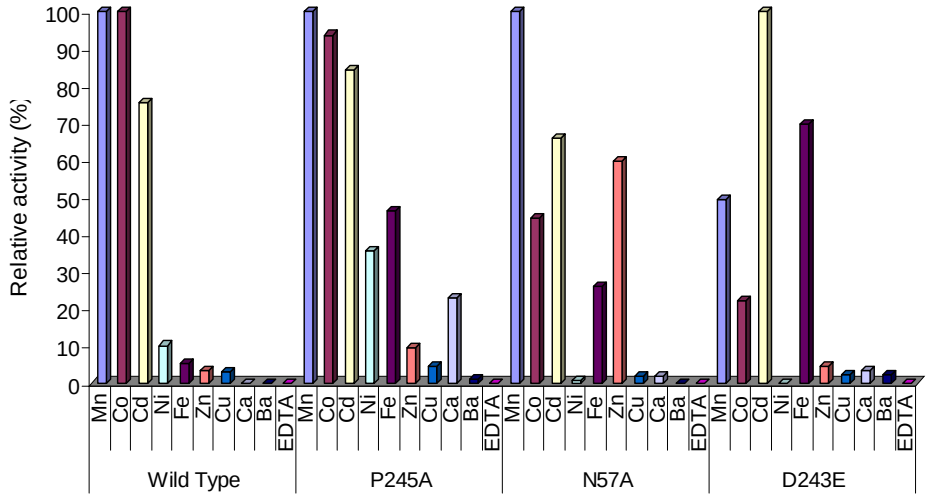

Figure 4.5 **Metal activation profile of *Afe* KDO8P synthase mutants.** Relative activity has been normalized to the highest activating metal ion for each respective mutant. Assays were carried out at 37 ºC using 100 μM A5P, 200 μM PEP and 110 μM of the respective metal ions in a final volume of 1 mL in BTP buffer (pH 7.2) with 10μM EDTA. Protein aliquots and concentrations used were: 1 μL Wild-type, 10 mg mL^{-1}; 1 μL P245A, 16.9 mg mL^{-1}; 2 μL N57A, 22.3 mg mL^{-1}; 1

μL D243E, 9.5 mg mL^{-1}. Reaction mixtures containing BTP buffer, PEP, $MnSO_4$ and enzyme were incubated for six minutes and the reaction was initiated by the addition of A5P.

Wild-type *Afe* KDO8P synthase is most activated by Mn^{2+} (100%), Co^{2+} (100%) and Cd^{2+} (75%) but shows little activity (< 10%) in the presence of any of the other metal ions tested. The metal activation profile for P245A *Afe* KDO8P synthase resembles the profile for the wild-type more than the other mutant *Afe* KDO8P synthases. The major differences are activation by Ni^{2+} (36%), Fe^{2+} (47%) and Ca^{2+} (24%) which suggests that substitution of this residue has slightly altered the shape or size of the metal-binding pocket in the active site.

The major differences in the profile for N57A *Afe* KDO8P synthase are the lower relative activity in the presence of Co^{2+} (45% of maximum activity) and the activation by Fe^{2+} (26%) and Zn^{2+} (60%). The relative maximum activity of this mutant compared to the wild-type when activated by Mn^{2+} was only 25% (table 4.2). This suggests that disruption of the conserved LysAla**Asn**ArgSer motif alters the position of A5P and PEP in relation to each other and that the catalytic mechanism may be less efficient with the substrates in the orientation that they have adopted. The altered position of A5P in this mutant could affect the size or shape of the metal-binding pocket, as suggested by the altered metal activation profile.

The metal activation profile for D243E *Afe* KDO8P synthase shows that activity in the presence of Mn^{2+} is only 49% compared to activity in the presence of the most activating metal ion (Cd^{2+}). Fe^{2+} (66%) is the next most activating metal cofactor for D243E *Afe* KDO8P synthase. Asp243 is a metal-binding residue, therefore substitution of this residue directly affects the metal-binding pocket of *Afe* KDO8P synthase so the different affinity for activating metal ions demonstrated by D243E *Afe* KDO8P synthase was to be expected. Cd^{2+} is the most activating metal ion for KDO8P synthase from *A.*

pyrophilus[21] and *H. pylori*[26] and is one of the most activating metal ions for *A. aeolicus* KDO8P synthase[11] and *C. tepidum* KDO8P synthase (chapter 2 of this thesis). This suggests that by creating a metal-binding pocket capable of binding Cd^{2+} efficiently, the substrates can still adopt the correct orientation required for the mechanism, perhaps simulating the metal-binding pocket of other Cd^{2+} activated KDO8P synthases. However, the high apparent K_m value this mutant has for A5P (see figure 4.7) suggests that A5P does not bind particularly efficiently. This could be due the interaction between the metal ion and the C2 hydroxyl of A5P being inefficient in this mutant due to the change in shape of the metal-binding pocket.

The N57A and P245A mutant proteins were expected to show similar metal activation profiles to that of the wild-type as the Asn57 residue is involved in A5P binding in the active site and Pro245 is not directly involved with substrate or metal ion binding. But there are significant differences, especially the activation of the N57A mutant by Zn^{2+} and the activation of the P245A mutant by Fe^{2+} and Ca^{2+}, suggesting that these mutations do alter the metal-binding site.

	Relative activity, %			
Divalent metal ion	**Wild-type**	**P245A**	**N57A**	**D243E**
Mn^{2+}	100	100	25	35
Co^{2+}	100	95	14	16
Cd^{2+}	76	86	19	80
Ni^{2+}	11	36	0	0
Fe^{2+}	9.5	47	8	49
Zn^{2+}	3.6	9.6	18	3
Cu^{2+}	2.9	4.8	1	2
Ca^{2+}	0	24	1	2
Ba^{2+}	0	1.1	0	2
EDTA	0	0	0	0

Table 4.2 **Metal activation of *Afe* KDO8P synthase mutants.** Relative activity has been normalized to maximum wild-type specific activity in the presence of Mn^{2+}. Assays were carried out exactly as described above (figure 4.5).

4.7 Metal independent activity of C21N *Afe* KDO8P synthase

With no metal ion added and in the presence of 1 mM EDTA, purified C21N *Afe* KDO8P synthase showed 0.5% (0.02 U mg^{-1}) activity when compared to maximum activity of the wild-type in the presence of Mn^{2+} (3.4 U mg^{-1}). In the presence of 1 mM EDTA the wild-type protein showed no activity and was activated by the addition of divalent metal ions, particularly Mn^{2+}, Co^{2+} and Cd^{2+} as discussed in section 4.6. The addition of Mn^{2+}, Co^{2+} or Cd^{2+} to the C21N mutant did not affect the activity at all. The rate of absorbance change at 232 nm due to the loss of PEP was proportional to the amount of protein solution included in the assay indicating that any activity being detected was due to C21N *Afe* KDO8P synthase. The same mutation has been carried out on the KDO8P synthases from *A. pyrophilus*[23] and *A. aeolicus*[22] and metal independent activity has been observed at levels of 10% and 70% respectively when compared to the metal-dependent activity levels of the respective wild-type enzymes. These results suggest a common mechanism between metallo and non-metallo KDO8P synthases and suggest that a direct catalytic role of the metal-ion in the activation of water is unlikely.[22, 23, 25] The results presented in this thesis suggest that the single Cys to Asn substitution is not the only important difference between metallo and non-metallo KDO8P synthases.

4.8 Kinetic parameters for *Afe* KDO8P synthase mutants

The steady-state kinetic parameters for purified D243E and P245A *Afe* KDO8P synthase were measured by following the consumption of PEP at pH 7.2 and 37 ºC. Initial rate values were determined as a function of various concentrations of one substrate at fixed concentration of the other. The apparent Michaelis-Menten constants (K_m) and the turnover number (k_{cat}) were determined by fitting the data to the Michaelis-Menten equation using Enzfitter (Biosoft).

Although the specific activity at maximum velocity for the wild-type, D243E and P245A *Afe* KDO8P synthase proteins was very similar, the kinetic parameters show that each protein has different properties with respect to substrate binding (summarized in table 4.3). The very high apparent K_m for A5P that D243E *Afe* KDO8P synthase has (2.6 mM) reflects the importance of this residue's position in the active site. Structures of *A. aeolicus* KDO8P synthase with A5P and Cd^{2+} bound show that the Asp residue is in a position to be able to bind to both the metal ion and to the C4 hydroxyl group of A5P (see figure 4.1).[20] Substituting Asp for Glu lengthens the side chain of this residue and so may change the size and shape of the spaces in which A5P and the metal ion have to bind in the active site. The position of A5P relative to PEP in the active site is important for catalytic activity, as implicated by the number of residues conserved throughout metallo and non-metallo KDO8P synthases that hold the two substrates in place.[25] The metal profile of D243E *Afe* KDO8P synthase suggests that there are changes to the metal-binding site (figure 4.5).

Changes to the Asp243 and Pro245 residues should not directly affect the binding pocket of PEP and this is reflected in the low apparent K_m the D243E and P245A mutants have for this substrate. It should also be noted that for the D243E mutant the apparent K_m value for PEP was calculated using only 1 mM A5P (less than half the apparent K_m value) due to a lack of available A5P and D243E having a considerably high apparent K_m for that substrate.

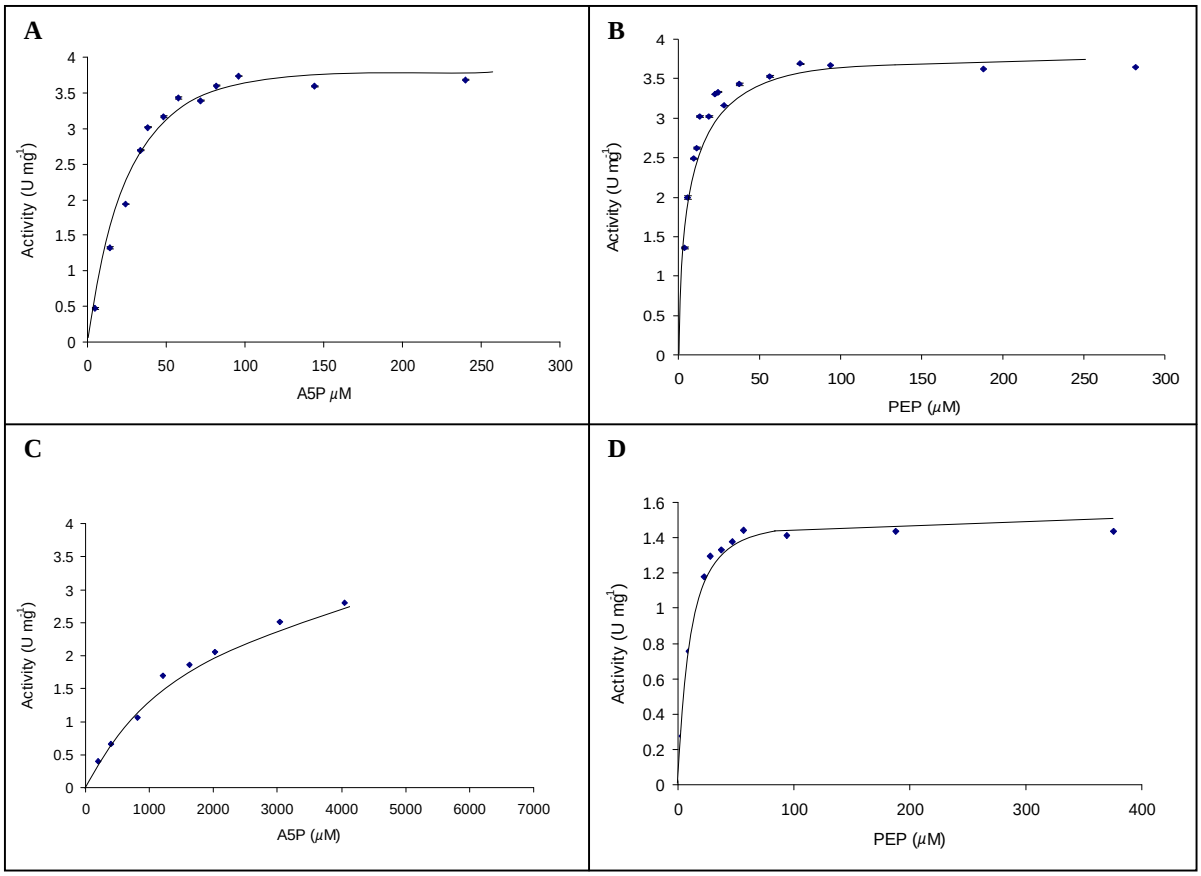

Figure 4.6 **Michaelis-Menten plots for the determination of K_m values for P245A and D243E *Afe* KDO8P synthase mutants.** Assays were performed at 37 ºC in 50 mM BTP buffer at pH 7.2 with 10 μM EDTA. Specific activity was measured by monitoring the absorbance change at 232 nm due to consumption of PEP. Assays for P245A (A and B) included 110 μM Mn^{2+}, 1 μL of P245A *Afe* KDO8P synthase (15.4 mg mL^{-1}), a fixed concentration of 200 μM of either A5P or PEP and varying concentrations of the other substrate. Assays for D243E K_m (A5P) (C) included 110 μM Cd^{2+}, 200 μM PEP, 1 μL of D243E *Afe* KDO8P synthase (9.5 mg ml^{-1}) and varying concentrations of A5P. Assays for D243E K_m (PEP) (D) included 110 μM Cd^{2+}, 1 mM A5P, 1 μL of D243E *Afe* KDO8P synthase (9.5 mg ml^{-1}) and varying concentrations of PEP.

Mutation	Activity (U mg^{-1})	K_m (A5P) μM	K_m (PEP) μM	k_{cat} s^{-1}
Wild-type	3.4	5.3 ± 0.8	34 ± 3	3.8 ± 0.08
P245A	3.4	24 ± 5	5.2 ± 0.5	3.9 ± 0.07
D243E*	3.3	2628 ± 29	13 ± 2.3	4.8 ± 0.3

Table 4.3 **Comparison between kinetic parameters of wild-type and *Afe* KDO8P synthase mutants.** Kinetic parameters presented here for wild-type and P245A *Afe* KDO8P synthase were obtained under identical conditions (see figure 4.6) using Mn^{2+} as the metal ion cofactor. Kinetic parameters presented here for D243E *Afe* KDO8P synthase were obtained using 110 μM Cd^{2+} as the metal ion cofactor.

*****Preliminary assays of D243E *Afe* DKO8P synthase using Mn^{2+} as the metal ion cofactor indicated that maximum velocity had not been achieved with the addition of A5P up to 2 mM. Kinetic parameters were therefore not calculated using Mn^{2+} due to the availability of A5P.

4.9 Conclusions and future directions

The results of the site-directed mutagenesis studies presented in this chapter have provided information about some of the amino-acid residues in and around the active site of *Afe* KDO8P synthase. This summary points out the relevant findings from each mutation studied and suggests future directions of study that may help provide more information on the mechanism of metallo KDO8P synthases and the relationships of these to their non-metallo partners.

D243A/D243E

It has been shown that the Asp243 residue of *Afe* KDO8P synthase is an essential residue for metal-dependent activity. When Asp243 was substituted for an Ala residue, taking away the negatively-charged carboxylate functional group of the side-chain, Mn^{2+} stimulated activity is reduced by over 99% when compared to the wild-type *Afe* KDO8P synthase. The importance of having a negatively charged group at this position

was shown by the substitution of a Glu residue for Asp243. The D243E *Afe* KDO8P synthase protein is capable of near maximal activity when compared to wild-type *Afe* KDO8P synthase, but altering this side-chain changes the preferred metal ion to Cd^{2+} and affects the affinity of the enzyme for A5P. This suggests that the D243E mutation has altered the size or shape of the metal-binding site. A Glu in this position may not interact correctly with the C4 hydroxyl of A5P, therefore altering the position of A5P and the efficiency of A5P binding in the active site, as reflected by the high K_m the D243E mutant has for this substrate.

P245A

The Pro245 residue of *Afe* KDO8P synthase was shown to be unimportant. Activity of P245A *Afe* KDO8P synthase was almost identical to activity of wild-type *Afe* KDO8P synthase when both proteins were activated by Mn^{2+}. A change in the metal-activation profile for the P245A mutant suggests that a change in this position may affect the metal binding site, possibly due to movement of the important residue Asp243 (mentioned above). Studies by Dr Fiona Cochrane at Massey University (2007, unpublished observations) show that the equivalent mutation to the non-metallo *N. meningitidis* KDO8P synthase (P249A) had only a relatively small apparent consequence to catalytic activity.[27] It remains unclear why this residue is absolutely conserved throughout the primary sequence of the non-metallo KDO8P synthases and not the metallo enzymes. It also remains unclear why this region of metallo and non-metallo KDO8P synthases appears to be mobile and is disordered in most KDO8P synthase structures. Further structural studies of metallo (including *Afe* KDO8P synthase) and non-metallo KDO8P synthases may help resolve these issues.

C21N

The Cys21 residue was also found to be important for metal-dependent activity of *Afe* KDO8P synthase. When Cys21 is substituted for an Asn residue the activity of the mutant *Afe* KDO8P synthase is only 0.5% when compared to the activity of the wild-type *Afe* KDO8P synthase in the presence of Mn^{2+}. Furthermore, the activity of C21N

Afe KDO8P synthase is not affected by the addition of Mn^{2+}, Cd^{2+}, Co^{2+} or EDTA, indicating enzyme catalysis was occurring in the absence of metal. The activity of this mutant is very low when compared to the activity of the equivalent mutant KDO8P synthases from *A. aeolicus* (70% of wild-type activity) and *A. pyrophilus* (10% of wild-type activity).[22, 23] This suggests that a single mutation at this position in *Afe* KDO8P synthase is not sufficient to convert the metallo enzyme to an efficient non-metallo enzyme.

Kinetic characterization of C21N *Afe* KDO8P synthase was not performed as part of this project and may give insight into how efficiently the mutant protein binds A5P and PEP when compared to the non-metallo KDO8P synthases. The introduction of multiple site-specific mutations may be required to further understand the relationship between the metallo and non-metallo enzymes. Structural studies of C21N *Afe* KDO8P synthase may help identify other residues that are important for metal-dependent activity and these could be targeted for mutagenesis. Although the same mutation has been carried out on *A.aeolicus* and *A. pyrophilus* KDO8P synthases, no structures of either mutant protein have been published.[22, 23]

The ability to perform the corresponding mutation (Asn to Cys) on the non-metallo *E. coli* KDO8P synthase to create a metal-dependent enzyme is disputed. Shulami *et al* report the *E. coli* N26C mutant to have up to 30% of the maximum wild-type when activated by Mn^{2+} or Cd^{2+} metal ions.[23] In contrast, studies by Li *et al* have reported that the N26C *E. coli* KDO8P synthase retains only 1.4% of wild-type activity and is not activated by metal ions, suggesting that there are other differences between metallo and non-metallo KDO8P synthases apart from this single-site substitution.[22]

N57A

Activity of N57A *Afe* KDO8P synthase is only 25% compared to maximum wild-type activity when activated by Mn^{2+}. This result reflects the importance of this residue in the active site of *Afe* KDO8P synthase. This Asn residue is part of the

LysAla**Asn**ArgSer motif which is conserved throughout all metallo and non-metallo KDO8P synthases. Structural studies of *A. aeolicus* KDO8P synthase show that this Asn residue provides an important binding contact for A5P in the active site, holding the aldehyde moiety of A5P close to the phosphate of PEP.[20] It has been proposed that this allows a hydrogen bond between the PEP phosphate and the aldehyde oxygen of A5P to form, activating the aldehyde group by protonation (Brønsted acid catalysis).[25] The results reported in this chapter give evidence of the important role of Asn57 in *Afe* KDO8P synthase but more information would be required to assess exactly how the mutation has affected A5P binding in the active site. Structural studies of wild-type *Afe* KDO8P synthase and N57A *Afe* KDO8P synthase in complex with A5P and PEP would help give insight to the specific role of this residue and would show the positions of the substrates relative to each other with or without the Asn present. Further mutagenesis experiments involving multiple mutations within the conserved LysAlaAsnArgSer motif of KDO8P synthase could give further insight into the differences between KDO8P synthase and DAH7P synthase. In the equivalent position of all DAH7P synthases is a conserved LysProArgThr motif which is proposed to be involved with binding of E4P in the active site.[33] Mutation of the Lys**AlaAsn**Arg**Ser** motif of *Afe* KDO8P synthase to Lys**Pro**Arg**Thr**, along with structural studies and substrate specificity studies, could help identify other key differences or similarities between the two enzymes and provide further evidence for a common ancestor.

CHAPTER 5.

EXPERIMENTAL PROCEDURES

5.1 General methods

Agarose gel electrophoresis

DNA fragments were separated by size using agarose gel electrophoresis. 1% (w/v) agarose gels were prepared by adding 0.3 g agarose to 30 mL 1x TAE buffer (40 mM Tris base, 20 mM acetic acid and 2 mM EDTA at pH 8.0) and heating until dissolved. 3 μL of SYBR-Safe® was added before the gels were set. All gels were run using a Sub-Cell® GT Agarose Gel electrophoresis system (Bio-Rad) in 1x TAE buffer. DNA sample were premixed with 6x DNA loading buffer (0.2% (w/v) bromophenol blue in 50% (v/v) glycerol) and loaded into the wells. Electrophoresis was carried out at 85 V until the dye front had migrated ¾ of the length of the gel. The DNA fragments were visualized on the gels by exposure to ultraviolet light (302 nm). Pictures of the gels were taken using an Alpha Imager gel documentation system (Alpha Innotech Corporation, USA) and edited and arranged using Microsoft Windows XP picture manager.

Purification of DNA from agarose gel

DNA fragments were purified from agarose gel using High Pure PCR Product Purification Kit (Roche). This consisted of cutting out the DNA band from the gel and dissolving it in 3x solution 1 (3 M guanidine-thiocyanate, 10 mM Tris-HCl pH 6.6, 5%

(v/v) ethanol) and then adding 1x isopropyl alcohol. The mixture was mixed gently, left at room temperature for 10 minutes and then added to a filter tube. 700 μL of washing buffer (2 mM Tris-HCl pH 7.5, 20 mM NaCl, 80% (v/v) ethanol) was added and the tube was centrifuged at 14000 rpm for 60 seconds. The flowthrough was discarded and the DNA was eluted from the filter tube by adding 30 μL of sterilized water and centrifuging into a sterile 0.6 mL Eppendorf tube at 13000 rpm for 1 minute. Purified DNA was stored at -20 ºC.

Transformation of DNA fragments into* E. coli *XL1-blue cells

Competent XL-1 Blue cells were kindly prepared by Dr Fiona Cochrane. 1 μL of the relevant plasmid DNA or PCR product was mixed with 20 μL of competent XL1-blue cells and incubated on ice for 30 minutes. The cells were heat shocked for 45 seconds at 42 ºC and then incubated on ice for a further 5 minutes. 40 μL of LB and 6 μL of 100 mM glucose were added and the cells were plated on pre-warmed (37 ºC) LB agar plates containing 100 μg mL^{-1} ampicillin (Sigma) and incubated for 12-16 hours at 37 ºC. Glycerol stocks of cells were prepared by adding 0.5 mL of 50% glycerol to 1 mL of cells with an optical density at 600 nm (OD_{600}) of ~0.6, flash frozen in liquid nitrogen and stored at -80 ºC.

Preparation of plasmid DNA

Plasmid DNA was prepared using a High Pure Plasmid Isolation Kit (Roche). This consisted of spinning down 4 ml of cells which had been grown for 12-16 hours at 37 ºC at 14000 rpm for 60 seconds. The cells were resuspended in 250 μL of suspension buffer (50 mM Tris-HCl pH 8.0, 10 mM EDTA, 0.1 mg mL^{-1} RNase A) and 250 μL of lysis buffer (0.2 M NaOH, 1% (w/v) SDS) was added. The mixture was incubated at room temperature for 5 minutes. 350 μL of chilled binding buffer (4 M guanidine hydrochloride, 0.5 M potassium acetate pH 4.2) was added and the mixture was incubated on ice for 10 minutes. The precipitate was spun down for 10 minutes at 14000

rpm and the supernatant was added to a filter tube. The tube was centrifuged at 14000 rpm for 60 seconds. 700 μL of washing buffer (2 mM Tris-HCl pH 7.5, 20 mM NaCl, 80% (v/v) ethanol) was added and the tube was centrifuged at 13000 rpm for 60 seconds. The flowthrough was discarded and the plasmid DNA was eluted from the filter tube by adding 80 μL of sterilized water and centrifuging into a sterile 1.5mL Eppendorf tube at 13000 rpm for 1 minute. Pure plasmid DNA was stored at -20 ºC.

Transformation of plasmid DNA into* E. coli *BL21(DE3) cells

Competent BL21(DE3) cells were kindly prepared by Dr Fiona Cochrane. 1 μL of ~20 ng μL^{-1} plasmid DNA was mixed with 20μL competent BL21(DE3) cells and transformation was carried out exactly the same as described for the transformation of DNA into *E. coli* XL1-blue cells.

Quantification and size determination of DNA fragments

The concentration of a DNA sample was estimated by visual comparison with DNA samples of a known concentration run alongside on an agarose gel. The approximate size of a DNA band was estimated by comparing its migration through the agarose gel against that of DNA standards with a known size (1 Kb Plus DNA Ladder, Invitrogen) which were run alongside the DNA sample of interest.

DNA sequencing

DNA sequencing services were provided by the Allan Wilson Centre for Molecular Evolution and Ecology Genome Service at Massey University. DNA sequencing was carried out on either an ABI Prism 377-64 sequencer or an ABI Prism 3730 capillary sequencer using BIGDYE labeled dideoxy chain termination chemistries (Applied Biosystems). Sequencing reactions contained at least 300 ng DNA and 3.2 pmol of T7 promoter (or reverse primer) in a total volume of 15 μL in sterile Milli-Q water.

Media

All *E. coli* cultures in this project were grown in Luria Broth (LB) made up (25 g L^{-1}) with Milli-Q water and sterilized by autoclaving at 121 ºC and 15 psi for 20 minutes. Agar media for agar plates was prepared by adding 1% agar (Invitrogen) to the liquid LB media prior to autoclaving and adding 100 μg mL^{-1} ampicillin immediately before pouring and setting the plates.

Centrifugation

All centrifugation in this project was performed in one of three centrifuges: a SORVALL® Heraeus multifuge 1S/1S-R or a MiniSpin® centrifuge (Eppendorf).

pH measurement

The pH of buffers used in this project was measured using a Sartorius PP-15 Professional Meter equilibrated with 3 M KCl.

Growth of* E. coli *cells

5 mL of LB containing 100 μg mL^{-1} ampicillin was inoculated with a scraping of a glycerol stock of the appropriate strain of *E. coli* cells. The cells were grown overnight, shaking, at 37 ºC. 2.5 mL of the overnight culture was added to 250 mL LB (with 100 μg mL^{-1} ampicillin) and was grown until mid-logarithmic phase (OD_{600} 0.4 – 0.6). All cell cultures used in this project for large scale protein purifications were multiple 250 mL cultures of cells growing along side each other in the same conditions.

Induction of protein expression

Expression of genes inserted into the multiple cloning site of pT7-7 is under the control of the *lac* promoter and is therefore induced by the addition of lactose or isopropyl-β-D-thiogalactopyranoside (IPTG) (Applichem). IPTG was used because it is a non-physiological analogue of lactose which is not metabolized by the cell, unlike lactose. IPTG was added to a final concentration of 1 mM to induce protein expression.

Harvesting and lysis of cells

The cells were harvested 4 – 5 hours after induction by centrifuging at 4500 rpm for 20 minutes at 4 ºC. Cell pellets were stored at -80 ºC until lysis.

Cell pellets were resuspended on ice in the appropriate lysis buffer. Cell pellets from 5 mL cultures were resuspended in 400 μL of lysis buffer and lysed by sonication on ice. Cell pellets from 250 mL cultures were resuspended in 10 mL of lysis buffer and lysed by using a French Press (8000 psi). The DNA was broken up by sonication and the cell debris was removed by centrifugation at 10150 rpm for 20 minutes 4 ºC.

The lysis buffer used for *Cte* KDO8P synthase consisted of 10 mM BTP pH 8.5, 1 mM EDTA, 1 mM DTT, 200 μM PEP. The lysis buffer used for *Afe* KDO8P synthase consisted of 10 mM BTP pH 7.0, 1 mM EDTA, 1 mM DTT, 0.2 M KCl, 200 μM PEP.

Sonication

All sonication was performed using a VirTis VirSonic digital 475 ultrasonic cell disrupter using a 1/8 inch probe at ~60 Watts.

Polyacrylamide gel electrophoresis

Sodium dodecyl sulfate polyacrylamide gel electrophoresis (SDS-PAGE) was performed using the method of Laemmli[60] with a 4% (w/v) stacking gel and a 12% (w/v) resolving gel, using a Mini Protean III cell (Bio-Rad). All samples were added to SDS loading buffer and boiled for two minutes before being loaded to gels. A current of 260 V was applied until the dye front ran off the bottom of the resolving gel. Bio-Rad low range molecular weight standards or Bio-Rad Precision Plus protein standards were used. Protein in the gels were detected by staining the gels for at least 60 minutes in a solution consisting of 1 g L^{-1} Coomassie Brilliant Blue R 250 (Park Scientific) in 50%

(v/v) methanol and 10% (v/v) acetic acid in water. Excess dye was removed by soaking gels for 20 – 30 minutes in an identical solution but without the Coomassie dye.

Fast protein liquid chromatography (FPLC)

FPLC was carried out using a Bio-Rad Biologic protein chromatography system at 4 ºC (for ion exchange and size-exclusion chromatography) or using an AKTAprime™ plus chromatography system (Amersham Biosciences) at room temperature (for hydrophobic interaction chromatography). All buffers and solvents used during FPLC were treated with Chelex resin (Bio-Rad) for 1 – 2 hours and filtered using a 0.45 μm filter (Millipore) before use.

Ion exchange chromatography (IEC)

IEC separates proteins according to their different net charges at a given pH. The side chains of surface amino-acid residues can be protonated or deprotonated depending on the pH of the environment and the overall charge on the protein will dictate the protein's behaviour on an ion exchange matrix. Anion exchange chromatography (AEC) uses a stationary phase that is positively charged with a counter ion such as Cl^- balancing the charge and cation exchange chromatography (CEC) uses a stationary phase that is negatively charged with a counter ion such as Na^+ balancing the charge. AEC in this project was performed at 4 ºC using a SOURCE™ 15Q (Amersham) column with the buffers at ~1 pH unit above the isoelectric point (pI) of the protein being purified. CEC was performed at 4 ºC using a SOURCE™ 15S (Amersham) column with the buffers at ~1 pH unit below the pI of the protein being purified.

Size-exclusion chromatography (SEC)

SEC, or gel filtration chromatography, separates proteins according to their molecular mass. The matrix is porous, acting like a molecular sieve that excludes large proteins that are eluted from the column with the void volume and retains smaller proteins that are eluted between the void volume and the total column volume in order of decreasing molecular mass. SEC in this project was used as a final purification step before

crystallization trials and as a way of determining the molecular mass of *Afe* KDO8P synthase. A Superdex S200 HR (10/300) column (Amersham) was used. All SEC was performed using a buffer consisting of 10 mM BTP pH 7.0, 10 μM EDTA, 200 μM PEP and 50 mM KCl at a flow rate of 0.4 mL min^{-1} for 100 minutes.

Molecular mass determination using SEC

SEC was used to determine the molecular mass of *Afe* KDO8P synthase in solution by comparing elution time of the sample protein with the elution times of molecular mass standards (MW-GF-200, Sigma). The molecular mass standards used were cytochrome C (12.4 kDa), carbonic anhydrase (29 kDa), alcohol dehydrogenase (150 kDa) and β-amylase (200 kDa).

Hydrophobic interaction chromatography (HIC)

HIC separates proteins based on differences in their surface hydrophobicity. The stationary phase is a matrix of phenyl agarose that binds to hydrophobic groups on the surface of a protein at neutral pH (close to the pI of the protein). Proteins can be eluted from the column by lowering the salt concentration (usually ammonium sulfate) of the aqueous mobile phase, which decreases the entropy of water and weakens the hydrophobic interactions. HIC in this project was carried out at room temperature using a SOURCE™ 15Phe (Amersham) column equilibrated with 1 M ammonium sulfate in BTP buffer at pH approximately equivalent to the pI of the target protein.

Standard enzyme assays and kinetic measurements

The assay system used for KDO8P synthase was a modified form of the assay used by Schoner and Herrmann[61] for DAH7P synthase. The consumption of PEP was monitored at 232 nm (ε = 2.8 x 10^3 M^{-1} cm^{-1} at 37 ºC) using a Varian Cary 100 UV Visible spectrophotometer. Measurements were made using 1 cm path length quartz cuvettes. Standard reaction mixtures contained PEP (~200 μM) (Sigma), A5P (~200 μM) (Sigma) and $MnSO_4$ (~100 μM) (Sigma) in BTP buffer (50 mM, pH 7.2) containing 10 μM

EDTA and enzyme to make a total volume of 1 mL. The BTP buffer solution was treated with Chelex before use. PEP and A5P solutions were made up in the BTP buffer solution. $MnSO_4$ solutions were made up in Milli-Q water that had been treated with Chelex. Reaction mixtures containing BTP buffer, PEP, $MnSO_4$ and enzyme were incubated for 6 minutes at 37 ºC and the reaction was initiated by the addition of A5P. Initial rates of reaction were determined by a least-squares fit of the initial rate data. One unit (1 U) of enzyme activity is defined as the loss of 1 μmol of PEP per minute at 37 ºC. Specific activity is defined as the loss of 1 μmol of PEP per minute at 37 ºC per mg of protein (U mg^{-1}). K_m and k_{cat} values were determined by fitting the data to the Michaelis-Menten equation using Enzfitter (Biosoft, 1999).

Determination of PEP and A5P concentrations

PEP and A5P concentrations were determined by using the standard assay method described above. For example, to determine the concentration of A5P a reaction mixture consisting of >200 μM PEP, ~100 μM $MnSO_4$ and ~5 μL A5P solution (of unknown concentration) is made up in BTP buffer, equilibrated to 37 ºC and initiated with enzyme to give a final volume of 1 mL. The reaction is allowed to go to completion and the difference between the absorbance before initiation and the absorbance after completion is measured (ΔA1). An identical reaction is set up in the absence of A5P to determine how much change in absorbance is due to the addition of the enzyme (ΔA2). The correct change in absorbance is given by ΔA1 + ΔA2. To convert absorbance into concentration Beer's Law is applied ($A = \varepsilon.c.\ell$ where ℓ = 1 cm and εPEP = 2.8 x 10^3 M^{-1} cm^{-1} at 37 ºC).

Determination of protein concentration

Protein concentration was determined by the method of Bradford, 1976[62] using bovine serum albumin (BSA) as a standard. BSA protein standards were made to protein concentrations of 0 mg mL^{-1}, 0.05 mg mL^{-1}, 0.1 mg mL^{-1}, 0.2 mg mL^{-1} and 0.4 mg mL^{-1} by dilution of a 20 mg mL^{-1} stock BSA solution (Bio-Rad). 1 mL of a 1/5 dilution of

stock Bradford reagent (Bio-Rad) was added to 100 μL of each standard and a standard curve was produced by taking absorbance readings at 595 nm of the standard mixtures after 5 minutes at room temperature. Protein samples of unknown concentration were diluted to 100 μL, 1 mL of Bradford reagent added and absorbance recorded in the same manner as above. Protein concentrations were determined in mg mL^{-1} using the Cary UV concentration software.

Storage of enzymes

All purified enzyme samples were concentrated to 10 – 50 mg mL^{-1} in filtered (0.2 μm) and Chelex treated BTP buffer pH 7.0 containing 200 μM PEP, flash frozen in liquid nitrogen and stored in 100 μL aliquots at -80 ºC.

Purified water

Water was purified by passage through a Sybron/Barnstead NANOpure II filtration system (Maryland, USA), containing two ion-exchange and two organic filters. This is referred to as Milli-Q water throughout this thesis. All Milli-Q water used in cloning of genes was autoclaved at 121 ºC and 15 psi for 20 minutes before use.

Amino-acid sequence alignments

Alignment of KDO8P synthase amino-acid sequences used for this project were obtained by copying and pasting the required primary sequences into ClustalW (EMBL-EBI) (http://www.ebi.ac.uk/ClustalW) and performing a multiple sequence alignment.

5.2 Experimental for chapter 2

Expression and Purification of *Chlorobium tepidum* KDO8P Synthase

Cloning of the Cte *KDO8P synthase gene*

Glycerol stocks of *E. coli* BL21(DE3) expression cells transformed with the cloned *Cte* KDO8P synthase gene in a pT7-7 vector were prepared by Dr Mark Patchett (Massey University, Palmerston North) prior to the start of this project.

Expression trials

Expression trials were carried out varying growth temperatures after induction, growth time after induction and testing the effect of different lysis buffers. Multiple overnight cultures of expression cells were grown in 5 mL LB with 100 μg mL^{-1} ampicillin (LB + amp). 200 μL of each overnight culture was used to inoculate 5 mL LB + amp and were grown at 37 ºC until mid-logarithmic phase (OD_{600} = 0.4 – 0.6). Expression was induced with 5 μL IPTG and cells were left to grow at the appropriate temperature for the appropriate time depending on which treatment was being tested. Equivalent numbers of cells from each treatment were harvested by centrifugation at 14000 rpm for 60 seconds at room temperature in 1.5 mL Eppendorf tubes. Cell pellets were resuspended in 400 μL of the appropriate lysis buffer and lysed by 3 x 15 seconds sonication at ~60 W. A 2 μL sample of the crude lysate was taken before the cell debris was spun down at 14000 rpm for 10 minute at 4 ºC. The supernatants were pipetted off and the pellets were resuspended in 200 μL 20 % SDS and 200 μL 6 M urea. 10 μL samples of the supernatants and the resuspended pellets were run alongside 2 μL samples of crude lysate on SDS-PAGE gels. Expression levels of soluble and insoluble proteins, including KDO8P synthase from each treatment, were compared by visually comparing the darkness and thickness of the bands on the gels after staining.

Purification by AEC and CEC

The supernatant fraction was collected after cell lysis and centrifugation was filtered using a 0.45 μm filter (Millipore), diluted 2 fold with buffer A (10 mM BTP pH 8.5, 1 mM EDTA, 1 mM DTT, 200 μM PEP) and loaded onto a SOURCE™ 15Q column (Amersham) equilibrated with buffer A at 4 ºC. The unbound protein was removed with 2 column volumes (~16 mL) of and the bound protein was eluted with a 90 mL linear gradient between buffer A and buffer A + 0.2 M NaCl, at a flow rate of 1.5 mL min^{-1}. SDS-PAGE was performed on samples of fractions (3 mL) corresponding to a peak on the UV trace and were tested for activity to identify the presence of KDO8P synthase. Fractions containing KDO8P synthase were pooled and concentrated using either a 20 mL Vivaspin 10 kDa MWCO concentrator (Vivascience) or a 15 mL Amicon Ultra 10 kDa MWCO concentrator (Millipore) and washed and diluted 2 fold with buffer B (10 mM BTP pH 6.5, 1 mM EDTA, 1 mM DTT, 200 μM PEP). The diluted sample was loaded onto a SOURCE™ 15S column (Amersham) and the unbound protein was removed with 2 column volumes (~16 mL) of buffer B. The bound protein was eluted with a 90 mL linear gradient between buffer B and buffer B + 0.2 M NaCl, at a flow rate of 1.5 mL min^{-1}. Fractions containing KDO8P synthase (as determined by SDS-PAGE) were pooled and concentrated using either a 2 mL Vivaspin 10 kDa MWCO concentrator or a 4 mL Amicon Ultra 10 kDa MWCO concentrator. The concentrated sample was washed and stored at -80 ºC in 10 mM BTP pH 7.4, 10 μM EDTA, 200 μM PEP.

Purification by HIC

After AEC, as described above, fractions containing KDO8PS were pooled and $(NH_4)_2SO_4$ was added to a final concentration of 1 M. The sample was filtered with a 0.45 μm filter (Millipore), diluted 2 fold and loaded onto a SOURCE™ 15Phe column (Amersham) equilibrated with buffer C (10 mM BTP pH 8.5, 1 mM EDTA, 1 mM DTT, 200 μM PEP, 1 M $(NH_4)_2SO_4$), at room temperature. Unbound protein was

removed with 2 column volumes (~16 mL) buffer C and bound protein was eluted with a 100 mL linear gradient between 100 % buffer C and 100 % buffer A at 1 mL min^{-1}.

Metal-dependency

Activity assays at each step of purification were carried out as described in general methods. 10 μL aliquots of *Cte*-KDO8P synthase solution were used in each assay. The assay buffer contained 50 mM BTP pH 7.4 and 10 μM EDTA. Metal activation was tested using 10 μL aliquots of protein after the anion exchange step but before buffer exchange, as this was when the protein was found to be most active. The effect of EDTA was tested by adding 0.5 M solution of EDTA to the assay mixture to a final concentration of 10 mM, equilibrating at 37 ºC for 6 minutes and then adding $MnSO_4$ until activity was restored.

Production of C24N and D246A mutants

The mutations were produced using the QuickChange® II Site-Directed Mutagenesis Kit (Stratagene). PCR was carried out using the pT7-7 plasmid preparation from *Cte* KDO8P synthase transformed XL1-blue cells as the double-stranded DNA template and synthetic primers incorporating the C24N mutation. The primers used for C24N were: (site-specific mutations underlined)

Forward 5'– CTCATCGCGGGGCCTAACCTTATCGAAAACC

Reverse 5'– GGTTTTCGATAAGGTTAGGCCCCGCGATGAG

The primers used for D246A were:

Forward 5'- ATGTCCGCTGCTTCGACCCAGGCTCCGCTC

Reverse 5'- GAGCGGAGCCTGGGTCGAAGCAGCGGACAT

The PCR reaction mixture consisted of ~ 10 ng of plasmid DNA template, 6 pmol of each primer, 250 μM of each of the deoxyribonucleotide triphosphates (dNTPs), 1x polymerase buffer + $MgSO_4$ and 1 unit *Pwo* DNA polymerase in a total volume of 25 μL. The thermo-cycling program used was as described by the Stratagene QuickChange® II Site-Directed Mutagenesis Kit (initial denaturation at 95 ºC for 3

minutes followed by 16 cycles of primer annealing at 55 ºC for 60 seconds and extension at 68 ºC for 4 minutes). 1 unit of *Dpn*1 restriction endonuclease was added to digest the parental of DNA, and the reaction was incubated at 37 ºC for 2 hours. 1 μL of PCR product was then used to transform 20 μL of XL1-blue cells as described in general methods. Subsequent plasmid preparation and transformation of BL21(DE3) cells was carried out as described in general methods.

Restriction enzyme digests

Success of plasmid preparation was monitored by digesting 1.5 μL of plasmid DNA with 1 unit of *Bam*HI in a total volume of 15 μL in 1x SuRE/cut buffer B (10 mM Tris-HCl pH 8.0, 0.1 M NaCl, 5 mM $MgCl_2$, 1 mM β-mercaptoethanol, Roche) at 37 ºC for at least 1 hour, then running on a 1% agarose gel to observe the result.

5.3 Experimental for chapter 3

Cloning, Expression, Purification and Characterization of Wild-Type *Acidithiobacillus ferrooxidans* KDO8P Synthase

Amplification of the* Afe *KDO8P synthase gene by PCR

Afe genomic DNA (ATCC, 23270) of unknown concentration was kindly donated by Dr Mark Patchett. DNA corresponding to the open reading frame of the KDO8P synthase gene was amplified using *Pwo* DNA polymerase (Stratagene).

The primers used were:

Forward 5' – GGTGGTCATATGCGTCTCTGTGGCTTCGAAGCAGGTC incorporating an *Nde*I restriction site (underlined).

Reverse 5' – GGTGGATCCTCATACTAACTCCTCAGGGTAGTTTTCAG incorporating a *Bam*HI restriction site (underlined).

Duplicate PCR reaction mixtures contained ~1 μg genomic DNA, 15 pmol of each primer, 250 μM of each of the dNTPs, 1x polymerase buffer + $MgSO_4$ and 2 units *Pwo* DNA polymerase in a total volume of 50 μL per reaction. The thermo-cycling program consisted of initial denaturation at 94 ºC for 3 minutes followed by 30 cycles of primer annealing at 58 ºC for 60 seconds and extension at 72 ºC for 60 seconds. The 846 bp PCR product was purified from a 1 % agarose gel as described in general methods and stored at -20 ºC.

Ligation of* Afe *KDO8P synthase gene into pT7-7

A 5 mL culture of pT7-7 in BL21(DE3) (kindly donated by Dr Mark Patchett) was grown for 12 – 16 hours at 37 ºC and pure plasmid was prepared as described in general methods. ~600 ng of pT7-7 and ~1 μg of the *Afe* KDO8P synthase gene (prepared above) were digested separately with 2 units of *Nde*I in a total volume of 25 μL in 1x SuRE/cut buffer H (50 mM Tris-HCl pH 7.5, 10 mM $MgCl_2$, 100 mM NaCl, 100 μM DTT, Roche) at 37 ºC overnight. ~600 ng of the singly digested plasmid and ~1 μg of the singly digested *Afe* KDO8P synthase gene were digested separately with 2 units of *Bam*HI in a total volume of 25 μL in 1x SuRE/cut buffer B (10 mM Tris-HCl pH 8.0, 0.1 M NaCl, 5 mM $MgCl_2$, 1 mM β-mercaptoethanol, Roche) at 37 ºC for 2 hours. The DNA was gel purified as described in general methods.

The ligation reaction consisted of ~150 ng digested pT7-7, ~450 ng digested *Afe* KDO8P synthase gene, 4 units of T4 DNA ligase (Roche) made up to a total volume of 30 μL in 1x ligation buffer (66 mM Tris-HCl pH 7.5, 5 mM DTT, 5 mM $MgCl_2$, 1 mM ATP) and incubated overnight at 16 ºC.

Transformation of XL1-blue and BL21(DE3)

2 μL of ligation mixture was used to transform 20 μL of Stratagene XL1-blue cells as described in the general methods. Colony PCR was performed to identify transformants.

Each PCR reaction mixture consisted of 5 μL GoTaq Green Master Mix (GoTaq Green buffer, 250 μM of each of the dNTPs, 5 U μL^{-1} *Taq* DNA polymerase, Pro Mega), ~5 ng reverse *Afe* KDO8P synthase primer and ~5 ng pT7-7 promoter primer made up to a volume of 10 μL with nuclease free H_2O (Pro Mega). Scrapings of each colony were streaked on an LB (amp) agar plate and added to the PCR reaction mixtures. The thermo-cycling program consisted of initial denaturation at 94 ºC for 3 minutes followed by 30 cycles of primer annealing at 50 ºC for 60 seconds and extension at 72 ºC for 60 seconds. Successful transformants were identified by band of ~930 bp on an agarose gel (*Afe* KDO8P synthase gene = 846 bp, T7 promoter = 80 bp upstream).

Overnight 5 mL culture of pT7-7-*Afe* KDO8P synthase transformed XL1-blue cells was grown and a 1 mL glycerol stock was prepared and stored at -80 ºC. A plasmid preparation was performed on the remaining 4 mL as described in general methods. 20 μL of BL21(DE3) cells were transformed with 1 μL of plasmid as described in general methods.

Purification by AEC and HIC

Purification by AEC and HIC was performed exactly as described above for *Cte* KDO8P synthase except that buffers A, B and C were all pH 7.0. Bound protein was eluted from the SOURCE™ 15Q column with a 90 mL linear gradient between buffer A and buffer A + 0.2 M NaCl, at a flow rate of 1.5 mL min^{-1}. Bound protein was eluted from the SOURCE™ 15Phe column with a 100 mL linear gradient between buffer C and buffer A at a flow rate of 1 mL min^{-1}.

Effect of pH and temperature

Standard 1 mL assays were performed in duplicate at varying temperatures (26 ºC – 60 ºC) to determine at which temperature *Afe* KDO8P synthase was most active.

50 mM BTP buffers (pH 6.1 – 8.8) and 50 mM sodium acetate buffers (pH 4.5 – 6.22) were prepared at 37 ºC and standard duplicate assays were carried out to determine at which pH *Afe* KDO8P synthase was most active.

All subsequent assays were performed in 50 mM BTP buffer at pH 7.2 and 37 ºC.

Metal activation To determine which metal ions best activated *Afe* KDO8P synthase, standard 1 mL assays were used containing a final concentration of 100 μM of various metal salts. The metal salts used were: $MnSO_4$; $CoSO_4$; $CdSO_4$; $NiCl_2$; $FeSO_4$; $CuSO_4$; $BaCl_2$; $CaCl_2$; $ZnSO_4$ all made up in chelex treated Milli-Q water at concentrations of 10 mM. All assays were performed in duplicate at 37 ºC and were initiated with the addition of A5P.

Metal-binding affinity assays were performed by using saturating concentrations of PEP (~200 μM) and A5P (~100 μM) and varying the final concentration of metal ion (2 μM – 400 μM) in the standard assay mixture.

Michaelis-Menten kinetics

To determine the kinetic parameters K_m and k_{cat}, PEP (15 μM – 1 mM) or A5P (2.42 μM – 242 μM) concentrations were varied while keeping the other substrate and $MnSO_4$ at saturating levels. Reactions were initiated with the addition of A5P and were performed in duplicate at 37 ºC.

Crystallization trials

Screening for crystallization conditions was performed using hanging-drop vapor diffusion in 24-well plates (1 μL + 1 μL drops and 400 μL of the appropriate mother liquor). Crystal trays were set up and stored at room temperature or set up and stored at 4 ºC. Initial screens included the Hampton Crystal Screens I and II (Hampton Research). Further screens included a Tris-HCl pH screen (Hampton Research) and

systematic PEG and salt concentration screens. Hampton Additive Screen I (Hampton Research) was performed using sitting-drop vapor diffusion on 96-well plates (0.5 μL + 0.5μL and 100 μL of appropriate mother liquor with additive). All screening was set up manually. All prepared solutions used were centrifuged at 14000 rpm for 2 minutes and crystal trays, pipette tips and cover slips were blown using compressed air to remove any dust.

X-ray diffraction

Crystals were transferred straight from the mother liquor drop onto the goniostat using an appropriate sized loop attached to a crystal mount (Hampton). If a cryo-protectant was necessary the crystals were transferred into a ~5 μL drop of cryo-solution before being mounted. Crystals were frozen upon mounting onto the goniometer by a stream of gaseous nitrogen at 110 K. Two images were collected at 90^{o} to each other with an exposure time of 10 - 20 minutes with the detector set at 100 mm from the loop.

The apparatus used in the attempted collection of crystal data was a Rigaku MicroMax-007 rotating anode X-ray generator (λ = 1.5418 nm, 800 W, 40 kV), with Osmic Blue confocal optics, R-Axis IV++ image plate detector and an Oxford series 700 cryostream.

5.4 Experimental for chapter 4

Investigating the Role of Important Amino-Acids in and Around the Active Site of *Acidithiobacillus ferrooxidans* KDO8P Synthase

Production of mutants

Site-specific mutations were introduced to *Afe* KDO8P synthase using the QuickChange® II Site-Directed Mutagenesis Kit (Stratagene). Primers used to create the mutations were:

C21N: *Forward* 5'- ATGGCAGGCCCCAACGCGATCGAGAGTGAA

Reverse 5'- TTCACTCTCGATCGCGTTGGGGCCTGCCAT

N57A: *Forward* 5'- CCTACGATAAAGCGGCACGTTCTTCGGGGCAG

Reverse 5'- CTGCCCCGAAGAACGTGCCGCTTTATCGTAGG

D243A: *Forward* 5'- GATGCTTTGTCTGCTGGTCCCAACGC

Reverse 5'- GCGTTGGGACCAGCAGACAAAGCATC

D243E: *Forward* 5'- GATGCTTTGTCTGAAGGTCCCAACGCCTG

Reverse 5'- CAGGCGTTGGGACCTTCAGACAAAGCATC

P245A: *Forward* 5'- CTTTGTCTGATGGTGCAAACGCCTGGCCGCTG

Reverse 5'- CAGCGGCCAGGCGTTTGCACCATCAGACAAAG

The template DNA for all the single mutation primers was pT7-7 plasmid preparation from XL1-blue cells incorporating the wild-type *Afe* KDO8P synthase gene. The procedure was exactly the same as described for production of *Cte* KDO8P synthase mutants.

Expression, purification and characterization of mutant proteins

Each protein was expressed and purified separately using exactly the same procedures as wild-type *Afe* KDO8P synthase. All chromatography columns used were washed thoroughly between purifications.

All assays were carried out in the same buffer as used for characterization of wild-type *Afe* KDO8P synthase (50 mM BTP pH 7.2, 10 μM EDTA). Determination of K_m and k_{cat} values for each mutant was subject to how much A5P was available to use in the assays.

REFERENCES

1. Levin, D. H. R., E., Condensation of arabinose 5-phosphate and phosphorylenol pyruvate by 2-keto-3-deoxy-8-phosphooctonic acid synthase. *J. Biol. Chem.* **1959,** 234, (10), 2532-2539.
2. Raetz, C. R. H., Biochemistry of endotoxins. *Annu. Rev. Biochem.* **1990,** 59, 129-170.
3. Delmas, F. P., J.; Joubes, J.; Seveno, M.; Paccalet, T.; Hernould, M.; Lerouge, P.; Mouras A.; Chevalier, C., The gene expression and enzyme activity of plant 3-deoxy-D-*manno*-octulosonic acid-8-phosphate synthase are preferentially associated with cell division in a cell cycle-dependent manner. *Plant Physiol.* **2003,** 133, 348-360.
4. Wyckoff, T. J. O. R., C. R. H.; Jackman, J. E., Antibacterial and anti-inflammatory agents that target endotoxin. *Trends Microbiol.* **1998,** 6, (4), 154-159.
5. Holst, O., Chemical structure of the core region of lipopolysaccharides - an update. *Trends Glycosci. Glycotech.* **2002,** 14, 87-103.
6. Rick, P. D. O., M. J., Isolation of a mutant of *Salmonella typhimurium* dependent on D-arabinose-5-phosphate for growth and synthesis of 3-deoxy-D-*manno*-octulosonate-8-phosphate (ketodeoxyoctonate). *Proc. Natl. Acad. Sci. U. S. A.* **1972,** 69, 3756-3760.
7. Rick, P. D. Y., D. A., Isolation and characterization of a temperature-sensitive lethal mutant of *Salmonella typhimurium* that is conditionally defective in 3-deoxy-D-*manno*-octulosonate-8-phosphate synthesis. *J. Bacteriol.* **1982,** 150, (2), 447-455.
8. Meredith, T. C. A., P.; Mamat, U.; Lindner, B.; Woodard, R. W., Redefining the requisite lipopolysaccharide structure in *Escherichia coli*. *ACS Chem. Biol.* **2006,** 1, (1), 33-42.

9. Luke, R. N. A., S.; Gibson, B. W.; Campagnari, A. A., Identification of a 3-deoxy-D-*manno*-octulosonic acid biosynthetic operon in *Moraxella catarrhalis* and analysis of a KdsA-deficient isogenic mutant. *Infect. Immun.* **2003,** 71, (11), 6426-6434.
10. Ray, P. H., Purification and characterization of 3-deoxy-D-*manno*-octulosonate 8-phosphate synthetase from *Escherichia coli*. *J. Bacteriol.* **1980,** 141, 635-644.
11. Duewel, H. S. W., R. W., A metal bridge between two enzyme families: 3-Deoxy-D-*manno*-octulosonate-8-phosphate synthase from *Aquifex aeolicus* requires a divalent metal for activity. *J. Biol. Chem.* **2000,** 275, (30), 22824-22831.
12. DeLeo, A. B. S., D. B., Mechanism of 3-deoxy-D-*arabino*-heptulosonate 7-phosphate (DAHP) synthetase. *Biochem. Biophys. Res. Commun.* **1968,** 32, (5), 873-877.
13. Jensen, R. A. X., G.; Calhoun, D. H.; Bonner, C. A., The correct phylogenetic relationship of KdsA (3-deoxy-D-*manno*-octulosonate 8-phosphate synthase) with one of two independently evolved classes of AroA (3-deoxy-D-*arabino*-heptulosonate 7-phosphate synthase). *J. Mol. Evol.* **2002,** 54, 416-423.
14. Baasov, T. K., J. R., Is the first enzyme of the shikimate pathway 3-deoxy-D-*arabino*-heptulosonate-7-phosphate synthase (tyrosine sensitive), a copper metalloenzyme? *J. Bacteriol.* **1989,** 171, (11), 6155-6160.
15. Schnappauf, G. H., M.; Kunzler, M.; Braus, G. H., The two 3-deoxy-D-*arabino*-heptulosonate-7-phosphate synthase isoenzymes from *Saccharomyces cerevisiae* show different kinetic modes of inhibition. *Arch. Microbiol.* **1998,** 169, 517-524.
16. Stephens, C. M. B., R., Analysis of the metal requirement of 3-deoxy-D-arabino-heptulosonate 7-phosphate. *J. Biol. Chem.* **1991,** 266, (31), 20810-20817.
17. Schofield, L. R. A., B. F.; Patchett, M. L.; Norris, G. E.; Jameson, G. B.; Parker, E. J., Substrate ambiguity and crystal structure of *Pyrococcus furiosus* 3-deoxy-D-*arabino*-heptulosonate-7-phosphate synthase: an ancestral 3-deoxyald-2-ulosonate-phosphate synthase? *Biochemistry* **2005,** 44, (36), 11950-11962.

18. Gosset, G. B., C. A.; Jensen, R. A., Microbial origin of plant-type 2-keto-3-deoxy-D-*arabino*-heptulosonate 7-phosphate synthases, exemplified by the chorismate and tryptophan-regulated enzyme from *Xanthomonas campestris*. *J. Bacteriol.* **2001,** 183, 4061-4070.
19. Birck, M. R. W., R. W., *Aquifex aeolicus* 3-deoxy-D-*manno*-2-octulosonic acid 8-phosphate synthase: A new class of KDO 8-P synthase? *J. Mol. Evol.* **2001,** 52, 205-214.
20. Duewel, H. S. R., S.; Wang, J.; Woodard, R. W.; Gatti, D. L., Substrate and metal comlexes of 3-deoxy-D-*manno*-octulosonate-8-phosphate synthase from *Aquifex aeolicus* at 1.9-A resolution. *J. Biol. Chem.* **2001,** 276, (11), 8393-8402.
21. Shulami, S. Y., O.; Rabkin, E.; Shoham, Y.; Baasov, T., Cloning, expression, and biochemical characterization of 3-deoxy-D-*manno*-2-octulosonate-8-phosphate (KDO8P) synthase from the hyperthermophilic bacterium *Aquifex pyrophilus*. *Extremophiles* **2003,** 7, 471-481.
22. Li, J. W., J.; Fleischhacker, A. S.; Woodard, R. W., Conversion of *Aquifex aeolicus* 3-deoxy-D-*manno*-octulosonate 8-phosphate synthase, a metalloenzyme, into a nonmetalloenzyme. *J. Am. Chem. Soc.* **2004,** 126, (24), 7448-7449.
23. Shulami, S. F. C. A., N.; Shoham, Y.; Anderson, K. S.; Baasov, T., A reciprocal single mutation affects the metal requirement of 3-deoxy-D-*manno*-2-octulosonate-8-phosphate (KDO8P) synthases from *Aquifex pyrophilus* and *Escherichia coli*. *J. Biol. Chem.* **2004,** 279, (43), 45110-45120.
24. Oliynyk, Z. B.-R., L.; Janowitz, T.; Sondergeld, P.; Fersht, A. R., Designing a metal-binding site in the scaffold of *Escherichia coli* KDO8PS. *Protein Eng. Des. Sel.* **2004,** 17, (4), 383-390.
25. Ahn, M. P., A. L.; Schofield, L. R.; Parker, E. J., Mechanistic divergence of two closely related aldol-like enzyme-catalysed reactions. *Org. Biomol. Chem.* **2005,** 3, 4046-4049.

26. Krosky, D. J. A., R.; Berg, M.; Carmel, G.; Tummino, P. J.; Xu, B.; Yang, W., *Helicobacter pylori* 3-deoxy-D-*manno*-octulosonate-8-phosphate (KDO-8-P) synthase is a zinc-metalloenzyme. *Biochim. Biophys. Acta* **2002,** 1594, 297-306.
27. Cochrane, F. C., Unpublished data. In 2007.
28. Subramaniam, P. S. X., G.; Xia, T.; Jensen, R. A., Substrate ambiguity of 3-deoxy-D-*manno*-octulosonate 8-phosphate synthase from *Neisseria gonorrhoeae* in the context of its membership in a protein family containing a subset of 3-deoxy-D-*arabino*-heptulosonate 7-phosphate synthases. *J. Bacteriol.* **1998,** 180, (1), 119-127.
29. Wu, J. P., M. A.; Sundaram, A. K.; Woodard, R. W., Functional and biochemical characterization of a recombinant *Arabidopsis thaliana* 3-deoxy-D-*manno*-octulosonate 8-phosphate synthase. *Biochemistry* **2004,** 381, 185-193.
30. Duewel, H. S. S., G. Y.; Woodard, R. W., Functional and biochemical characterization of a recombinant 3-deoxy-D-*manno*-octulosonic acid 8-phosphate synthase from the hyperthermophilic bacterium *Aquifex aeolicus*. *Biochem. Biophys. Res. Commun.* **1999,** 263, (2), 346-351.
31. Taylor, W. P. S., G. Y.; Woodard, R. W., A single point mutation in 3-deoxy-D-*manno*-octulosonate-8-phosphate synthase is responsible for temperature sensitivity in a mutant strain of *Salmonella typhimurium*. *J. Biol. Chem.* **2000,** 275, (41), 32141-32146.
32. Radaev, S. D., P.; Patel, M.; Woodard, R. W.; Gatti, D. L., Structure and mechanism of 3-deoxy-D-*manno*-octulosonate-8-phosphate synthase. *J. Biol. Chem.* **2000,** 275, (13), 9476-9484.
33. Shumilin, I. A. B., R.; Wu, J.; Woodard, R. W.; Kretsinger, R. H., Crystal structure of the reaction complex of 3-deoxy-D-*arabino*-heptulosonate-7-phosphate synthase from *Thermotoga maritima* refines the catalytic mechanism and indicates a new mechanism of allosteric regulation. *J. Mol. Biol.* **2004,** 341, (2), 455-466.
34. Webby, C. J. B., H. M.; Lott, J. S.; Baker, E. N.; Parker, E. J., The structure of 3-deoxy-D-*arabino*-heptulosonate 7-phosphate synthase from *Mycobacterium*

tuberculosis reveals a common catalytic scaffold and ancestry for type I and type II enzymes. *J. Mol. Biol.* **2005,** 354, (4), 927-939.

35. Wang, J. D., H. S.; Woodard, R. W.; L. Gatti, D. L., Structures of *Aquifex aeolicus* KDO8P synthase in complex with R5P and PEP, and with a bisubstrate inhibitor: role of active site water in catalysis. *Biochemistry* **2001,** 40, (51), 15676-15683.
36. Furdui, C. Z., L.; Woodard, R. W.; Anderson, K. S., Insights into the mechanism of 3-deoxy-D-*arabino*-heptulosonate 7-phosphate synthase (Phe) from *Escherichia coli* using a transient kinetic analysis. *J. Biol. Chem.* **2004,** 279, (44), 45618-45625.
37. Wang, J. D., H. S.; Stuckey, J. A.; Woodard, R. W.; Gatti, D. L., Function of His 185 in *Aquifex aeolicus* 3-deoxy-D-*manno*-octulosonate 8-phosphate synthase. *J. Mol. Biol.* **2002,** 324, (2), 205-14.
38. Dotson, G. D. D., R. K.; Clemens, J. C.; Wooten, E. W.; Woodard, R. W., Overproduction and one step purification of *Escherichia coli* 3-deoxy-D-*manno*-octulosonic acid 8-phosphate synthase and oxygen transfer studies during catalysis using isotopic-shifted heteronuclear NMR. *J. Biol. Chem.* **1995,** 270, 13698-13705.
39. Hedstrom, L. A., R., 3-Deoxy-D-*manno*-octulosonate-8-phosphate synthase catalyzes the C-O bond cleavage of phosphoenolpyruvate. *Biochem. Biophys. Res. Commun.* **1988,** 157, (2), 816-820.
40. Wooten, E. W. D., R. K.; Dotson, G. D.; Woodard, R. W., Homo- and heteronuclear multiple quantum filters for measurement of NMR isotope shifts. *J. Magn. Reson.* **1994,** 107, 50-55.
41. Dotson, G. D. N., P.; Reily, M. D.; Woodard, R. W., Stereochemistry of 3-deoxy-D-*manno*-2-octulosonate 8-phosphate synthase. *Biochemistry* **1993,** 32, 12393-12397.
42. Kohen, A. J., A.; Baasov, T., Mechanistic studies of 3-deoxy-D-*manno*-2-octulosonate-8-phosphate synthase from *Escherichia coli*. *Eur. J. Biochem.* **1992,** 208, 443-449.

43. Howe, D. L. S., A. K.; Wu, J.; Gatti, D. L.; Woodard, R. W., Mechanistic insight into 3-deoxy-D-*manno*-octulosonate 8-phosphate synthase and 3-deoxy-D-*arabino*-heptulosonate 7-phosphate synthase utilizing phosphorylated monosaccharide analogues. *Biochemistry* **2003,** 42, 4843-4854.

44. Baasov, T. S.-D.-N., S.; Kohen, A.; Jakob, A.; Belakhov, V., Catalytic mechanism of 3-deoxy-D-*manno*-octulosonate-8-phosphate synthase. *Eur. J. Biochem.* **1993,** 217, 991-999.

45. Baasov, T. T., R.; Sheffer-Dee-Noor, S.; Belakhov, V., Catalytic mechanism of 3-deoxy-D-*manno*-2-octulosonate-8-phosphate synthase. *Curr. Org. Chem.* **2001,** 5, (2), 127-138.

46. Li, Z. S., A. K.; Shen, S.; Whitehouse, C.; Baasov, T.; Anderson, K. S., A snapshot of enzyme catalysis using electrospray ionization mass spectrometry. *J. Am. Chem. Soc.* **2003,** 125, (33), 9938-9939.

47. Asojo, O. F., J.; Adir, N.; Belakhov, V.; Shoham, Y.; Baasov, T., Crystal structures of KDOP synthase in its binary complexes with the substrate phosphoenolpyruvate and with a mechanism-based inhibitor. *Biochemistry* **2001,** 40, (21), 6326-6334.

48. Furdui, C. S., A. K.; Yaniv, O.; Belakhov, V.; Woodard, R. W.; Baasov, T.; Anderson, K. S., The use of (E)- and (Z)-phosphoenol-3-fluoropyruvate as mechanistic probes reveals significant differences between the active sites of KDO8P and DAHP synthases. *Biochemistry* **2005,** 44, (19), 7326-7335.

49. Xu, X. K., F.; Wang, J.; Lu, J.; Stemmler, T.; Gatti, D. L., The catalytic and conformational cycle of *Aquifex aeolicus* KDO8P synthase: Role of the L7 loop. *Biochemistry* **2005,** 44, (37), 12434-12444.

50. Sheflyan, G. Y. D., H. S.; Chen, G.; Woodard, R. W., Identification of essential histidine residues in 3-deoxy-D-*manno*-octulosonic acid 8-phosphate synthase: analysis by chemical modification with diethyl pyrocarbonate and site-directed mutagenesis. *Biochemistry* **1999,** 38, 14320-14329.

51. Wahlund, T. M. W., C. R.; Castenholz, R. W.; Madigan, M. T., A thermophilic green sulfur bacterium from New Zealand hot springs, *Chlorobium tepidum*. *Arch. Microbiol.* **1991,** 159, 81-90.

52. Eisen, J. A. N., K. E.; Paulsen, I. T.; Heidelberg, J. F.; Wu, M.; Dodson, R. J.; Deboy, R.; Gwinn, M. L.; Nelson, W. C.; Haft, D. H.; Hickey, E. K.; Peterson, J. D.; Durkin, S. A.; Kolonay, J. L.; Yang, F.; Holt, I.; Umayam, L. A.; Mason, T.; Brenner, M.; Shea, T. P.; Parksey, D.; Nierman, W. C.; Feldblyum, T. V.; Hansen, C. L.; Craven, M. B.; Radune, D.; Vamathevan, J.; Khouri, H.; White, O.; Gruber, T. M.; Ketchum, K. A.; Venter, J. C.; Tettelin, H.; Bryant, D. A.; Fraser, C. M., The complete genome sequence of *Chlorobium tepidum* TLS, a photosynthetic, anaerobic, green-sulfur bacterium. *Proc. Natl. Acad. Sci. U. S. A.* **2002,** 99, (14), 9509-9514.

53. Webby, C. J. P., M. L.; Parker, E. J., Characterization of a recombinant type II 3-deoxy-D-*arabino*-heptulosonate-7-phosphate synthase from *Helicobacter pylori*. *Biochem. J.* **2005,** 390, 223-230.

54. Schofield, L. R. P., M. L.; Parker, E. J., Expression, purification and characterization of 3-deoxy-D-*arabino*-heptulosonate 7-phosphate synthase from *Pyrococcus furiosus*. *Protein Expr. Puif.* **2004,** 34, 17-27.

55. Sau, A. K. L., Z.; Anderson, K. S., Probing the role of metal ions in the catalysis of *Helicobacter pylori* 3-deoxy-D-*manno*-octulosonate-8-phosphate synthase using a transient kinetic analysis. *J. Biol. Chem.* **2004,** 279, (16), 15787-15794.

56. Kelly, D. P. W., A. P., Reclassification of some species of *Thiobacillus* to the newly designated genera *Acidithiobacillus* gen. nov., *Halothiobacillus* gen. nov. and *Thermithiobacillus* gen. nov. *Int. J. Syst. Evol. Microbiol.* **2000,** 50, 511-516.

57. Holt, J. G., *Bergey's manual of determinative bacteriology*. Williams & Wilkins: Baltimore, Md., 1993.

58. Barron, J. L. L., D. R., Growth and maintenance of *Thiobacillus ferrooxidans* cells. *Appl. Environ. Microbiol.* **1990,** 56, 2801-2806.

59. Sheflyan, G. Y. S., A. K.; Taylor, W. P.; Woodard, R. W., Substrate ambiguity of 3-deoxy-D-*manno*-octulosonate 8-phosphate synthase from *Neisseria gonorrhoeae* revisited. *J. Bacteriol.* **2000,** 182, (17), 5005-5008.

60. Laemmli, U. K., Cleavage of structural proteins during the assembly of the head of bacteriophage T4. *Nature* **1970,** 227, 680-685.

61. Schoner, R. H., K. M., 3-Deoxy-D-*arabino*-heptulosonate 7-phosphate synthase. Purification, properties and kinetics of the tyrosine-sensitive enzyme from *Escherichia coli*. *J. Biol. Chem.* **1976,** 251, 5440-5447.

62. Bradford, M. M., A rapid and sensitive method for the quantification of microgram quantities of protein using the principles of protein-dye binding. *Anal. Biochem.* **1976,** 72, 248-254.